Alma Mater Studiorum · University of Bologna

School of Science
Department of Physics and Astronomy
Master Degree in Physics

Generalized hydrodynamics of a $(1+1)$-dimensional integrable scattering theory with roaming trajectories

Supervisor:
Prof. Francesco Ravanini

Co-supervisor: Prof. Olalla Castro-Alvaredo

Submitted by:
Michele Mazzoni

Academic Year 2019/2020

Abstract

The emergence of hydrodynamic features in off-equilibrium $(1 + 1)$-dimensional integrable quantum systems has been the object of increasing attention in recent years. In this Master Thesis, we combine Thermodynamic Bethe Ansatz (TBA) techniques for finite-temperature quantum field theories with the Generalized Hydrodynamics (GHD) picture to provide a theoretical and numerical analysis of Zamolodchikov's staircase model both at thermal equilibrium and in inhomogeneous generalized Gibbs ensembles. The staircase model is a diagonal $(1 + 1)$-dimensional integrable scattering theory with the remarkable property of roaming between infinitely many critical points when moving along a renormalization group trajectory. Namely, the finite-temperature dimensionless ground-state energy of the system approaches the central charges of all the minimal unitary conformal field theories (CFTs) $\mathcal{M}_p$ as the temperature varies. Within the GHD framework we develop a detailed study of the staircase model's hydrodynamics and compare its quite surprising features to those displayed by a class of non-diagonal massless models flowing between adjacent points in the $\mathcal{M}_p$ series. Finally, employing both TBA and GHD techniques, we generalize to higher-spin local and quasi-local conserved charges the results obtained by B. Doyon and D. Bernard [1] for the steady-state energy current in off-equilibrium conformal field theories.

Contents

Introduction

In the last forty years, integrable models have proven an ideal landscape for the understanding of equilibrium and off-equilibrium properties of interacting quantum many-body systems. This is true on two levels.

Theoretically, the presence of an extensive number of conserved quantities allows one to exactly solve the dynamics at all orders in perturbation theory by simply requiring some analytical and self-consistency properties of the scattering data of the theory. This is the essence of the S-matrix approach to integrable quantum field theories (QFTs). Originally developed to provide an alternative route for the theoretical understanding of low-energy processes in quantum chromodynamics (QCD), which could not be dealt with the usual techniques of perturbative quantum field theory, the analytic theory of scattering amplitudes was soon understood to work at its best with integrable quantum models in one spatial dimension [2, 3]. The reason is that the presence of too many conservation laws poses severe constraints on the interactions allowed in the theory. In fact, so severe that if there are two or more spatial dimensions a "no-go"theorem forbids any non-supersymmetric integrable QFT to present non-trivial interactions [4]. Luckily, among $(1+1)$-dimensional theories there is a vast class of models which can be exactly solved, as any two-dimensional lattice model which is classically integrable can be mapped into a quantum spin chain, and the latter can in turn be regarded as the non-relativistic, discretized limit of some integrable field theory. Towards the end of the 1980s, a series of pioneering works by Al. B. Zamolodchikov [5, 6, 7] made it clear that the S-matrix content of an integrable relativistic QFT, togheter with the knowledge of its mass spectrum, is sufficient to determine the thermodynamic properties of the model when the latter is at finite temperature. This is done by generalizing a procedure already known for non-relativistic interacting gases [8], which involves the solution of a set of nonlinear integral equations, the thermodynamic Bethe ansatz (TBA) equations.

On the other hand, quantum integrable systems can be realized and studied in a laboratory. For instance, a spin-$\frac{1}{2}$ Heisenberg chain is well-reproduced by a magnetic crystal in which ions are arranged in one-dimensional rays and the locality of interactions is preserved by non-magnetic atoms screening long-distance effects [9]. A Lieb-Liniger gas, the non-relativistic limit of the celebrated sinh-Gordon QFT, can obtained by trapping rubidium atoms using an optical lattice [10]. Moreover, the recent development

of sophisticated experimental techniques has made it possible to investigate quantum many-body systems out of thermal equilibrium [11]: in a partitioning protocol, two quantum systems connected to thermal reservoirs at different temperatures are joined together and the global system is let evolve with an interaction Hamiltonian. It turns out that integrability plays a key role in determining the thermalization properties of the system at large time scales. Indeed, if there are few conserved charges the relaxation process inevitably leads to a homogeneous Gibbs ensemble, where there are no transport phenomena at the macroscopic scale. On the other hand, if there are infinitely many conserved charges thermalization cannot take place in a proper sense: a pre-thermalization process occurs, and the final state is a spatially inhomogeneous ensemble with infinitely many generalized thermodynamic potentials coupled to the conserved charges[12]. This is known as a generalized Gibbs ensemble (GGE). The absence of proper thermalization in a GGE is manifested by non-equilibrium steady state currents, *i.e.* diffusive phenomena due to ballistic motion of charge carriers even at large space-time scales [13]. In particular, a universal formula for the steady state energy current has been found by D. Bernard and B. Doyon [1, 14] in a partitioning protocol realized by joining togheter two $(1+1)$-dimensional critical systems modeled by a certain conformal field theory (CFT). The emergent hydrodynamic picture in the theory of off-equilibrium integrable models is coherently described within the recently-developed framework of generalized hydrodynamics (GHD), where the TBA techniques are extensively used [15, 16].

The present manuscript is set within this context. Its aim is to provide a detailed theoretical and numerical study of the generalized hydrodynamics of Zamolodchikov's staircase model [17]. This is a $(1+1)$-dimensional integrable scattering theory with a diagonal S-matrix, obtained by analytic continuation of the sinh-Gordon S-matrix at the self-dual point. In spite of the apparent simplicity of the model, which contains only one neutral massive particle with no bound states, there is a rather peculiar feature which is manifested at the TBA level. This is the fact that at intermediate temperatures, between the infrared and the ultraviolet regimes, the scaling free-energy of this model approaches the central charges of all the minimal unitary conformal models, that is, the renormalization group (RG) trajectory roams between infinitely many conformal fixed points. An accurate analysis of the staircase's reduced TBA equations reveals unexpected connections to a class of non-diagonal theories, the A_n massless perturbations of unitary minimal models. The numerical implementation of the partitioning protocol, with some refinements introduced by the author in order to account for specific features of the staircase model, shows that this connection holds also at the GHD level. A comprehensive theoretical study to support numerical observations in this direction is in preparation [18]. Within the context of GHD, we employ TBA techniques to obtain an expression for the steady-state energy current in a partitioning protocol, which reproduces in the UV limit the result obtained in [1]. This result is then generalized to all the local and quasi-local higher-spin charges in the staircase model, which display a universal power-law

dependence on the temperatures of the thermal reservoirs, with coefficients depending on the spin and on the limiting central charge. The numerical simulations performed with Phyton are in very good agreement with the theoretical predictions in the UV regime. The work is structured as follows.

- In chapter 1 we introduce the main ideas and tools in the theory of $(1 + 1)$-dimensional integrable quantum systems, starting from from the well-established notion of Liouville integrability in discrete classical systems. We then discuss the S-matrix approach to integrable quantum field theories and illustrate the role of integrability in obtaining the exact analytical structure of the scattering amplitudes.

- In chapter 2 we present the thermodynamic Bethe ansatz technique and use it to derive the finite-temperature properties of integrable $(1 + 1)$-dimensional QFTs with diagonal scattering, showing also how the central charge of the underlying conformal field theory is recovered form the dimensionless free energy of the model in the UV limit. In the last part of the chapter we outline the universal classification of TBA systems in terms of ADE simply-laced algebras and describe how it can be generalized to non-diagonal theories, with a particular attention to A_n massless models flowing between critical points in the minimal unitary series.

- The scattering theory and TBA structure of Zamolodchikov's staircase model are discussed in chapter 3. A detailed analysis of the kinks-plateaux structure displayed by the L-function of the model is followed by a comparison between the staircase's reduced TBA equations and the stationary solutions of Y-systems in A_n massless models. By adapting arguments presented in [19, 20], we provide an analytic derivation of the roaming behaviour displayed by the staircase's model scaling function.

- In chapter 4 we outline the main ideas and techniques of generalized hydrodynamics (GHD), starting from the off-equilibrium description of systems with finitely-many conserved charges. We then show how integrability, combined with the local entropy maximization assumption, lead to the notion of generalized Gibbs ensembles. These can be studied using a quasi-particle formulation based on the TBA techniques introduced in chapter 2. The second part of the chapter is devoted to the analysis of some curious features displayed by the staircase model in a GHD setting. In particular, we present a numerical implementation of the partitioning protocol which accounts for the non-monotonicity of the effective velocity, and suggest how this feature can be related to the behaviour of magnons in A_n massless models.

- The final chapter is devoted to the study of steady-state average currents and charges in the off-equilibrium staircase model. By means of the quasi-particle description of GGEs we derive the exact UV limit of the average energy current and

density in the steady state which is formed by joining two independently thermalized reservoirs. A slight generalization of this procedure is then used to treat the case of steady-state higher-spin currents, which display different UV behaviours according to the initial GGE in which the two reservoirs are prepared.

Chapter 1

Integrability in $(1+1)$-dimensional quantum field theories

In this chapter we outline the basic notions about integrable quantum field theories in $(1+1)$ dimensions, which are the main ingredients of the thermodynamic Bethe ansatz and the hydrodynamic approach developed in the following chapters. Starting from the definition of Liouville integrability in discrete classical systems [21], we show how it is possible to extend this notion to discrete quantum systems and then to quantum field theories by taking a scaling limit of one-dimensional spin chains. In particular, we underline the essential role of locality when dealing with systems having an extensive number of degrees of freedom.

In the second part of the chapter we present a different approach to integrable QFTs, the analytic theory of scattering amplitudes [2, 3]. In this formulation, the fundamental objects are asymptotic multi-particle states and S-matrix elements rather than quantum fields. The presence of infinitely many conserved charges has profound implications on the structure of the S-matrix in one spatial dimensions, as the scattering processes are completely elastic and factorizable. Therefore, the physical content of an integrable $(1+1)$-dimensional quantum field theory is completely unveiled by the spectrum of its conserved charges and by the analytic structure of its two-particle S-matrix.

1.1 From classical to quantum integrability

The notion of integrability finds application in diverse areas of theoretical physics, from classical mechanics to quantum field theories. In this section we review the main issues which arise when trying to extend a classical definition of integrability to quantum systems, and show how they can be overcome [21, 22].

1.1.1 Discrete classical systems

Let us see how integrability is defined and works in discrete classical systems. The space of states of a classical system with n degrees of freedom is a $2n$-dimensional manifold parametrized by n coordinates $q_i \in \mathbb{R}$ and their canonically conjugated momenta $p_i \in \mathbb{R}$, $i = 1, \dots, n$. The manifold is symplectic, which means that it is endowed with a bilinear antisymmetric operation, the Poisson brackets $\{\cdot\,,\,\cdot\}$, acting on two copies of the algebra $\mathcal{F}$ of smooth functions over the phase space:

$$\{F, G\} \equiv \sum_{i=1}^{n} \left(\frac{\partial F}{\partial p_i} \frac{\partial G}{\partial q_i} - \frac{\partial F}{\partial q_i} \frac{\partial G}{\partial p_i} \right) , \quad F, G \in \mathcal{F} \,. \tag{1.1}$$

The time evolution of any observable $F \in \mathcal{F}$ is ruled by the Hamiltonian function $H(q_i, p_i)$ through the relation:

$$\dot{F} = \{H, F\} \,, \tag{1.2}$$

which in particular entails the well-known Hamilton equations for the canonical coordinates and momenta:

$$\dot{q}_i = \{H, q_i\} = \frac{\partial H}{\partial p_i} \,, \quad \dot{p}_i = \{H, p_i\} = -\frac{\partial H}{\partial q_i} \,, \quad i = 1, \dots, n \,. \tag{1.3}$$

A conserved quantity, or classical integral of motion, is a function $F \in \mathcal{F}$ which is invariant under the time evolution generated by H, that is $\{H, F\} = 0$. We define a dynamical system (with a $2n$-dimensional phase space) classically integrable, or Liouville-integrable, if it admits n independent integrals of motion $F_i \in \mathcal{F}$ which are in involution, that is $\{F_i, F_j\} = 0$ for all $i, j = 1, \dots, n$. Independence of the conserved quantities means that at any point in phase space, the tangent space to the surface:

$$\mathcal{M}_f = \{(q_i, p_i) : F_i = f_i \,, \forall\, i = 1, \dots, n\} \,, \tag{1.4}$$

with f_i constant quantities, exists and it is n-dimensional. Clearly there cannot be more than n of such quantities which are independent, and the Hamiltonian must therefore be a function of the F_i, so that we can always choose it to coincide with one of them. When a system admits several conserved quantities, however, the choice of which of them plays the role of time-evolution generator is essentially a matter of convenience: we will see in the last chapter a situation in which the time-evolution is not ruled by the Hamiltonian.

The fundamental consequence of Liouville integrability is that if a system is classically integrable according to the previous definition, then we can solve the equations of motion by quadrature. This means that it is possible to find a canonical transformation from (q_i, p_i) to action-angle variables (I_i, φ_i), such that the dynamics is trivial in these new coordinates:

$$\dot{I}_i = \{H, I_i\} = 0 \,, \quad \dot{\varphi}_i = \{H, \varphi_i\} = \frac{\partial H}{\partial I_i} = \Omega_i(\{I_j\}) \,. \tag{1.5}$$

One usually refers to the problem of finding the canonical transformation to action-angle coordinates as the direct problem of classical dynamics, whereas the inverse problem consists in re-expressing the latter as functions of the original variables (q_i, p_i) in order to obtain their time-evolution. The inverse problem is usually the more difficult one from the computational point of view, and it is the one which is generalized to the inverse scattering method in classical field theory.

Our main problem is, however, how to decide whether a theory with a given Hamiltonian is integrable in the above sense. There is no general answer to this question, but several techniques are available to find the integrals of motion of the theory. Let us briefly discuss the concept of *Lax pairs*, which is one of the integrability tools most easily generalized to classical field theories and quantum systems. A Lax pair is a couple of d-dimensional square matrices L, M with entries in the functional space $\mathcal{F}$ such that the dynamic of L is given by:

$$\dot{L} = [M, L]\,, \tag{1.6}$$

being $[\cdot\,,\cdot]$ in the right-hand side the usual matrix commutator. With a Lax pair at hand, one can directly construct integrals of motions. For instance, for all $m \in \mathbb{N}$:

$$\frac{\mathrm{d}}{\mathrm{d}t}\,\mathrm{Tr}(L^m) = m\,\mathrm{Tr}\Big(L^{m-1}\dot{L}\Big) = m\,\mathrm{Tr}\big(L^{m-1}[M,L]\big) = \mathrm{Tr}([M,L^m]) = 0\,. \tag{1.7}$$

In particular, if L is diagonalizable, it is not difficult to show that (1.6) implies the conservation of all the d eigenvalues of L (which are not necessarily independent functions of (q_i, p_i)). However, this is not sufficient to have Liouville integrability, as the conserved quantities should be in involution. Let $\mathcal{M}$ be the space of d-dimensional square matrices with entries in $\mathcal{F}$, so that $L, M \in \mathcal{M}$. Then it is possible to show [21] that the condition of mutual involution for the eigenvalues of L is equivalent to the existence of a quantity $r = \sum_{\alpha,\beta} a_\alpha \otimes b_\beta$ with constant entries belonging to the Lie algebra[1] $\mathcal{M} \otimes \mathcal{M}$ such that the following equation holds:

$$[r_{12}\,,\, r_{13}] + [r_{12}\,,\, r_{23}] + [r_{32}\,,\, r_{13}] = 0\,, \tag{1.8}$$

where $r_{12} = \sum_{\alpha,\beta} a_\alpha \otimes b_\beta \otimes \mathbb{1}$, $r_{13} = \sum_{\alpha,\beta} a_\alpha \otimes \mathbb{1} \otimes b_\beta$ and similarly for other indices. If we further require $r_{12} = -r_{21}$ then r is called a classical r-matrix and the previous equation is the classical Yang-Baxter equation, a fundamental constraint which appears in many situations when integrability is at stake. As we will see in the next section, the quantum version of the previous equation is strictly related to the factorizability of the S-matrix in $(1+1)$-dimensional integrable quantum field theories.

As we have previously mentioned, the Lax pair formalism is usually employed to provide conserved quantities in integrable field theories at the classical level [21, 22]. Without enetering into details, we just mention that when dealing with continuously

[1] The Lie-algebraic structure of $\mathcal{M} \otimes \mathcal{M}$ is induced by the Poisson brackets in $\mathcal{F}$.

many degrees of freedom, one usually introduces a non physical *spectral parameter* λ in order to avoid the use of infinite-dimensional matrices. A Lax pair is thus given by two finite-dimensional matrices $L(\lambda)$, $M(\lambda)$ which smoothly depend on λ and such that:

$$\frac{\mathrm{d}}{\mathrm{d}t}L(\lambda) = [M(\lambda), L(\lambda)]\,, \tag{1.9}$$

which implies that $\mathrm{Tr}[L(\lambda)]$ is conserved for every λ. The expansion of $\mathrm{Tr}[L(\lambda)]$ in powers of λ thus provides infinitely many conserved charges which are in involution if a continuous generalization of (1.8) holds.

1.1.2 Quantum spin chains and integrable QFTs

Our main purpose is to provide a sensible definition of integrable quantum field theories. To do so, let us start by considering quantum systems with a finite number of degrees of freedom. In a quantum-mechanical system of finitely-many interacting particles, the phase space is replaced by an Hilbert space $\mathcal{H}$ which in general is infinite-dimensional and does not admit a countable basis if the particles move in a non-compact space. To make things easier, suppose that each particle is "freezed"in a fixed position so that there are only spin degrees of freedom. Assuming that there are N spin-$\frac{1}{2}$ particles lying on a straight line, what we are considering is the (anti-ferromagnetic) Heisenberg XXX quantum spin chain [23], with Hilbert space $\mathcal{H} = (\mathbb{C}^2)^{\otimes N}$ and Hamiltonian:

$$\frac{1}{4}\sum_{j=1}^{N}(\boldsymbol{\sigma}_j \cdot \boldsymbol{\sigma}_{j+1} - 1)\,, \quad \boldsymbol{\sigma}_{N+1} \equiv \boldsymbol{\sigma}_1\,. \tag{1.10}$$

For any finite N, this Hamiltonian is an Hermitean $2^N \times 2^N$ matrix, which is diagonalizable. In the diagonal basis, it is possible to find as much as 2^N other pairwise-commuting diagonal matrices which commute also with H. According to our definition of integrability in classical discrete systems, this model seems integrable (and it is indeed). However, we could in principle build other spin chains with similar properties, and that would suggest that any of these model is integrable. Moreover, they would admit a number of conserved charges larger than the number of degrees of freedom. To avoid this absurd conclusion, we have to provide a different definition of integrability in quantum spin chains, which makes sense in the thermodynamic limit $N \to +\infty$ and is strictly related to the notion of *locality*.

In a quantum chain we say that an operator $\mathcal{O}$ is local if it is supported on a finite number of sites of the chain. More specifically, let $h_j \equiv \boldsymbol{\sigma}_j \cdot \boldsymbol{\sigma}_{j+1}$ be the Hamiltonian density supported on the sites j and $j+1$. This is by definition local. Then we say that the operator $\mathcal{O}_k$, with a support centered on the site k, is local if:

$$[\mathcal{O}_k, h_j] = 0\,, \quad |i-j| \quad \text{large enough}\,, \tag{1.11}$$

where the expression "large enough"is meaningful only in the thermodynamic limit. At this point we say that a quantum spin chain is integrable if as $N \to +\infty$ it admits infinitely many local conserved charges which are pairwise commuting. As it will become clear in the next section, it is essential for integrability techniques that the system has one spatial dimension.

We can now proceed and generalize this definition to quantum field theories. A first way to obtain a QFT is of course through quantization of the corresponding classical field theory. However, renormalization is then necessary to deal with divergences arising from the strong fluctuations of interacting fields. The renormalization procedure can be put on a more solid ground by starting from a well-behaved lattice theory[2] and then taking its scaling limit. This is, roughly speaking, the limit in which the system's size is sent to infinity and at the same same its correlation lenght ξ diverges. Practically this means that if $\mathcal{O}^{(1)}, \mathcal{O}^{(2)}$ are two local operators at lattice sites j_1 and j_2 then we scale the system's size in such a way that $j_1, j_2, \dots \to +\infty$ while all the ratios $j_1/\xi, j_2/\xi, \dots$ are kept finite and constant. In order for the correlator $\langle \mathcal{O}^{(1)} \mathcal{O}^{(2)} \rangle$ to remain finite as $\xi \to +\infty$ we have to multiply it by $\xi^{d_1} \xi^{d_2}$, with d_1 and d_2 appropriate scaling dimensions of the operators. What we obtain in this way is a quantum theory of local fields largely independent on the details of the original lattice model.

In a $(1+1)$-dimensional relativistic QFT, a local conserved charge:

$$Q = \int \mathrm{d}x \, q(x) \tag{1.12}$$

is expressed as the spatial integral of a local density $q(x)$ built solely from fields in the theory and their derivatives at the point x. To make a contact with definition (1.11), we can rephrase the locality condition for the density $q(x)$ by introducing the Hamiltonian density $h(x)$, such that:

$$H = \int \mathrm{d}x \, h(x) \tag{1.13}$$

is the Hamiltonian of the theory. Then we say that $q(x)$ is a local density if:

$$[q(x), h(x')] = 0 \,, \quad |x - x'| \quad \text{space-like} \,. \tag{1.14}$$

We can now formulate a sensible definition of integrable quantum field theories in one spatial dimension: a $(1+1)$-dimensional QFT is integrable if there exist infinitely many pairwise-commuting conserved charges $Q_i = \int \mathrm{d}x \, q_i(x)$ such that the densities $q_i(x)$ are local.

Before turning to the S-matrix description of integrable scattering theories, we mention the fact that two-dimensional conformal field theories are integrable according to

[2]We are thinking of a two-dimensional classical lattice theory or, equivalently, a one-dimensional quantum chain.

our definition[3]. A conformal field theory is a quantum field theory which describes the universality class of a certain critical phenomenon (second-order phase transition), and it is scale-invariant at the local level, *i.e.* it is symmetric under conformal transformations. In two dimensions, invariance under infinitesimal conformal transformations in the complex plane implies the splitting of the theory into an holomorphic and an anti-holomorphic sector. In particular, using complex variables $(z, \bar{z})$, this means that the stress-energy tensor components satisfy:

$$\partial_{\bar{z}} T_{zz} = \partial_z T_{\bar{z}\bar{z}} = 0\,, \tag{1.15}$$

and as a consequence we have the conservation of all the higher-spin charges in the conformal families of T_{zz} and $T_{\bar{z}\bar{z}}$ [26]. One can always build combinations of these charges which are pairwise commuting and therefore a two-dimensional conformal field theory is an integrable quantum field theory.

The interesting question is whether a perturbation of a CFT by one of its relevant operators is still an integrable model. A general criterion, known as "counting argument", was developed by A. B. Zamolodchikov [27] in order to establish when this is the case. We will say something more about integrable deformation of conformal field theories in the next chapter.

1.2 S-matrix theory

We have described how a quantum field theory can be thought of as a scaling limit of a lattice model. In this section, we will consider a different description of integrable QFTs, which relies solely on the scattering data of a given theory. The main ingredients of the S-matrix formalism are the asymptotic scattering states needed to describe the Hilbert space and the transition amplitudes encoding the details of the interactions. The advantage of this approach is that it can be used in a consistent way even when a lagrangian description of the QFT is not available: the latter is a situation of great interest in this thesis, as it is precisely what happens with Zamolodchikov's staircase model, which will be introduced in chapter 3.

The S-matrix description of integrable QFTs is based on some fundamental physical principles:

- short range of the interactions;
- unitarity of time evolution;
- Lorentz invariance of the scattering amplitudes;

[3]We do not provide here an introduction to the vast subject of two-dimensional CFTs. See [24] for a review and [25, 26] for a more exhaustive treatment of this topic.

- causality principle and analyticity.

Let us briefly discuss the implications of these principles in a generic $(d+1)$-dimensional scattering theory, $d \geq 1$.

1.2.1 General properties

The short range of the interactions is necessary in order to define the asymptotic states in the Hilbert space $\mathcal{H}$. If the particles participating in a scattering process are well separated from each other except for a small space-time region in the proximity of the interaction, then off-shell effects can be neglected and for the incoming and outgoing particles the on-shell condition holds:

$$p_\mu p^\mu = m^2 \,. \tag{1.16}$$

In an infinite volume of course both the energy and the spatial momentum eigenvalues form a continuous spectrum, but let us adopt for simplicity the notation $|n\rangle$ to indicate a generic multi-particle state and assume that $\{|n\rangle\}_n$ is a basis for $\mathcal{H}$, so that orthonormality and completeness relations read:

$$\langle m|n\rangle = \delta_{m,n} \,, \quad \sum_n |n\rangle \langle n| = \mathbb{1} \,. \tag{1.17}$$

Let $|\text{in}\rangle$ be the asymptotic state in the remote past $t \to -\infty$ and $|\text{out}\rangle$ the asymptotic state in the remote future $t \to +\infty$, way after the interaction has taken place. The scattering matrix S is the linear operator such that:

$$|\text{out}\rangle = S\,|\text{in}\rangle \ . \tag{1.18}$$

If the scattering theory admits an Hamiltonian description, then S is expressed as the time-ordered exponential:

$$S = \mathcal{T} \exp\left[-i \int_{-\infty}^{+\infty} \mathrm{d}^{d-1}x \, H_{\text{int}}(x)\right] \,, \tag{1.19}$$

from which unitarity immediately follows. However, this property is easily proved even if an Hamiltonian description is not available[4]. Indeed, suppose that the initial state is a normalized linear superposition:

$$|\text{in}\rangle = \sum_n a_n \,|n\rangle \ , \quad \sum_n |a_n|^2 = 1 \,, \tag{1.20}$$

[4]This is for instance the case of the staircase model.

then conservation of probability implies that $|\text{out}\rangle$ must be a normalized superposition of basis states as well. Therefore:

$$1 = \sum_m |\langle m| S |\text{in}\rangle|^2 = \langle \text{in}| S^\dagger S |\text{in}\rangle = \sum_{n,m} a_n^* a_m \langle n| S^\dagger S |m\rangle \ , \tag{1.21}$$

which thanks to (1.20) implies:

$$S^\dagger S = \mathbb{1} \, . \tag{1.22}$$

Concerning the Lorentz invariance principle, this is simply the statement that the transition amplitude between any two states $|n\rangle$, $|m\rangle$ is invariant when the latter are transformed according to some representation $\mathrm{U}(\Lambda)$ of the Lorentz group, that is:

$$\langle m'| S |n'\rangle = \langle m| S |n\rangle \Rightarrow \mathrm{U}^{-1}(\Lambda) S \mathrm{U}(\Lambda) = S \, , \tag{1.23}$$

and therefore the scattering matrix can depend only on Lorentz-invariant quantities.

Let us finally comment on the causality and analyticity principles. Causality is the principle according to which the correlation function of any two physical observables $\mathcal{O}^{(1)}(x_1)$, $\mathcal{O}^{(2)}(x_2)$ vanishes when $|x_1 - x_2|$ is a space-like interval. In ordinary quantum systems, the causality principle allows to extract information on the analytic properties of the transition amplitude thanks to dispersion relations satisfied by the Green functions. However, it is generally very difficult to pin down the analytic structure of the S-matrix in a relativistic scattering theory by relying only on causality. The assumption that one usually makes when dealing with an integrable scattering theory is that the physical transition amplitudes coincide with the real boundary values of meromorphic functions in the complex plane, having a minimum number of singularities dictated by the physical features of the theory, and which can be inferred via a self-consistent bootstrap method [3]. We will come back to this point later on.

1.2.2 Conserved charges and factorization

We can now turn to the case of $(1+1)$-dimensional scattering theories: as it will become clear in a while, this is indeed the only situation where integrability can be fully realized at the quantum level in non-supersymmetric theories. The infinite-dimensional Hilbert space of the theory is specified by assigning the masses $\{m_a, \, a \in I\}$ and the internal charges of all the particle species which enter the asymptotic scattering states, being I the set of particle types. In one spatial dimension, we can parametrize the on-shell energy and momentum of a particle by means of its relativistic rapidity θ:

$$E_a(\theta) = m_a \cosh(\theta) \, , \quad p_a(\theta) = m_a \sinh(\theta) \, , \tag{1.24}$$

so that (1.16) is satisfied. Notice that a generic Lorentz transformation amounts to a translation $\theta \mapsto \theta + \alpha$ and therefore any rapidity difference is Lorentz-invariant.

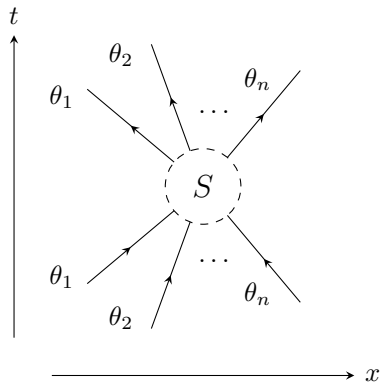

Figure 1.1: Ordering prescription for the rapidities in a n-to-n particle scattering.

The asymptotic states are created by acting on the vacuum $|0\rangle$ with the (bosonic or fermionic) creation operators $A_a^\dagger(\theta)$, and are annihilated by the operators $A_a(\theta)$. A generic n-particle state thus reads:

$$|\theta_1, \dots, \theta_n\rangle_{a_1,\dots,a_n} \equiv A_{a_1}^\dagger(\theta_1) \dots A_{a_n}^\dagger(\theta_n) \, |0\rangle \ . \tag{1.25}$$

Since particles are forced to move on a line and no further interaction can take place as $t \to \pm\infty$, the fastest particle must be at the far right in the remote future and at the far left in the remote past. Thus we adopt the following ordering prescription for the asymptotic states, see figure 1.1:

$$|\theta_1, \dots, \theta_n\rangle_{a_1,\dots,a_n}^{(\text{in/out})} \ , \quad \begin{cases} \theta_1 > \dots > \theta_n \in \mathbb{R} & (\text{in}) \\ \theta_1 < \dots < \theta_n \in \mathbb{R} & (\text{out}) \end{cases} \ . \tag{1.26}$$

The S-matrix elements are now defined by the overlaps between the *in* and *out* states:

$$S_{a_1,\dots,a_n}^{b_1,\dots,b_{n'}}(\theta_1, \dots, \theta_n; \theta'_1, \dots, \theta'_{n'}) = {}_{a_1,\dots,a_n}^{(\text{in})}\langle \theta_1, \dots, \theta_n | \theta'_1, \dots, \theta'_{n'} \rangle_{b_1,\dots,b_{n'}}^{(\text{out})} \ , \tag{1.27}$$

where because of Lorentz invariance (1.23) the left-hand side must be a function of difference rapidities only, $\theta_{ij} = \theta_i - \theta_j$.

In an integrable theory, the presence of infinitely many conserved charges in involution severely constrains the S-matrix. If the theory is relativistic, local conserved charges can always be arranged in such a way that they are labelled by a spin index $s \in \mathbb{Z}$:

$$Q_s = \int_{-\infty}^{+\infty} \mathrm{d}x \, q_s(x) \, , \quad [Q_s, Q_{s'}] = 0 \, , \tag{1.28}$$

with $q_s(x)$ a local density. Of course, not all the possible values of s are present in a given integrable model. These charges are defined so that they act on the asymptotic

states (1.26) as the conserved charges of free theories act on free particle states. That is, they have additive eigenvalues which are well-defined functions of the rapidity and can always be chosen so to commute with internal symmetries. The first charges are by definition the light-cone components of the energy-momentum:

$$Q_{\pm 1} = H \pm P \,, \tag{1.29}$$

so that:

$$Q_{\pm 1} \, |\theta_1, \theta_2, \ldots\rangle^{(\text{in/out})}_{a_1, a_2 \ldots} = \sum_k m_{a_k} e^{\pm \theta_k} \, |\theta_1, \theta_2, \ldots\rangle^{(\text{in/out})}_{a_1, a_2 \ldots} \,, \tag{1.30}$$

and in a similar way the higher-spin local charges act as higher-rank representations of the Lorentz group:

$$Q_s \, |\theta_1, \theta_2, \ldots\rangle^{(\text{in/out})}_{a_1, a_2 \ldots} = \sum_k \chi^{(s)}_{a_k} e^{s\theta_k} \, |\theta_1, \theta_2, \ldots\rangle^{(\text{in/out})}_{a_1, a_2 \ldots} \,. \tag{1.31}$$

Notice that the equation above automatically ensures that the Q_s commute with internal symmetries. For this reason, the numbers $\chi^{(s)}$ are the same for different particle types falling inside a symmetry multiplet.

The consequences on the scattering amplitudes following from the presence of infinitely many conserved charges Q_s are the following:

- no particle production or annihilation can take place: n-to-n' scattering processes are forbidden if $n \neq n'$;
- the set of rapidities must be the same in the incoming and outgoing states, and permutations of rapidities can occur only among particles belonging to a symmetry multiplet, that is:

$$\{\theta_k\} = \{\theta'_k\} \,, \quad \chi^{(s)}_{a_k} = \chi^{(s)}_{a'_k} \quad \text{for} \quad \theta_k = \theta'_k \,; \tag{1.32}$$

- the scattering amplitudes are completely factorizable: every n-to-n S-matrix is expressed as a product of $n(n-1)/2$ two-particle S-matrices.

The first two properties are summarized by saying that in an integrable QFT the scattering is purely elastic. This immediately follows from (1.31). Indeed, by taking the product of both sides of the equations with the *out* state ${}^{(\text{out})}_{a'_1, a'_2, \ldots}\langle \theta'_1, \theta'_2, \ldots|$, one sees that the overlap is non-vanishing iff the following holds:

$$\sum_{k \,\in\, (\text{in})} \chi^{(s)}_{a_k} e^{s\theta_k} = \sum_{k \,\in\, (\text{out})} \chi^{(s)}_{a'_k} e^{s\theta'_k} \,. \tag{1.33}$$

This is an infinite set of equations (one for each value of s present in the theory) which admits (1.32) as unique solution.[5]

To prove factorizability, we will follow an heuristic argument which goes along the line of the more formal proof in [28]. Suppose that the scattering theory is parity-invariant, so that whenever Q_s is a conserved charge also Q_{-s} is such, and consider the odd combination:

$$P_s = Q_s - Q_{-s} \Rightarrow P_s \left|\theta_1, \theta_2, \ldots\right\rangle^{(\text{in/out})}_{a_1,a_2\ldots} = \sum_k \chi^{(s)}_{a_k} \sinh(s\theta_k) \left|\theta_1, \theta_2, \ldots\right\rangle^{(\text{in/out})}_{a_1,a_2\ldots} . \tag{1.34}$$

Assuming for simplicity that all the quantities $\chi^{(s)}_{a_k}$ are of order $\mathcal{O}(1)$ (as is usually the case), the dominant contribution at large rapidities in the right-hand side of the previous equation is the one with the s^{th} power of the particles' momenta p. Thus the action of the operator e^{icP_s}, $c \in \mathbb{R}$, on a localized wavepacket:

$$\psi(x_0, p_0) = \int_{-\infty}^{+\infty} \mathrm{d}p\, e^{-a^2(p-p_0)^2} e^{ip(x-x_0)} , \tag{1.35}$$

is given by:

$$e^{icP_s}\psi(x_0, p_0) \simeq \int_{-\infty}^{+\infty} \mathrm{d}p\, e^{-a^2(p-p_0)^2} e^{ip(x-x_0)} e^{icp^s} \simeq \psi(x_0 - scp_0^{s-1}, p_0) , \tag{1.36}$$

where the second approximate equality follows from a saddle-point evaluation of the integral. Hence we see that when we act with a higher-spin conserved charge on a wavepacket localized around x_0 in position space and p_0 in momentum space, x_0 is shifted by a quantity $\propto p_0^{s-1}$.

If the incoming particles in a scattering event are localized wavepackets, then the application of a higher-spin operators to one of the latter amounts to change the impact parameters of the state, *i.e.* the relative positions of the particles at the interaction time. But as $[Q_s, H] = 0\,, \forall s$, the conserved charges commute with the S-matrix and the transition amplitude is unaffected by this change. Therefore, considering for instance a 3-to-3 scattering process, the three S-matrices corresponding to the configurations in figure 1.2:

$$\begin{cases} S^{b_1,b_2,b_3}_{a_1,a_2,a_3}(\theta_1,\theta_2,\theta_3) & \text{(a)} \\ S^{d,c}_{a_2,a_3}(\theta_2,\theta_3) S^{e,b_3}_{a_1,c}(\theta_1,\theta_3) S^{b_1,b_2}_{e,d}(\theta_1,\theta_2) & \text{(b)} \\ S^{d,c}_{a_1,a_2}(\theta_1,\theta_2) S^{b_1,e}_{d,a_3}(\theta_1,\theta_3) S^{b_1,b_3}_{c,e}(\theta_2,\theta_3) & \text{(c)} \end{cases} \tag{1.37}$$

[5] To prove uniqueness one actually needs a slightly stronger condition, namely that the function $f_{a_k}(\alpha) = \sum_{s>0} e^{-s\alpha} \chi^{(s)}_{a_k}$ has only singular point on the real line, which is the same for every a_k. The quantities $\chi^{(s)}_{a_k}$ are such that this condition holds for every integrable QFT studied so far [22].

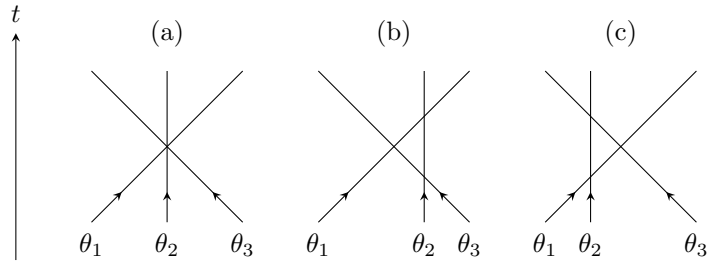

Figure 1.2: Three different configurations for a 3-to-3 scattering corresponding to different impact parameters of the incoming particles. Particle-type indices in the worldlines are omitted for the sake of clarity.

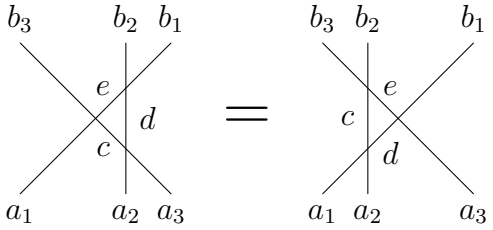

Figure 1.3: Pictorial representation of the quantum Yang-Baxter equation (1.39). The incoming particle a_i has rapidity θ_i, $i = 1, 2, 3$.

must be equal[6], as each configuration can be mapped in any of the other two by displacing the incoming wavepackets with an higher-spin operator. Therefore, we obtain at once the factorization of a 3-to-3 S-matrix into 3 two-body S-matrices:

$$S^{b_1,b_2,b_3}_{a_1,a_2,a_3}(\theta_1,\theta_2,\theta_3) = S^{d,c}_{a_2,a_3}(\theta_2,\theta_3)S^{e,b_3}_{a_1,c}(\theta_1,\theta_3)S^{b_1,b_2}_{e,d}(\theta_1,\theta_2)\,, \tag{1.38}$$

and a consistency relation for the different ways in which the factorization can be performed:

$$S^{d,c}_{a_2,a_3}(\theta_2,\theta_3)S^{e,b_3}_{a_1,c}(\theta_1,\theta_3)S^{b_1,b_2}_{e,d}(\theta_1,\theta_2) = S^{d,c}_{a_1,a_2}(\theta_1,\theta_2)S^{b_1,e}_{d,a_3}(\theta_1,\theta_3)S^{b_1,b_3}_{c,e}(\theta_2,\theta_3)\,. \tag{1.39}$$

This is the celebrated quantum Yang-Baxter equation, represented in figure 1.3). The Yang-Baxter equation appears in both quantum spin chains and integrable QFTs. By exploiting the relation between a one-dimensional quantum system and a two-dimensional classical lattice system [23] it is possible to show that (1.39) is nothing but the quantum version of equation (1.8). Notice that in order to perform the previous manipulations, and in particular to obtain the Yang-Baxter equation, one only needs two higher-spin conserved charges besides energy and momentum. This result was proved by S. Parke in [28].

[6]Sums over repeated indices are understood.

At this point it should be clear why integrable quantum field theories with non trivial scattering amplitudes can exist only in one spatial dimension. In $d > 1$ spatial dimensions particles are not forced to move on a line, and by acting with higher-spin operators on the localized wavepackets, the latter can be displaced in such a way that the particles never collide, so that any scattering can be mapped into a trivial one. This is the renowned Coleman-Mandula theorem [4], stating that the maximal symmetry allowed in a non trivial, non-supersymmetric $(d+1)$-dimensional scattering theory, $d \geq 2$, is the Poincaré group times (possibly) an internal symmetry group.

1.2.3 Two-particle S-matrix: analytic structure and bootstrap principle

Besides the Yang-Baxter equation, the S-matrix must satisfy some simple analytic properties which follow from general QFT principles. Since all the scattering processes are factorizable, we can focus on the analytic structure of the two-particle S-matrix[7]:

$$|\theta_1, \theta_2\rangle^{(\text{in})}_{a_1,a_2} = \sum_{b_1,b_2} S^{b_1,b_2}_{a_1,a_2}(\theta_1, \theta_2)\, |\theta_1, \theta_2\rangle^{(\text{out})}_{b_1,b_2} \,, \tag{1.40}$$

where of course other terms in the sums corresponding to 2-to-n contributions are forbidden by elasticity. The first property, that we have already mentioned, is Lorentz invariance, so that:

$$S^{b_1,b_2}_{a_1,a_2}(\theta_1, \theta_2) = S^{b_1,b_2}_{a_1,a_2}(\theta_{12})\,. \tag{1.41}$$

In terms of (real-valued) rapidities, the unitarity condition follows from the definition (1.40) and orthonormality of the asymptotic states:

$$\sum_{b_1,b_2} S^{b_1,b_2}_{a_1,a_2}(\theta)[S^{c_1,c_2}_{b_1,b_2}(\theta)]^* = \delta^{c_1}_{a_1}\delta^{c_2}_{a_2}\,. \tag{1.42}$$

If the scattering theory is ruled by a time-dependent Hermitean Hamiltonian then there is time-reversal symmetry in the S-matrix:

$$S^{b_1,b_2}_{a_1,a_2}(\theta) = S^{\bar{b}_2,\bar{b}_1}_{\bar{a}_2,\bar{a}_1}(\theta)\,, \tag{1.43}$$

where $\bar{a}$ denotes the antiparticle of a and the exchange of horizontal indices occurs because if a particle is travelling to the right then under time reversal its antiparticle is travelling to the left and vice-versa. In a two-particle scattering, it is possible to express

[7]Notice the different convention with respect to the definition (1.18): it is customary to define the two-particle S-matrix as a map from the outgoing to the incoming states, which would correspond to S^{-1} according to the general definition.

the S-matrix in terms of the Mandelstam variables s, t, u. Let p_1, p_2 be the momenta of the incoming particles and p_3, p_4 the momenta of the outgoing ones. Then:

$$\begin{aligned} s &= (p_1 + p_2)^2 = m_1^2 + m_2^2 + 2m_1 m_2 \cosh(\theta_{12}) \,, \\ t &= (p_1 - p_3)^2 = m_1^2 + m_3^2 - 2m_1 m_3 \cosh(\theta_{13}) \,, \\ u &= (p_1 - p_4)^2 = m_1^2 + m_4^2 - 2m_1 m_4 \cosh(\theta_{14}) \,, \end{aligned} \tag{1.44}$$

where because of elasticity and the ordering conventions $\theta_1 = \theta_4 > \theta_3 = \theta_2$, $m_1 = m_4$, $m_2 = m_3$. This implies that any u-channel contribution is identically vanishing. Furthermore, notice that:

$$s(i\pi - \theta) = t(\theta) \,, \tag{1.45}$$

so that the S-matrix depends only on the Mandelstam variable s.

In the complex s-plane $S(s)$ is a multi-valued function which possesses three branch points at $s = (m_1 - m_2)^2, (m_1 + m_2)^2, \infty$, and it is otherwise a meromorphic function. These branch points are of square-root type, as can be seen by expressing $\theta = \theta(s)$ through the first of equations (1.44), and the corresponding cuts along the real line are the usual u-cut $(-\infty, (m_1 - m_2)^2]$ and s-cut $[(m_1 + m_2)^2, +\infty]$, which start at the threshold energies corresponding to the creation of a particle pair in the u and s-channel respectively. Since in an integrable theory the scattering is purely elastic, there are no further cuts due to higher energy thresholds. The physical sheet is the Riemann sheet lying just above the s-cut, *i.e.* $s = s^+ + i0^+$, $s^+ > (m_1 + m_2)^2$, and the poles of the S-matrix in the real line between the two branch cuts correspond to possible *bound states* of the theory. Indeed, if $(m_1 - m_2)^2 < s^+ < (m_1 + m_2)^2$ the center-of-mass energy is less than the minimum value required to produce a pair of free particles in either the u or the s-channel. Coming back to the rapidity variables, it can be shown from (1.44) and

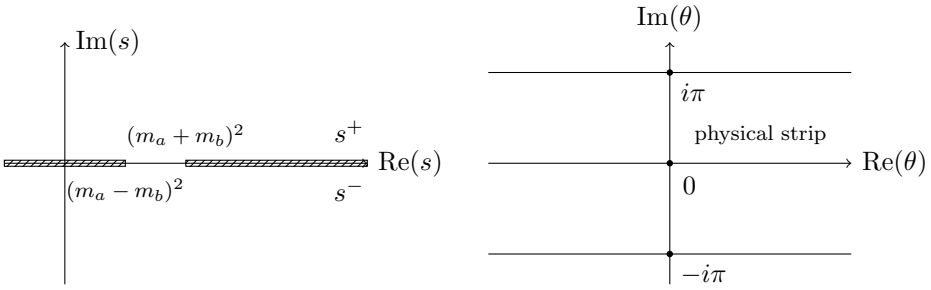

Figure 1.4: Analytic structure of the two-particle S-matrix in the s-plane (left) and θ-plane (right). The strip $\mathrm{Im}(\theta) \in [-i\pi, 0]$ corresponds to the second, unphysical Riemann sheet in the s-plane.

the unitarity condition that, as a function of $\theta \in \mathbb{C}$, $S(\theta)$ is meromorphic with no branch points. The branch points in the s-variable are mapped into the points $\theta = 0, i\pi, \infty$

which are now regular, and the cuts run along the points $\mathrm{Im}(\theta) = 0, \mathrm{Im}(\theta) = \pi$, meeting at infinity. The physical sheet is mapped into the strip $\mathrm{Im}(\theta) \in [0, \pi]$, and the physical bound states lie in the imaginary line within this strip. The analytic structure of S in both the s and the θ-plane is shown in figure 1.4.

An important analytical property of the two-particle scattering matrix is the so-called "Hermitean analyticity"on the physical sheet:

$$[S_{a_1,a_2}^{b_1,b_2}(\theta)]^* = S_{b_2,b_1}^{a_2,a_1}(-\theta^*) \qquad \mathrm{Im}(\theta) \in [0, \pi]\,. \tag{1.46}$$

This is the statement that the complex conjugate of the S-matrix on the physical sheet is the S-matrix evaluated at minus its complex conjugate θ-argument, which is still on the physical sheet. As $\theta \mapsto -\theta^*$ corresponds to $s \mapsto s^*$, in terms of the s-variable we have:

$$[S_{a_1,a_2}^{b_1,b_2}(s)]^* = S_{b_2,b_1}^{a_2,a_1}(s*) \qquad s = s^+ + i0^+\,. \tag{1.47}$$

Furthermore, if the theory is also parity-invariant:

$$S_{a_1,a_2}^{b_1,b_2}(\theta) = S_{a_2,a_1}^{b_2,b_1}(\theta)\,, \tag{1.48}$$

then Hermitean analyticity implies real analyticity on the physical sheet:

$$[S_{a_1,a_2}^{b_1,b_2}(\theta)]^* = S_{b_1,b_2}^{a_1,a_2}(-\theta^*)\,, \tag{1.49}$$

which is combined with unitarity (1.42) to give:

$$\sum_{b_1,b_2} S_{a_1,a_2}^{b_1,b_2}(\theta) S_{b_2,b_1}^{c_2,c_1}(-\theta^*) = \delta_{a_1}^{c_1}\delta_{a_2}^{c_2}\,. \tag{1.50}$$

Notice that in a scattering theory derived from a consistent QFT the simultaneous presence of time-reversal (1.43) and parity symmetry (1.48) implies that the S-matrix is also invariant under charge conjugation, so that there is full CPT-invariance:

$$S_{a_1,a_2}^{b_1,b_2}(\theta) = S_{b_1,b_2}^{a_1,a_2}(\theta)\,. \tag{1.51}$$

Finally, the two-particle S-matrix enjoys a crossing symmetry, *i.e.* it is unaffected by an exchange of space and time directions. This symmetry is encoded in the equivalence (1.45) between the s and t-channel and reads (see figure 1.5):

$$S_{a_1,a_2}^{b_1,b_2}(i\pi - \theta) = S_{\bar{b}_2,a_1}^{\bar{a}_2,b_1}(\theta)\,. \tag{1.52}$$

To conclude our discussion of the analytic properties of two-particle S-matrices, let us turn to the constraints coming from the presence of bound states in the theory. As we have pointed out, the latter are due to simple poles in the physical strip. Suppose that the two-particle matrix $S_{a_1,a_2}^{b_1,b_2}$ has a simple pole at $\theta = iu_{a_1a_2}^k$, with k a label for the

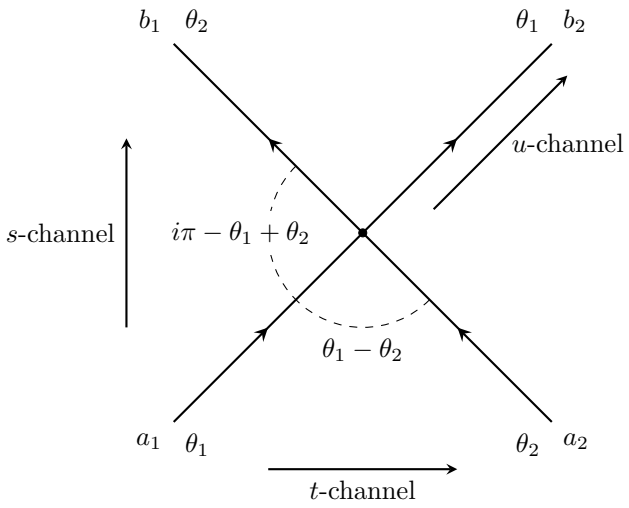

Figure 1.5: Pictorial representation of the available channels in a 2-to-2 scattering event. A rotation $\theta_{12} \mapsto i\pi - \theta_{12}$ maps the s-channel into the t-channel and leaves the S-matrix unchanged.

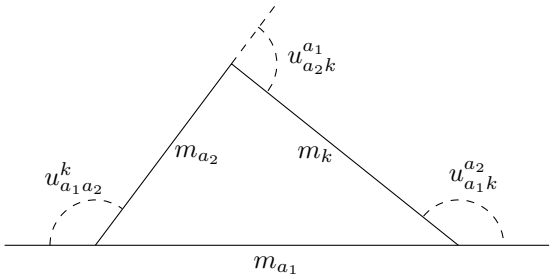

Figure 1.6: Mass triangle and the fusing angles.

bound state. The residue corresponding to this pole must be purely imaginary, so that we can write:

$$S^{b_1,b_2}_{a_1,a_2} \propto i \frac{R^{(k)}}{\theta - i u^k_{a_1 a_2}} \,, \tag{1.53}$$

where $R^{(k)} > 0$ if the process is in the direct channel (a_1 and a_2 are the incoming particles) and $R^{(k)} < 0$ if it is instead in the crossed channel. The mass of the bound state k can be read from the first of equations (1.44):

$$m_k^2 = m_{a_1}^2 + m_{a_2}^2 + 2 m_{a_1} m_{a_2} \cos\big(u^k_{a_1 a_2}\big) \,. \tag{1.54}$$

This is the Carnot relation for a triangle with sides of lengths m_{a_1}, m_{a_2}, m_k, and by looking at figure 1.6 one sees that the angles $u^k_{a_1 a_2}, u^{a_2}_{a_1 k}$ and $u^{a_1}_{a_2 k}$, called *fusing angles*,

must satisfy the geometric relation:

$$u^{k}_{a_1 a_2} + u^{a_2}_{a_1 k} + u^{a_1}_{a_2 k} = 2\pi \,. \tag{1.55}$$

This geometric point of view highlights the presence of a "democracy principle" between elementary scattering particles and bound states of the theory. Indeed, one can regard each of the three fusing angles as the imaginary part of the pole corresponding to the scattering of two of the particles k, a_1, a_2. Proceeding further, one can scatter a bound state with a different elementary particle, looking for other bound states. By requiring that the procedure closes upon itself, one obtains a set of constraints which must be satisfied by the scattering amplitudes. This is the essence of the S-matrix bootstrap approach[3], which allows to determine the location of the poles by considering bound states and elementary particles on the same ground.

1.2.4 The sinh-Gordon S-matrix

Thanks to factorization of multi-particle scattering processes and the analytic properties which must be satisfied by the scattering amplitudes, the problem of finding the S-matrix of an integrable quantum field theory is reduced to that of finding a set of meromorphic functions $S^{b_1,b_2}_{a_1,a_2}(\theta)$ which satisfy:

1. Yang-Baxter equations (1.39);
2. unitarity and Hermitean analyticity (1.50);
3. crossing symmetry (1.52);
4. consistency relations due to bound states.

The solution of this problem is much simpler if the S-matrix is diagonal, *i.e.* there is no exchange of particle types during the scattering:

$$S^{b_1,b_2}_{a_1,a_2} = \delta^{b_1}_{a_1}\delta^{b_2}_{a_2} S_{a_1,a_2} \tag{1.56}$$

as in this case the Yang-Baxter equations are trivially satisfied while unitarity and crossing symmetry relations are simplified as follows:

$$\sum_{a_1,a_2} S_{a_1,a_2}(\theta) S_{a_1,a_2}(-\theta^*) = 1 \,, \quad S_{a_1,a_2}(i\pi - \theta) = S_{\bar{a}_2,a_1}(\theta) \,, \tag{1.57}$$

and the most general solution of these equations can be written as a product of meromorphic functions[29, 3]:

$$S_{a,b}(\theta) = \prod_{x \in \mathcal{A}_{a,b}} \frac{\sinh\left[\frac{1}{2}(\theta + i\pi x)\right]}{\sinh\left[\frac{1}{2}(\theta - i\pi x)\right]} \,, \tag{1.58}$$

being $\mathcal{A}_{a,b}$ a set of complex numbers which can always be chosen to lie in the strip $\mathrm{Re}(x) \in [-1, 1]$. In particular, if $\mathrm{Re}(x) \in [-1, 0]$ there are no poles in the physical strip.

Requiring also that the scattering is neutral, so that every particle coincides with its antiparticle, the solution of (1.57) is:

$$S_{a,b}(\theta) = \prod_{x \in \mathcal{A}_{a,b}} \frac{\tanh\left[\frac{1}{2}(\theta + i\pi x)\right]}{\tanh\left[\frac{1}{2}(\theta - i\pi x)\right]} \,. \tag{1.59}$$

The simplest non-trivial S-matrix having the form above is the celebrated sinh-Gordon S-matrix [30, 2]:

$$S_{shG}(\theta) = \frac{\tanh[\frac{1}{2}(\theta - i\gamma)]}{\tanh[\frac{1}{2}(\theta + i\gamma)]} \,, \tag{1.60}$$

which describes the scattering theory of a single neutral particle. This S-matrix can be obtained via a perturbative expansion from the sinh-Gordon action:

$$S_{\mathrm{shG}} = \int \mathrm{d}^2 x \left[\frac{1}{2}(\partial_\mu \phi)^2 - 2\mu \cosh(\beta\phi)\right] \,, \quad 2\mu = \frac{m_0^2}{\beta^2} \,, \tag{1.61}$$

m_0 being the bare mass of the particle. The coupling constant β is related to the parameter γ in (1.60) via:

$$\gamma = \frac{\beta^2/8}{1 + \beta^2/(8\pi)} < \pi \tag{1.62}$$

from which it immediately follows that there are no bound states in the physical strip.

To conclude, we notice that any solution to the analyticity requirements listed above can be always multiplied by a factor (1.58) if $\mathrm{Re}(x) \in [-1, 0]$, so that no new physical bound states are introduced. This is called a CDD ambiguity factor, and in general it cannot be determined solely from integrability techniques. The sinh-Gordon S-matrix can be regarded as a pure CDD factor.

Chapter 2

Thermodynamics of diagonal scattering theories

In this chapter we present the main technique used to study finite-temperature properties of $(1+1)$-dimensional massive integrable quantum field theories, the thermodynamic Bethe ansatz (TBA). Originally introduced by C.N. Yang and C.P. Yang to derive the thermodynamics of a non-relativistic gas of interacting bosons [8], the TBA approach was soon extended to relativistic integrable QFTs thanks to the works of Al. B. Zamolodchikov [5, 7], T. R. Klassen and E. Melzer [29, 31]. The main idea behind relativistic TBA is that space-time symmetry enforces an equivalence between the finite-size ground state energy of a QFT and the finite-temperature free energy density of the very same theory in an infinite volume. This allows to obtain a set of nonlinear integral equations (TBA equations) which result from the thermodynamic limit of the Bethe quantization condition for the asymptotic states in an integrable theory.

Via the TBA equations, the finite-temperature properties of a massive integrable QFT can be reconstructed once its S-matrix and mass spectrum are known. When the high energy limit is performed, any massive integrable theory in $(1+1)$ dimensions reaches a critical point in Wilson's space of actions where its correlation lenght diverges, that is, a conformal field theory. The scaling free energy of an off-critical theory therefore reproduces the central charge of some CFT in the UV limit: if the massive QFT is obtained as a perturbation of the former via some relevant operator, this limit provides a good consistency check for its bootstrapped S-matrix, which rules the thermodynamics.

We mainly discuss here the thermodynamics of diagonal integrable models, for which the TBA equations can be obtained via a simple and well-established procedure. Moreover, if the diagonal theory is related to a certain affine Lie algebra of the A, D or E series, the TBA equations can be cast in a universal way. However, in the last section of this chapter we also provide a heuristic argument showing how these universal TBA systems can be used to describe the finite-temperature properties of non-diagonal scattering

theories [6, 7, 32, 33].

2.1 Zamolodchikov's mirror argument

Suppose that we have a (1+1)-dimensional integrable QFT confined in a finite volume and we wish to evaluate its ground state energy. The groundbreaking result obtained by Al. B. Zamolodchikov is that this is equivalent to obtain the finite-temperature free energy of the theory in the thermodynamic limit. The argument goes as follows. Assume that the theory is defined on a cylinder with periodic boundary conditions in both directions, that is, on a torus generated by two circumferences $\mathcal{C}_L$, $\mathcal{C}_R$ of lengths L and R respectively, as in figure 2.1. Thanks to relativistic invariance, we can choose the time direction to be either along $\mathcal{C}_L$ or $\mathcal{C}_R$, obtaining two different but equivalent quantization schemes.

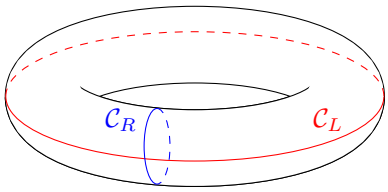

Figure 2.1: Toroidal geometry of the mirror argument.

Let x be the coordinate in the direction of $\mathcal{C}_R$ and y the coordinate along the direction of $\mathcal{C}_L$. The stress-energy tensor of the theory is $T_{\mu\nu}$. We can proceed in two way:

- if y is the time coordinate and x the space coordinate, then the time evolution is ruled by the Hamiltonian:
$$H_R = \frac{1}{2\pi}\int_{\mathcal{C}_R} \mathrm{d}x\, T_{yy} \tag{2.1}$$
and the corresponding quantization scheme is called "L-channel"quantization

- if instead we take y to be the space coordinate and $-x$ the time coordinate[1] then the Hamiltonian is:
$$H_L = \frac{1}{2\pi}\int_{\mathcal{C}_L} \mathrm{d}y\, T_{xx} \tag{2.2}$$
and now the quantization scheme is the "R-channel"one.

[1]The minus sign is chosen to preserve the relative orientation of the axis when we switch from one channel to the other.

Let $\mathcal{Z}(L,R)$ the partition function of the theory, with L and R both finite. Then we can equivalently write:

$$\mathcal{Z}(L,R) = \mathrm{Tr}_{\mathcal{H}_R}\, e^{-LH_R} = \mathrm{Tr}_{\mathcal{H}_L}\, e^{-RH_L} \tag{2.3}$$

where $\mathcal{H}_R$ and $\mathcal{H}_L$ are the Hilbert spaces of states living in $\mathcal{C}_R$ and $\mathcal{C}_L$ respectively. If we choose to quantize the theory in the L-channel then the limit $L \to +\infty$ corresponds to sending the (euclidean) time to infinity and therefore the trace is projected down to the ground state:

$$\mathcal{Z}(L,R) = \mathrm{Tr}_{\mathcal{H}_R}\, e^{-LH_R} \underset{L\to\infty}{\simeq} e^{-LE_0(R)} \tag{2.4}$$

On the other hand, if one chooses the R-channel scheme then $L \to +\infty$ corresponds to a thermodynamic limit and the euclidean time R, which is now periodic, is to be identified with the inverse temperature of the system, $R = \frac{1}{T}$. Thus:

$$\mathcal{Z}(L,R) = \mathrm{Tr}_{\mathcal{H}_L}\, e^{-RH_L} = \sum_n e^{-RE_n(L)} \underset{L\to\infty}{\simeq} e^{-RLf(R)} \tag{2.5}$$

where $E_n(L)$ are the discretized energy levels on the finite volume and $f(R)$ is the free energy per unit density at inverse temperature R. Therefore in the limit $L \gg R$ we obtain:

$$E_0(R) = Rf(R)\,. \tag{2.6}$$

This is the fundamental relation between the ground state energy in a finite volume (right-hand side) and the free energy density in the thermodynamic limit at finite temperature.

2.2 Derivation of the thermodynamics

We can now develop the thermodynamics of the theory by making use of the mirror argument. In the following we will work in the R-channel, as if L is large enough to neglect short-distance processes between particles then it is possible to obtain a basis of asymptotic states (Bethe states) which allows in principle to compute the sum in (2.5). In the case of a diagonal scattering theory this is done by means of a very simple procedure known as *coordinate Bethe ansatz*

2.2.1 Coordinate Bethe ansatz

Let us consider a $(1+1)$-dimensional diagonal scattering theory defined on a circle of lenght L. The spectrum of the theory consists of N particles of different species labelled by $a = 1, \dots, n$, with $\sum_{a=1}^{n} N_a = N$. Let m_a, $a = 1, \dots, n$ be the masses of the various species and define the correlation lenght through $\xi = 1/m_1$, m_1 being by convention the lowest mass in the spectrum.

Since the theory is diagonal, we can specify the interactions via the scattering phases δ_{ab} entering the two-particle S-matrices via $S_{ab}(\theta) \equiv e^{i\delta_{ab}(\theta)}$, θ being as usual the rapidity difference between the two particles involved. We are interested in the asymptotic regions in which the particles are well separated from each other, that is:

$$|x_i - x_{i+1}| \gg \xi\,, \quad i = 1, \dots, N-1 \tag{2.7}$$

there are $N!$ such regions in the total Hilbert space of the system, corresponding to the possible permutations of the positions x_i, and in every asymptotic region we can neglect any short-distance effect therein, so that the particles are on-shell and the multi-particle state is represented in position space by a plane wave:

$$\Psi(x_1, \dots, x_N) = \prod_{j=1}^{N} e^{ip_j x_j} \sum_{\mathcal{P}\in\mathcal{S}_N} A(\mathcal{P})\Theta(x_{\mathcal{P}})\,, \tag{2.8}$$

were the amplitude A only depends on the permutation $\mathcal{P}$ of the particle positions and:

$$\Theta(x_{\mathcal{P}}) = \begin{cases} 1 & , \quad \text{if } x_{\mathcal{P}_1} < \dots < x_{\mathcal{P}_N} \\ 0 & , \quad \text{otherwise} \end{cases}\,. \tag{2.9}$$

Exchanging the positions of two adjacent particles results in a modification of the amplitude due to the acquisition of a scattering phase, so that if $\mathcal{P} = (\dots, i, j, \dots)$ and $\mathcal{P}' = (\dots, j, i, \dots)$ then:

$$A\left(\mathcal{P}'\right) = S_{ij}(\theta_i - \theta_j) A\left(\mathcal{P}\right) \tag{2.10}$$

the quantization condition for the particles' momenta comes from the periodic (antiperiodic) boundary conditions, which must be imposed if the particles are bosons (fermions):

$$\Psi(\dots, x_i = L, \dots) = (-1)^{F_i}\Psi(\dots, x_i = 0, \dots)\,, \quad i = 1, \dots N \tag{2.11}$$

with $(-1)^{F_i} = \pm 1$ if the i^{th} particle is a boson (upper sign) or a fermion (lower sign). Using (2.8) the equation above reads:

$$\begin{aligned} A(i, \mathcal{P}_2, \dots, \mathcal{P}_N) &= (-1)^{F_i} e^{ip_i L} A(\mathcal{P}_2, \dots, \mathcal{P}_N, i) \\ &= (-1)^{F_i} e^{ip_i L} \left(\prod_{j\neq i} S_{ij}(\theta_i - \theta_j) \right) A(i, \mathcal{P}_2, \dots, \mathcal{P}_N)\,, \quad i = 1, \dots, N \end{aligned} \tag{2.12}$$

where $\mathcal{P}$ is any permutation in $\mathcal{S}_N$ such that $\mathcal{P}_1 = i$. Since the particles are on-shell we can parametrize their relativistic momenta using rapidities:

$$(E_i\,,\, p_i) = (m_i \cosh(\theta_i)\,,\, m_i \sinh(\theta_i)) \tag{2.13}$$

so that the quantization condition becomes

$$e^{im_i \sinh(\theta_i)} \prod_{j \neq i} S_{ij}(\theta_i - \theta_j) = (-1)^{F_i} \tag{2.14}$$

or equivalently, taking the logarithm and using $\delta_{ij}(\theta) = -i \ln S_{ij}(\theta)$:

$$Lm_i \sinh(\theta_i) + \sum_{j \neq i} \delta_{ij}(\theta_i - \theta_j) = 2\pi n_i \,, \quad i = 1, \ldots, N \tag{2.15}$$

with $n_i \in \mathbb{Z}$ if the i^{th} particle is a boson and $n_i \in \mathbb{Z} + \frac{1}{2}$ if it is a fermion.

Equation (2.15) is known as the coordinate Bethe ansatz equation, and directly follows from the plane-wave form of the asymptotic wavefunction in the space of coordinates. Notice that if all the interactions are trivial, *i.e.* $S_{ij}(\theta) = 1$ for all i, j, then the previous condition reduces to the usual momentum quantization condition for a particle in a box, $p_i = 2\pi n_i / L$.

The quantum numbers n_i specify the admissible rapidities, and for several specific models one can show that the solution is unique for every set $\{n_i\}$ of pairwise distinct numbers and that the totality of the resulting states form a basis for the interacting Hamiltonian. We will assume the latter condition as an hypothesis. However, there is an additional constraint on the possible values of the n_i which is due to the structure of the interaction. Indeed, unitarity of the S-matrix implies that for any particle species a it must be $S_{aa}^2(0) = 1$. This means that there are two possibilities:

1. $S_{aa}(0) = -1$. If there are two particles of the same species with the same rapidity, the wavefunction is antisymmetric under the exchange of their coordinates. If the species a is bosonic, this is incompatible with the statistics and the integers[2] $n_i^{(a)}$ must be all distinct. If instead the species a is fermionic, there are no restrictions on the values of the half-integers $n_i^{(a)}$. Therefore, in this case, bosons behave like fermions and fermions behave like bosons.

2. $S_{aa}(0) = 1$. This is the opposite situation: bosons can occupy each rapidity state in an arbitrary number and fermions are subject to an exclusion principle.

This shows the deep interplay between statistics and dynamics in one spatial dimensions, where it is impossible to exchange the positions of two particles without making them scatter against each other. In the TBA context, we therefore define the type of the particle species a in the following way:

$$t_a \equiv -(-1)^{F_a} S_{aa}(\theta = 0) = \begin{cases} +1 & , \quad \text{fermionic type} \\ -1 & , \quad \text{bosonic type} \end{cases} \tag{2.16}$$

[2]The superscript here designates the subset of $\{n_i\}_{i=1}^N$ relative to the species a.

In the following we will concentrate on fermionic-type particles. Once the Bethe equations (2.15) are solved for a given set $\{n_i\}$, the resulting multi-particle state $|\theta_1, \dots, \theta_N\rangle$ is an asymptotic eigenstate of the Hamiltonian, with total energy and momentum given by:

$$E(\{\theta_i\}) = \sum_{i=1}^{N} m_i \cosh(\theta_i), \quad p(\{\theta_i\}) = \sum_{i=1}^{N} m_i \sinh(\theta_i) \tag{2.17}$$

2.2.2 Ground state energy in the thermodynamic limit

Let us now derive the finite-temperature free energy of the system in the thermodynamic limit:

$$L \to \infty, \quad N \to \infty, \quad N/L \text{ fixed} \tag{2.18}$$

considering for simplicity the case in which all the N particles are of the same species (fermionic) with mass m. As the volume increases, the difference between two consecutive rapidities in the spectrum behaves as $|\theta_i - \theta_{i+1}| \sim 1/mL$ so that the occupied Bethe quantum numbers condense into a continuous distribution $\rho_p(\theta)$ of occupied states in the rapidity space. By definition, this particle density[3] is such that the number of particles with rapidity in the interval $[\theta, \theta + \Delta\theta]$ is given by $L\rho_p(\theta)(\theta)\Delta\theta$, and thus the discrete sum over occupied rapidities is replaced by an integral (here and below, all the integrations are over $\mathbb{R}$ unless otherwise specified):

$$\sum_i f(\theta_i) \underset{\text{TD}}{\longrightarrow} L \int \mathrm{d}\theta \, f(\theta)\rho_p(\theta) \tag{2.19}$$

this allows one to rewrite the total energy (2.17) as a linear functional of $\rho_p(\theta)$:

$$E[\rho_p(\theta)] = Lm \int \cosh(\theta)\rho_p(\theta)\mathrm{d}\theta \tag{2.20}$$

and the quantization condition (2.15) becomes:

$$m \sinh(\theta_i) + \int \delta(\theta_i - \theta)\rho_p(\theta)\mathrm{d}\theta = \frac{2\pi}{L} n_i, \quad i = 1, \dots, N. \tag{2.21}$$

Not all the allowed states n_i in the right-hand side of the previous equation are necessarily filled with particles: it is customary to introduce a density of *holes* (per unit of lenght and rapidity) $\rho_h(\theta)$, so that $L[\rho_p(\theta) + \rho_h(\theta)]\Delta\theta$ is the total number of Bethe states (occupied and unoccupied) in the rapidity interval $[\theta, \theta + \Delta\theta]$. To be more precise, let us define a counting function:

$$J(\theta) \equiv \frac{m}{2\pi} \sinh(\theta) + \frac{1}{2\pi}(\delta * \rho_p)(\theta) \tag{2.22}$$

[3]The distribution $\rho_p(\theta)$ is sometimes called *root density*, to highlight the fact that it is obtained as a limiting density of solutions of the Bethe equation.

where the symbol * stands for a convolution:

$$(f * g)(\theta) \equiv \int \mathrm{d}\theta' f(\theta - \theta') g(\theta') = (g * f)(\theta) \,. \tag{2.23}$$

By construction $J(\theta_i) = n_i/L$, so that using the counting function we can associate to each density $\rho_p(\theta)$ in the space of rapidities a distribution in the lattice $\mathbb{Z}/L$ of Bethe quantum numbers. By taking the derivative of equation (2.22) with respect to θ, one obtains therefore a constraint relating the densities of holes and particle in the thermodynamic limit:

$$\frac{\mathrm{d}}{\mathrm{d}\theta} J(\theta) = \rho_p(\theta) + \rho_h(\theta) = \frac{m}{2\pi} \cosh(\theta) + \frac{1}{2\pi} (\phi * \rho_p)(\theta) \tag{2.24}$$

where the kernel $\phi(\theta)$ has been introduced as the logarithmic derivative of $S(\theta)$:

$$\phi(\theta) \equiv \frac{d}{\mathrm{d}\theta} \delta(\theta) = -i \frac{d}{\mathrm{d}\theta} \ln S(\theta) \tag{2.25}$$

at this point, in order to obtain the physical distributions $\rho_p(\theta)$, $\rho_h(\theta)$ at thermal equilibrium it is sufficient to minimize the free energy functional[4]:

$$F[\rho_p, \rho_h] = E[\rho_p] - TS[\rho_p, \rho_h] = E[\rho_p] - \frac{1}{R} S[\rho_p, \rho_h] \tag{2.26}$$

subject to the constraint (2.24). The total entropy S of the (fermionic) system can be easily evaluated. In fact, if we consider a rapidity interval $[\theta_i, \theta_i + \Delta\theta]$ such that $(mL)^{-1} \ll \Delta\theta \ll 1$ (*i.e.* we are looking at the mesoscopic scale of the system), then we can reshuffle the $n_i \sim L\rho_p(\theta_i)\Delta\theta$ particles and the $m_i \sim L\rho_h(\theta_i)\Delta\theta$ holes in the interval without changing the macroscopic energy (2.20) of the system. Since we are considering a fermionic species the number of ways in which this can be done is:

$$\Omega_i = \frac{(n_i + m_i)!}{n_i!\, m_i!} \tag{2.27}$$

and therefore the total entropy is given by:

$$S[\rho_p, \rho_h] = \lim_{\mathrm{TD}} \prod_i \ln \Omega_i = L \int \mathrm{d}\theta \left[(\rho_p + \rho_h) \ln(\rho_p + \rho_h) - \rho_p \ln \rho_p - \rho_h \ln \rho_h \right] . \tag{2.28}$$

In order to enforce the Bethe constraint (2.24) let us define:

$$\Phi[\rho_p, \rho_h] \equiv L \int \mathrm{d}\theta \left[\rho_p(\theta) + \rho_h(\theta) - \frac{m}{2\pi} \cosh(\theta) - \frac{1}{2\pi} (\phi * \rho_p)(\theta) \right] \tag{2.29}$$

[4]Recall that we are working in the R-channel, so that R is identified as the system's inverse temperature.

the functional to minimize is then $F - \lambda\Phi$, with λ a Lagrange multiplier. Equation (2.24) is automatically recovered imposing $\frac{\delta(F-\lambda\Phi)}{\delta\lambda} = 0$, while the other two functional equations read:

$$\frac{\delta(F-\lambda\Phi)}{\delta\rho_p} = L\int \mathrm{d}\theta \left[m\cosh(\theta) - \frac{1}{R}\ln\left(\frac{\rho_p+\rho_h}{\rho_p}\right) + \frac{1}{2\pi}(\phi * \lambda)(\theta) - \lambda\right] \doteq 0 \tag{2.30}$$

$$\frac{\delta(F-\lambda\Phi)}{\delta\rho_h} = -L\int \mathrm{d}\theta \left[\frac{1}{R}\ln\left(\frac{\rho_p+\rho_h}{\rho_h}\right) + \lambda\right] \doteq 0 \tag{2.31}$$

solving (2.31) for λ and substituting the result into (2.30), one obtains:

$$mR\cosh(\theta) + \ln\left(\frac{\rho_p}{\rho_h}\right) - \frac{1}{2\pi}\left[\phi * \ln\left(\frac{\rho_p+\rho_h}{\rho_h}\right)\right](\theta) = 0\,. \tag{2.32}$$

We notice that the above equation involves only the ratio between the densities of particles and holes, as a consequence of the fact that the trace in (2.3) is over the full Hilbert space of the theory, *i.e.* $\mathcal{Z}(L,R)$ is the grand-canonical partition function at zero chemical potential. Let us therefore define the system's *pseudoenergy* $\varepsilon(\theta)$ and the related occupation function $n(\theta)$:

$$\varepsilon(\theta) \equiv -\ln\left(\frac{\rho_p}{\rho_h}\right), \quad n(\theta) = \frac{\rho_p}{\rho_p+\rho_h} = \frac{1}{1+e^{\varepsilon(\theta)}} \tag{2.33}$$

so that the equation (2.32) becomes:

$$\varepsilon(\theta) = mR\cosh(\theta) - \frac{1}{2\pi}\left[\phi * \ln\left(1+e^{-\varepsilon}\right)(\theta)\right] \tag{2.34}$$

this is the celebrated thermodynamic Bethe ansatz (TBA) equation [5, 29, 31] for a system of interacting fermions at inverse temperature R, where the interaction is encoded in the kernel ϕ. It is a self-consistency nonlinear integral equation which, once solved, allows one to express all the thermodynamic observables through the densities ρ_p and ρ_h. In particular, having solved the TBA equation we are finally able to evaluate the free energy at thermal equilibrium. To do so, first integrate (2.34) against $\rho_p(\theta)\mathrm{d}\theta$ and use the constraint (2.24) to obtain:

$$\begin{aligned}&\int \mathrm{d}\theta\, \rho_p(\theta)[Rm\cosh(\theta - \varepsilon(\theta)] \\ &= \int \frac{\mathrm{d}\theta}{2\pi}\ln\left(1+e^{-\varepsilon}\right)\left\{2\pi\left[\rho_p(\theta)+\rho_h(\theta)\right] - m\cosh(\theta)\right\}\end{aligned} \tag{2.35}$$

from the definition of the free energy functional (2.26) and writing $F(R) = Lf(R)$ we

have:

$$\begin{aligned} Rf(R) = \frac{R}{L}F(R) &= \frac{1}{L}(RE - S) \\ &= Rm\int \mathrm{d}\theta\, \cosh(\theta)\rho_p(\theta) - \int \mathrm{d}\theta\, [\rho_p \ln(1+e^{\varepsilon}) + \rho_h \ln\left(1+e^{-\varepsilon}\right)] \\ &= \int \mathrm{d}\theta\, [Rm\cosh(\theta) - \varepsilon(\theta)]\,\rho_p(\theta) - \int \mathrm{d}\theta\, (\rho_p+\rho_h)\ln\left(1+e^{-\varepsilon}\right)] \end{aligned} \tag{2.36}$$

finally, plugging (2.35) into the previous formula one obtains the expression for the equilibrium free energy density at temperature $1/R$, which coincides with the ground state energy $E_0(R)$ thanks to equation (2.6):

$$E_0(R) = Rf(R) = -\int \frac{\mathrm{d}\theta}{2\pi} m\cosh(\theta) L(\theta) \tag{2.37}$$

where we have defined:

$$L(\theta) \equiv \ln\left(1+e^{-\varepsilon(\theta)}\right). \tag{2.38}$$

Of course the same procedure can be carried out for bosonic-type particles (*i.e.* true bosons with $S(0) = 1$ or fermions with $S(0) = -1$). In that case relations (2.22) and (2.24) still hold as well as expression (2.20) for the total energy, but the entropy functional is modified according to the fact that multiple occupations are now possible. The bosonic TBA equation and the bosonic ground state energy read:

$$\varepsilon(\theta) = mR\cosh(\theta) + \frac{1}{2\pi}\left[\phi * \ln\left(1-e^{-\varepsilon}\right)(\theta)\right] \tag{2.39}$$

$$E_0(R) = +\int \frac{\mathrm{d}\theta}{2\pi} m\cosh(\theta)\ln\left(1-e^{-\varepsilon(\theta)}\right). \tag{2.40}$$

However, there are reasons to believe that the only consistent interacting theories in the TBA context are those of fermionic-type particles. The problem with the bosonic TBA equation comes from the term $\ln\left(1-e^{-\varepsilon(\theta)}\right)$: when varying the temperature the argument may become negative in a certain rapidity interval, and that would lead to complex solutions, which have no sound physical interpretation.

The generalization to purely diagonal scattering theories with n fermionic species of particles and a non-degenerate mass-spectrum m_a, $a = 1, \ldots, n$, is straightforward. Let $S_{ab}(\theta) = S_{ba}(\theta)$ the S-matrix elements and

$$\phi_{ab}(\theta) \equiv -i\frac{d}{d\theta}S_{ab}(\theta), \quad a, b = 1, \ldots, n. \tag{2.41}$$

If the theory is purely elastic, $\phi_{ab}(\theta) = \phi_{ab}(-\theta)$ as a consequence of unitarity. There is one TBA equation for each particle species:

$$\varepsilon_a(\theta) = \hat{m}_a\beta\cosh(\theta) - \frac{1}{2\pi}\sum_{a=1}^{n}(\phi_{ab} * L_b)(\theta) \tag{2.42}$$

where $L_a(\theta) \equiv \ln\left(1+e^{-\varepsilon_a(\theta)}\right)$, $\hat{m}_a \equiv m_a/m_1$ and the dimensionless inverse temperature $\beta = m_1 R$ has been introduced. the ground state energy is additive and simply given by:

$$E_0(R) = -\sum_{a=1}^{n} m_a \int \frac{d\theta}{2\pi} \cosh(\theta) L_a(\theta) \tag{2.43}$$

As a concluding remark, we notice that because of the very special role of the ground state energy in the mirror correspondence (2.6), the previous derivation does not allow one to obtain the excited states in the theory. The latter can nonetheless be obtained via other methods, as was first noticed in [34], were a method based on the analytic continuation of some of the system's parameter was proposed.

2.3 Infrared and ultraviolet limits

The correlation lenght of the theory on the torus is by definition the reciprocal of the lowest mass in its spectrum. Therefore if one works in the R-channel the ultraviolet and the infrared limits of the theory are obtained by sending $\beta \to 0$ and $\beta \to \infty$ respectively, $\beta \equiv m_1 R$. In the UV limit the theory should reproduce a certain conformal field theory, and it is possible to show from CFT first principles (see for instance [26]) that for the ground state energy it holds:

$$\lim_{\beta\to 0} E_0(R) = \frac{2\pi}{R}\left(\Delta_{\text{min}} + \bar{\Delta}_{\text{min}} - \frac{c}{12}\right) \tag{2.44}$$

where Δ_{min} and $\bar{\Delta}_{\text{min}}$ are the lowest conformal weights of the CFT and c its central charge. It is therefore useful to introduce a dimensionless scaling function $c(\beta)$ via:

$$E_0(R) \equiv -\frac{\pi c(\beta)}{6R} \tag{2.45}$$

so that in a theory[5] with $\Delta_{\text{min}} = \bar{\Delta}_{\text{min}}$ one has:

$$\lim_{\beta\to 0} c(\beta) = c_{\text{eff}} \equiv c - 24\Delta_{\text{min}} \tag{2.46}$$

that is, in the UV limit the scaling function of an integrable theory reproduces the effective central charge of the underlying conformal field theory. The expression of $c(\beta)$ in terms of the particles' pseudoenergies follows from (2.43):

$$c(\beta) = \frac{3}{\pi^2}\beta \sum_{a=1}^{n} \hat{m}_a \int_{-\infty}^{+\infty} \mathrm{d}\theta \, \cosh(\theta) L_a(\theta)\,. \tag{2.47}$$

[5]This is for instance the case when the primary fields are scalars.

Since the pseudoenergies -and therefore the functions $L_a(\theta)$- are fixed exclusively by the integrable dynamics contained in the kernels ϕ_{ab}, the fact that the scaling function correctly reproduces the effective central charge of the CFT in the UV limit is a good check of the correctness of the S-matrix obtained via bootstrap methods.

Let us now study in detail the UV and the IR limit of the scaling function, starting from the latter. As $\beta \to \infty$ the driving term in each TBA equation (2.42) is dominant over the convolution:

$$\varepsilon_a(\theta) = \hat{m}_a \beta \cosh(\theta) + \mathcal{O}(e^{-\beta}) \tag{2.48}$$

so that (using the fact that $\varepsilon_a(\theta) = \varepsilon_a(-\theta)$ and thus $L_a(\theta) = L_a(-\theta)$):

$$\lim_{\beta\to\infty} c(\beta) = \frac{6}{\pi^2}\beta \sum_{a=1}^{n} \hat{m}_a \int_0^{+\infty} \mathrm{d}\theta \, \cosh(\theta) e^{-\beta \hat{m}_a \cosh(\theta)} \left[1 + \mathcal{O}(e^{-\beta})\right] \tag{2.49}$$

$$= \frac{6}{\pi^2}\beta \sum_{a=1}^{n} \hat{m}_a K_1(\hat{m}_a \beta) + \mathcal{O}(e^{-2\beta}) \tag{2.50}$$

where K_1 is a modified Bessel function, exponentially dumped as $\beta \to \infty$. This is consistent with the fact that in the infrared regime the theory reduces to a collection of free massive particles, for which trivially $c = 0$.

To study the UV limit $\beta \to 0$ we shall consider here models for which the functions $\phi_{ab}(\theta)$ are peaked at $\theta = 0$ and rapidly decrease when $|\theta|$ increases. This is the most common scenario, which occurs whenever the S-matrices $S_{ab}(\theta)$ are given by products of minimal blocks with no extra CDD factors. If the kernels are peaked about the origin in the rapidity axis, as $\beta \to 0$ the pseudoenergies $\varepsilon_a(\theta)$ develop a plateau in the region $-\ln(2/\beta) \ll \theta \ll \ln(2/\beta)$, while tend to the asymptotic free values (2.48) for $|\theta| \gg \ln(2/\beta)$[6], see for instance the first plot in figure 3.4. The constant pseudoenergies ε_a are solutions of the following coupled transcendental equations:

$$\varepsilon_a = \sum_{a=1}^{n} N_{ab} \ln(1 + e^{-\varepsilon_b}) \tag{2.51}$$

where:

$$N_{ab} \equiv -\frac{1}{2\pi} \int_{-\infty}^{+\infty} \mathrm{d}\theta \, \phi_{ab}(\theta) = -\frac{1}{2\pi}[\delta_{ab}(+\infty) - \delta_{ab}(-\infty)] \tag{2.52}$$

is a matrix which is symmetric and positive definite in the models we are considering[7].

Along the edges of the plateau, *i.e.* along the *kinks* connecting the constant values ε_a to the asymptotic pseudoenergies, the TBA driving terms can be approximated as:

$$\hat{m}_a \beta \cosh(\theta) \simeq \frac{1}{2}\hat{m}_a \beta e^{\theta} = \hat{m}_a e^{\left(\theta - \ln\frac{2}{\beta}\right)} \tag{2.53}$$

[6] To see this, derive equation (2.42) with respect to θ and notice that $\beta \sinh(\theta) \to 0$ as $\beta \to 0$ whenever $|\theta| < \ln(2/\beta)$.

[7] With the very relevant exception of the the sinh-Gordon model, where $N \equiv N_{11} < 0$.

and the behaviour at the edges of the plateau is dictated by the universal kink TBA equations:

$$\tilde{\varepsilon}_a(\theta) = \frac{1}{2}\hat{m}_a\beta e^{\theta} - \frac{1}{2\pi}\sum_{b=1}^{n}(\phi_{ab} * \tilde{L}_b)(\theta) \tag{2.54}$$

where $\tilde{L}_a(\theta) \equiv \ln\left(1 + e^{-\tilde{\varepsilon}_a(\theta)}\right)$ and the kink pseudoenergies $\tilde{\varepsilon}_a$ assume the constant values ε_a for $\theta \ll \ln(2/\beta)$. The advantage of introducing these quantities lies in the fact that they only significantly differ from the pseudoenergies $\varepsilon_a(\theta)$ when $\theta \lesssim -\ln(2/\beta)$ and their dependence on β is trivial: it only amounts to a shift of θ to the right by $\ln(2/\beta)$. In terms of $\tilde{L}_a(\theta)$ the ultraviolet limit of the scaling function reads:

$$c(0) = \frac{6}{\pi^2}\lim_{\beta\to 0}\sum_{a=1}^{n}\int_0^{+\infty} \mathrm{d}\theta\, \tilde{L}_a(\theta)\frac{1}{2}\hat{m}_a\beta e^{\theta} \tag{2.55}$$

where we took advantage of the parity of $L_a(\theta)$ to reduce the integration domain in (2.47). The integral in the right-hand side of the previous equation can be evaluated as follows:

$$\begin{aligned} c(0) &= \frac{6}{\pi^2}\sum_{a=1}^{n}\int_0^{+\infty} \mathrm{d}\theta\, \tilde{L}_a(\theta)\left[\frac{d\tilde{\varepsilon}_a}{\mathrm{d}\theta} - \frac{1}{2\pi}\sum_{b=1}^{n}\left(\phi_{ab} * \frac{e^{-\tilde{\varepsilon}_b}}{1+e^{-\tilde{\varepsilon}_b}}\frac{d\tilde{\varepsilon}_b}{\mathrm{d}\theta}\right)(\theta)\right] \\ &= \frac{6}{\pi^2}\sum_{a=1}^{n}\left[\int_{\varepsilon_a}^{+\infty} \mathrm{d}\varepsilon\, \ln\left(1+e^{-\varepsilon}\right) + \frac{1}{2}\varepsilon_a \ln\left(1+e^{-\varepsilon_a}\right)\right] \\ &= \frac{6}{\pi^2}\sum_{a=1}^{n}\mathcal{L}\left(\frac{1}{1+e^{\varepsilon_a}}\right) \end{aligned} \tag{2.56}$$

in the first line we used the derivative of equation (2.54) with respect to θ to substitute $\frac{1}{2}\hat{m}_a\beta e^{\theta}$. The second line follows from a simple change of variable in the first term of the integral, where for the second term one has to exchange the convolution order, use equation (2.54) and then perform two integration by parts. In the third line we used the definition of Roger's Dilogarithm:

$$\mathcal{L}(z) \equiv -\frac{1}{2}\int_0^z \mathrm{d}t\, \left(\frac{\ln(1-t)}{t} + \frac{\ln(t)}{1-t}\right) \tag{2.57}$$

and the relation:

$$\mathcal{L}\left(\frac{1}{1+x}\right) = \mathrm{Li}_2(x) + \frac{1}{2}\ln(1-x)\ln(x)\,, \tag{2.58}$$

where $\mathrm{Li}_2(z)$ is the usual Dilogarithm function, with integral representation:

$$\mathrm{Li}_2(z) = \int_z^0 \mathrm{d}t\, \frac{\ln(1-t)}{t}\,. \tag{2.59}$$

Therefore in order to obtain the central charge of the CFT underlying a given purely elastic (diagonal) massive scattering theory one has to solve the transcendental equations (2.51) and then substitute the resulting ε_a in the last line of (2.56). The sum therein can be evaluated using Dilogarithm sum rules [35] once the ε_a are known.

2.4 Universal TBA for ADE diagonal theories

There is a vast class of two dimensional integrable quantum field theories for which the TBA equations can be presented in a universal way [32]: these are the so-called ADE theories, that is, diagonal scattering theories with an S-matrix related to a certain simply-laced affine Lie algebra[8] of the series A_n, D_n, E_6, E_7, E_8. Each of these theories is obtained as an integrable perturbation of a certain conformal field theory by some of its relevant operators. It was noticed [36, 29] that if the conformal families of the unperturbed CFT are classified according to an algebra in the ADE series[9], then it is possible to perturb the theory in such a way that the QFT describing the deformation is still integrable and the spins of the conserved charges are precisely the exponents of the Lie algebra $\mathcal{G}$ describing the underlying CFT, modulo the Coxeter number of $\mathcal{G}$. Moreover, the theory describes the (purely elastic) scattering of r massive particles (r being the rank of $\mathcal{G}$) and the masses of these particles are proportional to the components of the Perron-Frobenius eigenvector of I, the incidence matrix of the Dynkin diagram[10] of $\mathcal{G}$. For instance, the A_n series describes the deformation of $\mathbb{Z}_{n+1}$-parafermion CFTs deformed by the primary fields of dimensions $\Delta(A_n) = \frac{2}{n+3}$, while the D_n series S-matrices are those of sine-Gordon theory at the reflectionless points, *i.e.* free boson theories perturbed by operators with $\Delta(D_n) = \frac{1}{n}$.

One can also work the other way around and start from an off-critical action which is directly built from an algebra in the ADE series. Such theories are the so-called affine Toda field theories (ATFTs):

$$S = \int \mathrm{d}^2x \left[\frac{1}{2}\partial_\mu \phi_i \partial^\mu \phi_i - \frac{\beta^2}{m^2} \sum_{i=0}^{r} e^{\beta \alpha_i \cdot \phi} \right] \tag{2.60}$$

where β is a coupling constant, ϕ_i are real scalars, α_i, $i = 1, \ldots, r$ are the positive simple roots of the Lie algebra and α_0 is the negative of its maximal root. The minimal parts of the ATFTs S-matrices are precisely the ADE series S-matrices, though in this case there are also some extra CDD factors which depend on the couplings.

[8] We follow the notation introduced in chapter 13 of [26] for simply-laced algebras. See also [25] for a detailed discussion of the subject.

[9] See [37] for a review of ADE classification of conformal field theories.

[10] The incidence matrix elements I_{ab} of a Dynkin diagram (in general, of an undirected graph) are such that $I_{ab} = 1$ iff the nodes a and b are connected by a line and $I_{ab} = 0$ otherwise.

In order to obtain a universal TBA for ADE theories one starts from the usual TBA equations:

$$\nu_a(\theta) = \varepsilon_a(\theta) + \frac{1}{2\pi}\sum_{a=1}^{r}(\phi_{ab} * L_b)(\theta)\,, \quad \nu_a(\theta) \equiv m_a R\cosh(\theta) \tag{2.61}$$

with $r = \text{rank}\,\mathcal{G}$. For ADE S-matrices it is possible to show that the following relation holds [33]:

$$\ln S_{ab}\left(\theta + \frac{i\pi}{h}\right) + \ln S_{ab}\left(\theta - \frac{i\pi}{h}\right) = \sum_{c=1}^{r} I_{bc}\ln S_{ac}(\theta) - 2\pi i\Theta(\theta)I_{ab}\,, \tag{2.62}$$

where h is the Coxeter number of $\mathcal{G}$, I is the incidence matrix of its Dynkin diagram and Θ is the Heaviside step function with $\Theta(0) = \frac{1}{2}$. Deriving the previous equation with respect to θ and then taking the Fourier transform of both sides yields:

$$\tilde{\phi}_{ab}(k) = -2\pi\left[I\left(2\cos\left(\frac{\pi k}{h}\right) - I\right)^{-1}\right]_{ab} \tag{2.63}$$

where the Fourier transform of the kernel ϕ_{ab} has been introduced:

$$\tilde{\phi}_{ab}(k) = \int_{-\infty}^{+\infty} \mathrm{d}\theta\,\phi_{ab}(\theta)e^{ik\theta}\,. \tag{2.64}$$

Notice that by setting $k = 0$ in equation (2.63) one obtains a relation between the incidence matrix I and the matrix N defined in (2.52):

$$N = I(2 - I)^{-1} \tag{2.65}$$

this relation allows to rewrite the coupled transcendental equations for the plateau pseudoenergies of an ADE scattering theory in a more suitable way. Indeed, defining $y_a = e^{\varepsilon_a}$ equation (2.51) reads (with $n = r$):

$$y_a = \prod_{b=1}^{n}(1 + 1/y_b)^{N_{ab}}\,, \tag{2.66}$$

which becomes, thanks to (2.65):

$$y_a^2 = \prod_{b=1}^{n}(1 + y_b)^{I_{ab}}\,. \tag{2.67}$$

Using equation (2.63) it is possible to recast the TBA equations (2.61) in the following universal form:

$$\nu_a(\theta) = \varepsilon_a(\theta) + \frac{1}{2\pi} \sum_{a=1}^{r} I_{ab} \left[\phi_h * (\nu_b - \Lambda_b)\right](\theta)\,, \quad \Lambda_a(\theta) = \ln\left(1 + e^{\varepsilon(\theta)}\right) \tag{2.68}$$

where the kernel:

$$\phi_h(\theta) = \frac{h}{2\cosh\left(\frac{h\theta}{2}\right)} \tag{2.69}$$

is specified for each ADE theory once the Coxeter number h is given. The universality of the TBA structure for the ADE scattering theories can be shown to hold at a deeper level. Indeed, by performing an analytic continuation $\theta \mapsto \theta \pm \frac{i\pi}{h}$ it is possible to show that equations (2.68) are equivalent to the following set of functional equations (called Y-system):

$$Y_a\left(\theta - \frac{i\pi}{h}\right) Y_a\left(\theta + \frac{i\pi}{h}\right) = \prod_{b=1}^{n} (1 + Y_b(\theta))^{I_{ab}}\,, \quad a = 1, \ldots, n \tag{2.70}$$

where $Y_a(\theta) \equiv e^{\varepsilon_a(\theta)}$. The Y-system seems to play a very relevant role in the formal development of many theories which display integrability at the quantum level. Any solution of the previous system is also a solution of the universal TBA equations (2.68), but now the dependence on the driving terms $\nu_a(\theta)$ has completely disappeared. It has been proved [33] that for the previous system to have stationary (*i.e.* θ-independent) solutions the matrix I_{ab} must be the incidence matrix of an A_n, D_n, E_6, E_7, E_8 or $A_{2n}/\mathbb{Z}_2$ Dynkin diagram[11]: this provide a complete classification of the Y-systems.

The stationary solutions of the Y-systems are the quantities $y_a = e^{\varepsilon_a}$ in (2.67), which are used to evaluate the UV central charge through equation (2.56): a noticeable result is that for ADE theories the solutions of these coupled equations are *algebraic* rather then transcendental, as the entries of I_{ab} are non-negative integers. An important property of equation (2.70) is its periodicity, namely:

$$Y_a(\theta + i\pi P) = Y_{\bar{a}}(\theta)\,, \quad P = \frac{h+2}{h}\,, \quad \bar{a} \equiv n - a + 1\,. \tag{2.71}$$

On a physical ground, the TBA system (or Y-system) associated to a certain Dynkin diagram can be visually represented by "attaching"a particle of the system to each node, with driving term $\nu_a(\theta) = m_a R\cosh(\theta)$, $a = 1, \ldots, n$. There are interactions only between adjacent particles as the pseudoenergies are coupled through the adjacency matrix I_{ab}. Keeping up with this interpretation, the node $\bar{a}$ in (2.71) is the antiparticle

[11] The $A_{2n}/\mathbb{Z}_2$ diagrams are obtained through a folding procedure from the A_{2n} diagrams, and some additional considerations must be made when dealing with the corresponding TBA systems.

of a, and in the A_n case one has the further property that $Y_a(\theta) = Y_{\bar{a}}(\theta)$. The periodicity of the Y-system has a series of remarkable consequences, among which we only want to mention the fact that the period P determines both the Casimir energy expansion in powers of R when working in the finite-size channel (the L-channel) and the conformal dimension of the perturbing field Φ in the off-critical action:

$$S = S_{\text{CFT}} + \lambda \int \mathrm{d}^2x\, \Phi(x)\,, \quad \Delta(\Phi) = \begin{cases} 1 - \frac{1}{p} & , \quad \text{for} \quad A_n,\, D_n,\, E_n \\ 1 - \frac{2}{p} & , \quad \text{for} \quad A_{2n}/\mathbb{Z}_2 \end{cases} . \tag{2.72}$$

2.5 TBA equations of A_n massless flows

The classification of Y-systems in terms of the ADE series is based only on the structure of the matrix I_{ab} appearing in (2.67) and it is completely independent on h, so that it is in principle possible to write a physically consistent set of TBA equations leading to (2.70) for a certain value of h, but where the latter is no more a Coxeter number. In particular these equations may describe the thermodynamics of a theory with non-diagonal scattering. When the scattering is non-diagonal the usual coordinate Bethe ansatz for the asymptotic states cannot be employed (as in each interaction along the circle internal degrees of freedom are exchanged), and one has to adopt a far more sophisticated algebraic approach to diagonalise the S-matrix. We will not describe the *algebraic Bethe ansatz* technique (see [23] for a review), suffice it to say that in this approach fictitious degrees of freedom are introduced, called *magnons*, which are massless and carry no conserved charges. When the Hilbert space is extended so to include magnons, the S-matrix is diagonal.

In general the perturbation of a coset conformal model by one of its relevant operators may lead to non-diagonal scattering theories. This is true in particular for the perturbations of a unitary minimal model $\mathcal{M}_n$ by its least relevant operator $\Phi = \Phi_{(1,3)}$ of conformal dimension $\Delta = 1 - \frac{2}{n+3}$. The corresponding renormalisation group trajectory is massless or massive depending on the sign of λ in (2.72), and the TBA systems of both these integrable flows were proposed by A. B. Zamolodchikov In the seminal works [7], [6]:

$$\nu_a(\theta) = \varepsilon_a(\theta) + \frac{1}{2\pi} \sum_{b=1}^{n} I_{ab}^{(A)} (\phi * L_b)(\theta)\,, \quad \phi(\theta) = \frac{1}{\cosh(\theta)} \tag{2.73}$$

for $a = 1, \ldots, n$. $I_{ab}^{(A)}$ is the adjacency matrix of the A_n Dynkin diagram:

$$I_{ab}^{(A)} = \delta_{a,a+1} + \delta_{a+1,a} \tag{2.74}$$

and the driving terms are:

$$\nu_a(\theta) = \begin{cases} \delta_a^1 mR\cosh(\theta) & , \quad \lambda < 0 \quad \text{(massive)} \\ \\ \frac{mR}{2}(\delta_a^1 e^{\theta} + \delta_a^n e^{-\theta}) & , \quad \lambda > 0 \quad \text{(massless)} \end{cases} \tag{2.75}$$

that is, for $\lambda < 0$ we have one massive driving term attached to the first node of the Dynkin diagram and $n-1$ magnons attached to the other nodes. For $\lambda < 0$ instead there are $n-2$ magnons attached to the central nodes while the physical particles with driving terms $\frac{mR}{2}e^{\pm\theta}$ (usually referred to as "right-mover"and "left-mover") are attached to the first and the last nodes, see figure 2.2.

Figure 2.2: Dynkin diagrams for the the A_n massive (left) and massless (right) non diagonal flows, with magnons attached to white nodes and physical particles attached to black nodes.

To find the Y-system of the A_n flows we perform an analytic continuation $\theta \to \theta \pm \frac{i\pi}{2}$. If $\nu_a(\theta)$ are given as in (2.75) then one has $\nu_a\left(\theta + \frac{i\pi}{2}\right) + \nu_a\left(\theta - \frac{i\pi}{2}\right) = 0$ and, exploiting also the pole structure of $\frac{1}{\cosh(\theta)}$ and the explicit form of $I_{ab}^{(A)}$, this allows to recast equation (2.73) as:

$$Y_a\left(\theta + \frac{i\pi}{2}\right) Y_a\left(\theta - \frac{i\pi}{2}\right) = (1 + Y_{a+1}(\theta))(1 + Y_{a-1}(\theta)), \quad a = 1, \ldots, n \tag{2.76}$$

where now $Y_a(\theta) = e^{-\varepsilon_a(\theta)}$. The previous system is formally identical to the ADE Y-system (2.70) when we set $h = 2$ and I_{ab} as in (2.74), and it rules the UV behaviour of both massless and massive A_n flows. The stationary solutions of this systems correspond to the quantities $y_a = e^{-\varepsilon_a(0)}$ which satisfy equations (2.67), $\varepsilon_a(0)$ being the constant values of the pseudoenergies in the plateaux which form as $\beta \to 0$. They are the essential instruments used to compute the UV and the IR limit of the scaling function for the flow[12]. In particular it is possible to show [6, 38] that in the massless case, A_n interpolates between the $\mathcal{M}_{n+2}$ and the $\mathcal{M}_{n+1}$ minimal models ($n \geq 2$), so that both the UV and the IR central charges are non vanishing, whereas for the massive flow the UV limit is the same but in the IR case the model approaches a theory with $c = 0$.

[12]However in the infrared limit $\beta \to +\infty$ the stationary solutions must be interpreted as the values $e^{-\varepsilon_a(\infty)}$, with a a magnonic node. When a labels instead a massive node, the pseudoenergy asymptotically tend to infinity.

The staircase model that we will describe in the following chapter seems to be strictly related to the A_n massless flow. In this case, a detailed study of the reduced form of equation (2.73) shows that [33, 39]:

$$c_{\rm UV} = \lim_{\beta\to 0} c(\beta) = \frac{6}{\pi^2}\left(\sum_{a\in I} - \sum_{a\in I'}\right)\mathcal{L}\left(\frac{y_a}{1+y_a}\right) \tag{2.77}$$

$$c_{\rm IR} = \lim_{\beta\to \infty} c(\beta) = \frac{6}{\pi^2}\left(\sum_{a\in I} - \sum_{a\in I''}\right)\mathcal{L}\left(\frac{y_a}{1+y_a}\right) \tag{2.78}$$

where $I' \equiv I - \{L\}$ and $I'' \equiv I - \{L, R\}$, being I the adjacency matrix of the A_n Dynkin diagram, L the node to which the left-mover is attached and R the node with the right-mover attached. When I is given by (2.74), the stationary equations (2.67) can exactly solved, and this of course holds when we remove one or two nodes obtaining the reduced diagrams I', I''. The explicit solutions are the following [38]:

$$y_a^2 = \prod_{b=1}^{n}(1+y_b)^{I_{ab}} \Rightarrow 1+y_a = \frac{\sin^2\left[\pi(a+1)/(n+3)\right]}{\sin^2\left[\pi/(n+3)\right]} \tag{2.79}$$

$$y_a^2 = \prod_{b=2}^{n-1}(1+y_b)^{I_{ab}} \Rightarrow 1+y_a = \frac{\sin^2\left[\pi a/(n+1)\right]}{\sin^2\left[\pi/(n+1)\right]} \tag{2.80}$$

inserting these solutions in (2.77) and making use of the Dilogarithm sum rules one obtains

$$c_{\rm UV} = 1 - \frac{1}{(n+2)(n+3)}\,, \quad c_{\rm IR} = 1 - \frac{1}{(n+1)(n+2)} \tag{2.81}$$

which are the central charges of the $\mathcal{M}_{n+2}$ and $\mathcal{M}_{n+1}$ unitary minimal models, as announced.

Chapter 3

TBA structure of Zamolodchikov's staircase model

In this chapter we discuss the S-matrix and the TBA structure of Zamolodchikov's staircase model [17], the principal object of study in this thesis. The staircase model is a scattering theory obtained via analytic continuation of the sinh-Gordon S-matrix, and it does not posses a physically sensible lagrangian description. The mass spectrum and the analytic structure of the model are very simple, and yet a surprising phenomenon arises at finite temperatures: the scaling function approaches the central charges of all the unitary minimal models $\mathcal{M}_n$ when the temperature varies. We refer to this property by saying that there are roaming trajectories generated by the action of the renormalization group (RG). In the context of generalized hydrodynamics, which will be introduced in the next chapter, the presence of several UV fixed points allows to tests the predicted behaviour of steady state expectation values with a precision which would be inaccessible for other models.

Moreover, at the pure TBA level the equations of the staircase model are strictly related to those of the A_n non-diagonal massless flows, and this suggests that it is in some sense possible to regard the former as an effective scattering theory for more complicated models with magnons in their spectra. It is also possible to obtain generalized staircase-like theories via analytic continuation of the coupling constants in affine Toda field theories [20], [19].

3.1 The scattering theory

The staircase model originally proposed by Al. B. Zamolodchikov is perhaps the simplest scattering theory which displays roaming trajectories under the renormalization group

action. The particle content of the theory consists of a single neutral boson[1] of mass m, with the following two-body S-matrix:

$$S(\theta) \equiv \tanh\left(\frac{\theta-\theta_0}{2}-\frac{i\pi}{4}\right)\tanh\left(\frac{\theta+\theta_0}{2}-\frac{i\pi}{4}\right) \tag{3.1}$$

where $\theta = \theta_1 - \theta_2$ is the rapidity difference between the two scattering particles and $\theta_0 \in \mathbb{R}$ is a parameter of the model. It is immediate to check that this scattering amplitude satisfies the crossing symmetry (1.52) and unitarity (1.50) requirements:

$$S(\theta) = S(i\pi - \theta)\,, \qquad S(\theta)S(-\theta^*) = 1\,. \tag{3.2}$$

Thanks to the periodicity condition:

$$S(\theta) = S(\theta + 2\pi i) \tag{3.3}$$

the zeros and poles of the S-matrix are completely fixed by those in the physical strip $0 \leq \mathrm{Im}(\theta) < \pi$ and in the unphysical one $-\pi \leq \mathrm{Im}(\theta) < 0$. In the physical strip there are two simple zeros:

$$\theta = \pm\theta_0 + i\frac{\pi}{2}\,, \tag{3.4}$$

while two resonance poles are found in the unphysical strip:

$$\theta = \pm\theta_0 - i\frac{\pi}{2}\,. \tag{3.5}$$

The absence of zeros in the physical strip is a signal of the fact that there are no bound states in the model. We can re-express the scattering amplitude (3.1) in terms of the Mandelstam variable $s = 2m^2(1 + \cosh(\theta))$:

$$S(s) = \frac{\sqrt{s(s-4m^2)} - 2im^2\cosh(\theta_0)}{\sqrt{s(s-4m^2)} + 2im^2\cosh(\theta_0)} \tag{3.6}$$

from this expression we recognise the usual square-root branch points at $s = 0$ and $s = 4m^2$ originating the u-channel cut $(-\infty, 0]$ and the s-channel one $[4m^2, +\infty)$. In the s-plane the two zeros (3.4) are at the points $s = 2m^2 \pm 2im^2\sinh(\theta_0)$ in the first Riemann sheet, while the poles (3.5) are in the unphysical Riemann sheet just under the zeros, see figure 3.1.

On a physical ground, there are two possible interpretations for this scattering theory. The first one relies on the analogy with the massless flow between the tricritical and the critical Ising model, $A_2 : \mathcal{M}_4 \to \mathcal{M}_3$. In [6] the massless particles in the theory

[1] One could also choose the neutral particle to be a Majorana fermion by simply changing the overall sign of the scattering amplitude.

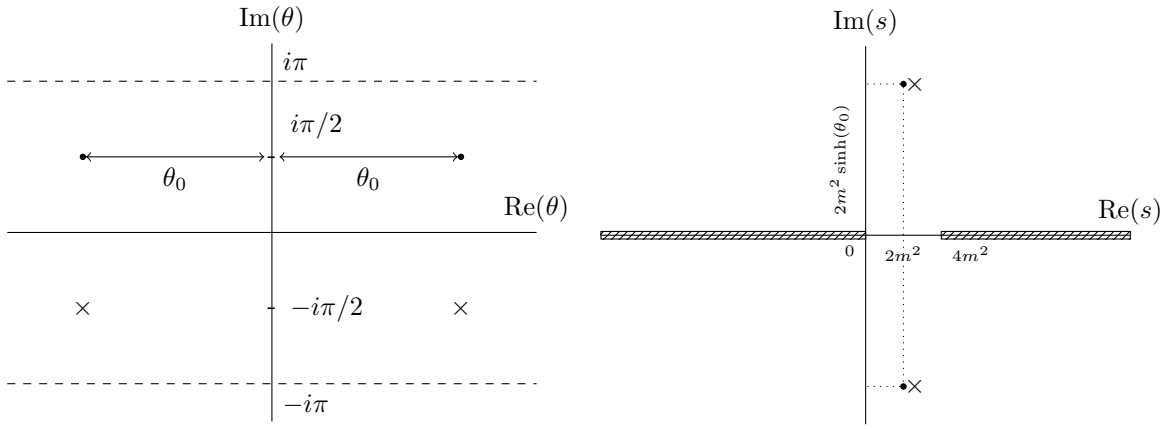

Figure 3.1: Zeros and poles of the staircase S-matrix in the θ-plane (left) and in the s-plane (right). Zeros are denoted by black dots and poles by crosses. In the s-plane the poles in the second sheet are misplaced a bit for transparency, as they are exactly under the zeros.

were interpreted as right-moving ($p = \frac{1}{2}Me^{\theta}$) and left-moving ($p = \frac{1}{2}Me^{-\theta}$) Goldstone fermions representing the spontaneous breaking of the $\mathcal{M}_4$ supersymmetry by the integrable $\Phi_{(1,3)}$ perturbation. The S-matrix which was proposed therein for the scattering between massless fermions is similar to the staircase's one (3.1):

$$S(\theta) = -\tanh\left(\frac{\theta}{2} - \frac{i\pi}{4}\right), \tag{3.7}$$

with θ the rapidity difference between the left mover and right mover. This scattering amplitude has a single pole in the unphysical sheet corresponding to a highly unstable Higgs boson in the theory. In light of this, one can argue that the S-matrix (3.1) represents a deformation of this theory in which SUSY is explicitly broken and the Goldstone fermions acquire a mass m related to the Higgs energy scale via $M^2 = m^2 e^{\theta_0}$.

The second interpretation of this massive scattering amplitude, to which we will stick from now on, is that of an analytic continuation of sinh-Gordon S-matrix at its self-dual point. To see this, it is useful to rewrite (3.1) as:

$$S(\theta) = \frac{\sinh(\theta) - i\cosh(\theta_0)}{\sinh(\theta) + i\cosh(\theta_0)} \tag{3.8}$$

and compare it to the sinh-Gordon S-matrix (1.60), which we recast as well:

$$S_{\text{shG}}(\theta) = \frac{\sinh(\theta) - i\sin(\gamma)}{\sinh(\theta) + i\sin(\gamma)}, \quad \gamma \equiv \frac{\beta^2/8}{1 + \beta^2/(8\pi)}. \tag{3.9}$$

We notice that $S_{\text{shG}}(\theta)$ has two zeros along the imaginary axis in the physical strip, which coincide when the self-dual point $\gamma = \frac{\pi}{2}$ (*i.e.* $\beta^2 = 8\pi$) is reached. If at that point we make the analytic continuation:

$$\gamma \mapsto \gamma = \frac{\pi}{2} \pm i\theta_0 \tag{3.10}$$

then the double zero of (3.9) splits into two distinct points with different real parts and the same happens to the pole in the unphysical strip, while we precisely recover the S-matrix (3.8):

$$S_{\text{ShG}}\left(\theta;\, \gamma = \frac{\pi}{2} \pm i\theta_0\right) = S(\theta;\, \theta_0) \tag{3.11}$$

One might be tempted to perform the analytic continuation (3.10) directly at the lagrangian level. The sinh-Gordon potential is proportional to the sum of two free-field exponential, $e^{\beta\phi} + e^{-\beta\phi}$, and because of the two possible signs in (3.10) there are two possible analytic continuation of each term, resulting in four exponential operators:

$$U_\pm = \exp\left(\pm i\sqrt{8\pi}\alpha_+\phi\right), \quad V_\pm = \exp\left(\pm i\sqrt{8\pi}\alpha_-\phi\right) \tag{3.12}$$

with $\alpha_\pm$ complex coefficients. From the CFT point of view these exponentials are *vertex operators* (see *e.g.* [25]) which have complex conformal weights. However, the sinh-Gordon conserved charges can be shown to survive under all these four perturbations, so that the action:

$$S = \int \mathrm{d}^2x \left[\frac{1}{2}(\partial_\mu\phi)^2 + \mu_+U_+ + \mu_-U_- + \nu_+V_+ + \nu_-V_-\right] \tag{3.13}$$

is still integrable at the quantum level [17]. This action would be a good candidate for a lagrangian description of the staircase model, were it not for the fact that even if we choose the coefficients $\mu_\pm, \nu_\pm$ in such a way that it is a real action, by no means the perturbing potential can be arranged bounded from below. Therefore, as far as it is presently known, there is no way to provide a physically sensible lagrangian description of this scattering theory.

3.2 TBA analysis

Let us now turn to the TBA structure of the model. From equation (3.8) one readily obtains the kernel $\phi(\theta) \equiv -i\partial_\theta \ln S(\theta)$:

$$\phi(\theta) = \frac{1}{\cosh(\theta - \theta_0)} + \frac{1}{\cosh(\theta + \theta_0)} \equiv \psi(\theta + \theta_0) + \psi(\theta - \theta_0) \tag{3.14}$$

where the function ψ is defined as the reciprocal of the hyperbolic cosine. The function $\phi(\theta)$ is plotted in figure 3.2 for two values of θ_0. Let us also define the kernel normalization

constant (notice the different choice of the overall sign with respect to the definition (2.52)):

$$C^{-1} \equiv \frac{1}{2\pi} \int_{-\infty}^{+\infty} \mathrm{d}\theta \, \psi(\theta) = \frac{1}{2} \,. \tag{3.15}$$

Since the particle content of the model consists only in one massive neutral particle, there is only one TBA equation, the solution of which gives the particle's pseudoenergy $\varepsilon(\theta)$:

$$\varepsilon(\theta) = \beta \cosh(\theta) - \frac{1}{2\pi} \left[(\psi * L)(\theta - \theta_0) + (\psi * L)(\theta + \theta_0) \right] \tag{3.16}$$

where $\beta \equiv mR$ and $L(\theta) \equiv \ln\left(1 + e^{-\varepsilon(\theta)}\right)$. Both the kernel and the driving term in the equation above are even functions of θ, thus also $\varepsilon(\theta)$ is even, as $\varepsilon(\theta)$ and $\varepsilon(-\theta)$ satisfy the same functional equation. This implies that $L(\theta) = L(-\theta)$ and the same holds for the occupation function $n(\theta)$ defined as in (2.33). In natural units β is dimensionless, and it is very useful to define the quantities $x \equiv \ln(\beta/2)$ and $y = -x$. We will be mainly interested in the UV regime(s) of the theory, where β is much smaller than 1, so that typically $x < 0$ and $y > 0$. It turns out more convenient to use y rather than β in the TBA equation:

$$\varepsilon(\theta) = 2e^{-y} \cosh(\theta) - \frac{1}{2\pi} \left[(\psi * L)(\theta - \theta_0) + (\psi * L)(\theta + \theta_0) \right] \,. \tag{3.17}$$

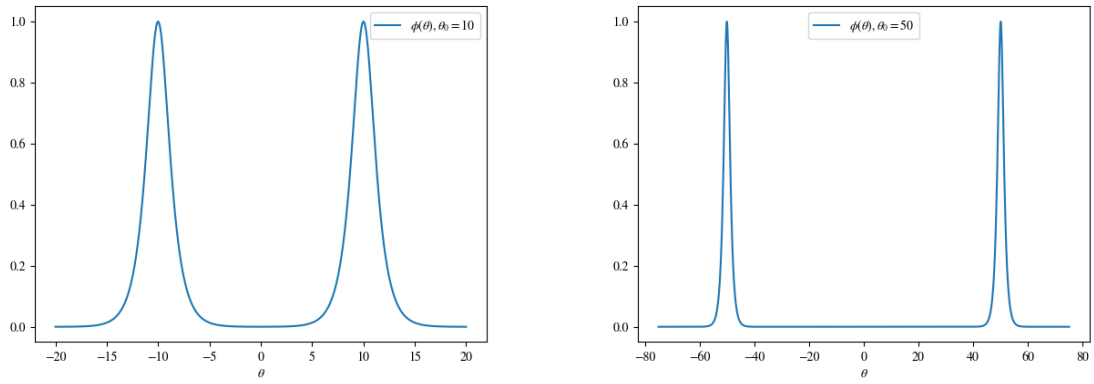

Figure 3.2: Kernel function $\phi(\theta)$ of the staircase model for $\theta_0 = 10$ (left) and $\theta_0 = 50$ (right). As θ_0 increases $\phi(\theta)$ flattens to zero in the region between the peaks, while the width of the latter is almost untouched.

3.2.1 Kinks and plateaux

Two important observations on equation (3.17) are in order. The first is that there are two dimensionless parameters, y and θ_0, which control the behaviour of the system. As we will show in the next section, it is the value of the ratio y/θ_0 which is responsible for the characteristic staircase profile of the scaling function:

$$c(\beta) = \frac{3\beta}{\pi^2} \int_{-\infty}^{+\infty} \mathrm{d}\theta \, \cosh(\theta) L(\theta) \tag{3.18}$$

as well as for the similar profiles of average charge currents and densities when the system is out of thermal equilibrium. When y and θ_0 are sent to infinity and their ratio is kept fixed and different from an integer or half-integer, $c(\beta)$ approaches the central charge of a unitary minimal model $\mathcal{M}_n$. On the other hand if θ_0 is fixed (and large enough) and y is increased the RG flow of the system roams between every unitary minimal model: as θ_0 gets larger, the scaling function gets arbitrarily close to each of them, and the "time"spent in proximity of every fixed point increases as well. The integer and half-integer values of y/θ_0 are the cross-over points where $c(\beta)$ leaves the basin of a unitary minimal model and enters the next one. The scaling function is plotted in figure 3.3 for different values of θ_0.

The second observation concerns the non-local nature of equation (3.17). As the function $\psi(\theta)$ is peaked at $\theta = 0$, the two convolution terms are peaked at $\theta - \theta_0$ and $\theta + \theta_0$ and become exponentially small as $|\theta \pm \theta_0|$ exceeds a few units. So the value of ε at θ is influenced by the values of ε in the very small intervals around $\theta + \theta_0$ and $\theta - \theta_0$. If $|\theta| \gg y$ then the driving term in (3.17) is largely dominant over the convolution terms and therefore the pseudoenergy becomes exponentially increasing:

$$\varepsilon(\theta) \simeq \begin{cases} e^{-y+\theta} & , \quad \theta \gg y \\ e^{-y-\theta} & , \quad \theta \ll -y \end{cases} \tag{3.19}$$

this means that when $|\theta| \gg y$, the occupation function falls-off exponentially and $L(\theta)$ suffers a double exponential decay, as $\ln(1 + e^{-\varepsilon}) \simeq \exp\left(e^{-y \pm \theta}\right)$ when $\theta \gg y$ (upper sign) or $\theta \ll -y$ (lower sign). This is the same behaviour displayed by scattering theories for which $\phi(\theta)$ is peaked at $\theta = 0$. Things however are quite different in the central region $-y < \theta < y$, where the staircase's TBA shows different structures depending on the ratio y/θ_0. To see that, let us start with $0 < y < \theta_0/2$. When $-y < \theta < y$ both $|\theta - \theta_0|$ and $|\theta + \theta_0|$ are larger than y, therefore $L(\theta - \theta_0)$ and $L(\theta + \theta_0)$ (the dominant contributions from the convolution) are essentially zero, so that approximately:

$$2e^{-y} \lesssim \varepsilon(\theta) \simeq 2e^{-y} \cosh(\theta) \lesssim 1 + e^{-y}, \quad -y < \theta < y. \tag{3.20}$$

In this interval therefore $L(\theta)$ varies very little and it develops a plateau which gets larger as y increases, in complete analogy with models having a single peak in $\phi(\theta)$. Two kinks at $\theta = \pm y$ connect the plateau value of L to the vanishing asymptotic values.

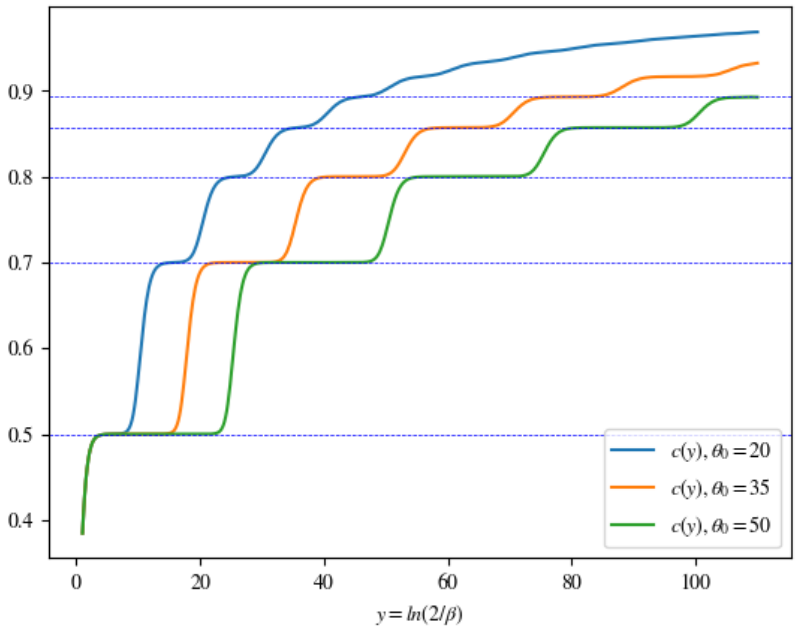

Figure 3.3: Staircase model's scaling function (3.18) for different values of θ_0 as the temperature varies. The plateaux are clearly visible and they match the values of the unitary minimal model central charges (3.58) (dashed horizontal lines).

If instead we take $\theta_0/2 < y < \theta_0$, and start at θ very large and negative, the behaviour of $L(\theta)$ is the same described above as long as $\theta < -y$. However, since the TBA equation relates the values of $L(\theta)$, $L(\theta-\theta_0)$ and $L(\theta+\theta_0)$ we expect the kink at $\theta = +y$ to originate another kink at $\theta = y - \theta_0 > -y$, as well as a kink at $-y + \theta_0 < y$ originated from the one at $\theta = y$. For $\theta > y$ again $L(\theta)$ drops to zero. So there are four kinks in this range, as it is confirmed by the numerical solution of the TBA equation.

One could then proceed and show that for $\theta_0 < y < 3\theta_0/2$ there are six kinks at the positions $\pm y$, $\pm(y - \theta_0)$, $\pm(y - 2\theta_0)$. These kinks form two alternating sequences generated from the right and left "seed"kinks, at $\theta = \pm y$ respectively. The general situation, supported by the numerical solution of equation (3.17) and represented in the plots in figure 3.4, is the following. When:

$$\frac{(k-1)\theta_0}{2} < y < \frac{k\theta_0}{2}\,, \quad k \in \mathbb{N} \tag{3.21}$$

$L(\theta)$ has $2k$ kinks, at the positions $\pm(y - i\theta_0)$, $i = 0, 1, \ldots, k-1$. The latter can be organized into two sequences originated from the left and the right seed kinks, so that

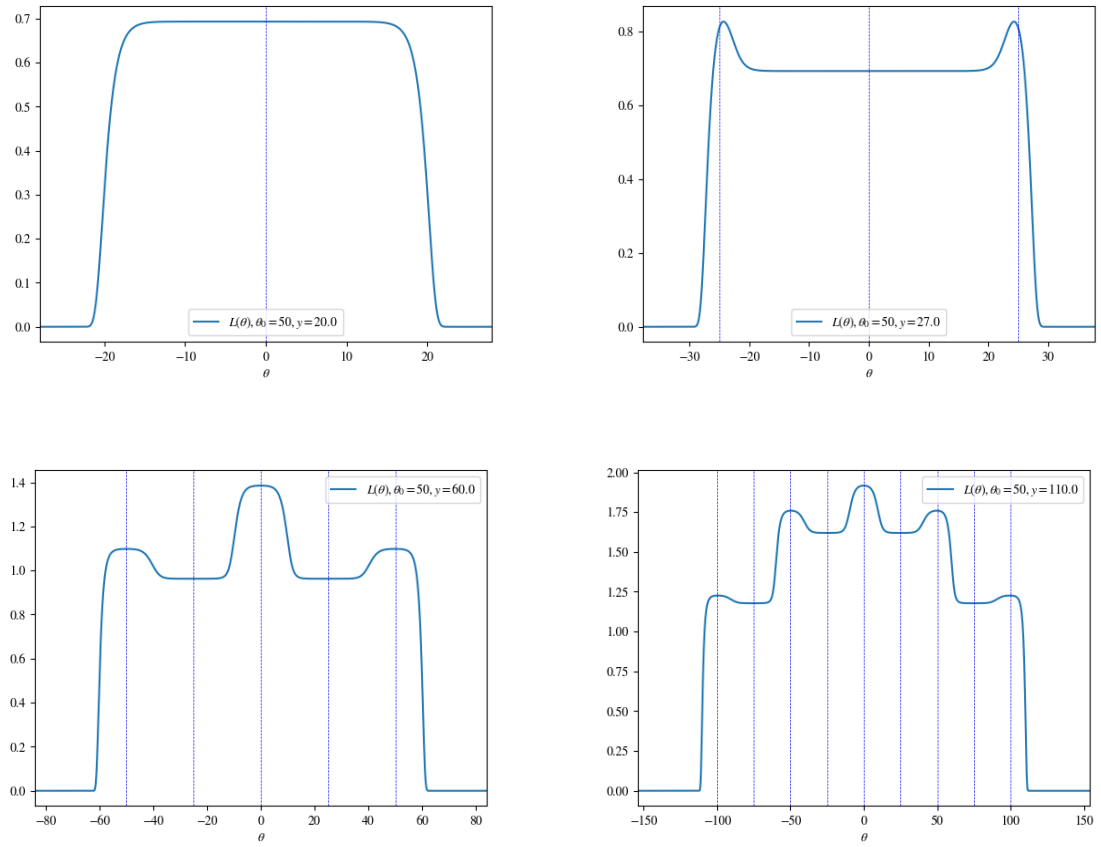

Figure 3.4: Profiles of $L(\theta)$ at different values of the ratio y/θ_0. The right plot in the top row is at the transition between the first ($k = 1$) and second ($k = 2$) fixed points, all the other plots are at values of y/θ_0 well inside (3.21). The vertical dashed lines are at the points z_i in (3.24).

we can label their positions as:

$$\begin{cases} \theta_{i,L} &= -y + (i-1)\theta_0 \\ \theta_{i,R} &= y - (k-i)\theta_0 \end{cases}, \quad i = 1, 2, \ldots, k \tag{3.22}$$

and clearly $\theta_{1,L} < \theta_{1,R} < \theta_{2,L} < \cdots < \theta_{k,L} < \theta_{k,R}$. Furthermore, $\theta_{i,R} = -\theta_{k-i+1,L}$ as expected from the parity of $L(\theta)$.

In each region between two adjacent kinks, the L-function shows very little variations, as can be argued [20] from a qualitative study of the integral equation satisfied by $L'(\theta)$, and this is also in agreement with the numerics. There are therefore $2k + 1$ plateaux of $L(\theta)$, the first and the last one being respectively in the regions $\theta < -y$ and $\theta > y$,

where $L(\theta)$ is effectively zero. The internal plateaux are of alternating width, as so is the distance between two adjacent kinks. Starting from $\theta = -y$, we can arrange the internal plateaux into two sequences:

$$\begin{cases} P_{2i-1} & = [\theta_{i,L}\,,\,\theta_{i,R}]\,, \quad i = 1,\dots,k\,, \quad |P_{2i-1}| = 2y - (k-1)\theta_0 \\ P_{2i} & = [\theta_{i,R}\,,\,\theta_{i+1,R}]\,, \quad i = 1,\dots,k-1\,, \quad |P_{2i}| = k\theta_0 - 2y \end{cases} \tag{3.23}$$

This structure gives us a hint of what happens to $L(\theta)$ when there is a transition between two fixed points in the UV limit, that is when k/θ_0 is equal to an integer or half integer (assuming both y and θ_0 very large). Setting $y = \alpha\theta_0$, with $(k-1)/2 < \alpha < k/2$, when α gets closer to $k/2$ the width of the even plateaux P_{2i} shrinks to zero, and a new bump forms at $\theta = 0$, which then gets larger as it effectively becomes a new plateau. Thus when α is just above k there are two more kinks and one more plateau, the "thin"plateaux being now the odd ones, P_{2i-1}. Of course when $\alpha \to (k-1)/2$ one only needs to interchange the roles of P_{2i} and P_{2i-1}.

We have tacitly assumed so far that the kinks are point-like jumps of $L(\theta)$ located at the positions (3.22), but they actually have a finite extension: this is the size of the interval where $\psi(\theta)$ is appreciably different from zero, which is of order $\mathcal{O}(1 \div 10)$, see Figure 3.2. The extension of the kinks does not depends, in first approximation, on the values of y, θ_0 and as these parameters get larger (with a fixed ratio) the former becomes negligible with respect to the size of the plateaux so that $L(\theta)$ is well-approximated by a piece-wise constant function. As long as y and θ_0 are finite, however, we should consider the finite size of the kinks. This requires just one more piece of notation. Let us define the points

$$z_i \equiv \frac{(i-k)\theta_0}{2}\,, \quad i = 0, 1\dots, 2k\,, \tag{3.24}$$

which are the equidistant midpoints of the internal plateaux (for $i \neq 0\,,\,2k$), namely z_i is the central point of P_i. The i^{th} kink, even though finite-sized, is well inside the interval:

$$K_i \equiv [z_{i-1}\,,\,z_i]\,, \quad i = 1, 2, \dots, 2k \tag{3.25}$$

as $z_0 < \theta_{1,L} < z_1 < \theta_{1,R} < \cdots < \theta_{k,L} < z_{2k-1} < \theta_{k,R} < z_{2k}$. Notice also that $L(z_0)$ and $L(z_{2k})$ are zero to all effects, so we can safely set:

$$\int_{-\infty}^{+\infty} \mathrm{d}\theta\, L(\theta) f(\theta) = \sum_{i=1}^{2k} \int_{K_i} \mathrm{d}\theta\, L(\theta) f(\theta) \tag{3.26}$$

as long as f is not doubly-exponentially increasing at large rapidities.

3.2.2 Reduced TBA equations and the relation to A_n massless flows

To conclude this section, let us derive the coupled algebraic equations for the constant quantities $\varepsilon(z_i) \equiv \varepsilon_i$, *i.e.* the pseudoenergies at the plateaux' midpoints. If $i = 1, \dots, 2k-1$ one has:

$$2e^{-y}\cosh(z_i) \leq 2\exp(|i-k|\theta_0/2 - y) \leq 2\exp((k-1)\theta_0/2 - y)\,, \tag{3.27}$$

so that the driving term in (3.17) is bounded by an exponentially decreasing quantity which is negligible when y and θ_0 are large enough. The TBA equation for ε_i is thus:

$$\varepsilon_i = -\sum_{i=1}^{2k} \int_{K_i} \frac{\mathrm{d}\theta'}{2\pi} L(z_i - \theta')\phi(\theta') \tag{3.28}$$

where (3.26) has been used. The kernel is effectively different from zero only inside the two plateaux containing $\theta = \pm\theta_0$, so that we can safely use the approximation:

$$\phi(\theta) \simeq 2\pi C^{-1}\left[\delta(\theta - \theta_0) + \delta(\theta + \theta_0)\right] \tag{3.29}$$

therefore, using the fact that $\varepsilon(z_i \pm \theta_0) = \varepsilon_{i\pm 2}$, equation (3.28) becomes:

$$\varepsilon_i = -C^{-1}\left[\ln\left(1 + e^{-\varepsilon_{i-2}}\right) + \ln\left(1 + e^{-\varepsilon_{i+2}}\right)\right] \quad i = 1, \dots, 2k-1\,, \tag{3.30}$$

with the boundary conditions $\varepsilon_{-1} = \varepsilon_0 = \varepsilon_{2k} = \varepsilon_{2k+1} = +\infty$. Furthermore, we notice that the interactions only involve even plateaux when i is even and odd plateaux when i is odd, so that we can write two disjoint sets of coupled equations. In fact, setting $x_i \equiv \exp\{(-\varepsilon_{2i-1})\}$ for $i = 1, \dots, k$ and $y_i \equiv \exp\{(-\varepsilon_{2i-2})\}$ for $i = 2, \dots, k$ the equations above split into:

$$\begin{cases} x_i &= [(1 + x_{i+1})(1 + x_{i-1})]^{C^{-1}}\,, \quad i = 1, \dots, k \\ y_i &= [(1 + y_{i+1})(1 + y_{i-1})]^{C^{-1}}\,, \quad i = 2, \dots, k \end{cases} \tag{3.31}$$

with boundary conditions $x_0 = x_{k+1} = y_1 = y_{k+1} = 0$. A manipulation of the staircase TBA equation similar to the one performed in the previous chapter leads to the kink equations for the quantities connecting the various ε_i [39].

Notice that, as $C^{-1} = 1/2$, the two sequences of coupled equations (3.31) can be re-written in the following way :

$$x_a^2 = \prod_{b=1}^{k}(1 + x_b)^{I_{ab}}\,, \quad y_a^2 = \prod_{b=2}^{k}(1 + y_b)^{I_{ab}} \tag{3.32}$$

where I_{ab} is the incidence matrix of a A-type Dynkin diagram, and in the first equation $a = 1, \dots, k$ while in the second one $a = 2, \dots, k$. These are exactly the equations (2.79) (renaming $y_a \equiv x_a$) and (2.80) for the ultraviolet and infrared stationary solutions of a massless A-type Y-system.

This coincidence had already been noticed in [20], but its consequences were not completely analyzed therein. As we are going to show in detail in the next section, when the ratio y/θ_0 is kept fixed as in (3.21) and y, θ_0 are sent to infinity, the staircase model approaches the unitary minimal model $\mathcal{M}_{k+2}$. But this is also the UV fixed point of the A_k massless flow and the IR fixed point of the A_{k+1} one, and the θ-independent values of the real-particle and magnonic rapidities in those models are precisely ruled by the first and the second equation in (3.32) respectively. Thus, it seems that when the staircase model, during its roaming, reaches the $\mathcal{M}_{k+2}$ fixed point, the midpoints of the "odd"plateaux of its L-function correspond to the particles in the A_k massless flow in its UV limit, while the ones of the "even"plateaux correspond to the particles of the A_{k+1} massless flow in its IR limit. This is not an innocuous analogy, as it indicates that somehow a diagonal scattering theory with only one massive particle in the spectrum encodes information about the particles contained in other non-diagonal models having the same high-energy and low-energy limits [18]. In the next chapter we will show that this relation seems to hold at the hydrodynamic level, where we can actually "see"the density peaks corresponding to these particles.

3.3 The scaling function

The scaling function of the staircase model depends on the two parameters $y \equiv \ln(2/\beta)$, θ_0 rather than on the temperature alone, so that we can conveniently re-write (3.18) as:

$$c(y, \theta_0) = \frac{6}{\pi^2} \int_{-\infty}^{+\infty} \mathrm{d}\theta \, e^{-y} \cosh(\theta) L(\theta) \,. \tag{3.33}$$

Thanks to (3.26) we can reduce the integration domain to $\bigcup_{i=1}^{i=2k} K_i$. Inside each K_i, $L(\theta)$ is bounded for every finite y and the quantity $2e^{-y}\cosh(\theta)$ is effectively different from zero (in the limit of large y) only in K_1 and K_{2k}, as it is roughly bounded by $\exp(|i-k|\theta_0/2 - y) \to 0$ when $i \neq 1, 2k$, that is:

$$2e^{-y}\cosh(\theta) \simeq \begin{cases} e^{-y-\theta} & , \quad \theta \in K_1 \\ 0 & , \quad \theta \in K_2 \dots, K_{2k-1} \\ e^{-y+\theta} & , \quad \theta \in K_{2k} \end{cases} \tag{3.34}$$

therefore the only relevant contributions to the scaling functions come from the kinks in K_1 and K_{2k}:

$$c(y, \theta_0) = c_- + c_+ \tag{3.35}$$

where:

$$c_- \equiv \frac{3}{\pi^2}\int_{K_1} \mathrm{d}\theta\, e^{-y-\theta} L(\theta)\,, \quad c_+ \equiv \frac{3}{\pi^2}\int_{K_{2k}} \mathrm{d}\theta\, e^{-y+\theta} L(\theta)\,. \tag{3.36}$$

Notice that, as $L(\theta) = L(-\theta)$ and the two intervals K_1 and K_{2k} are symmetric with respect to $\theta = 0$, $c_- = c_+$ and therefore we only need to evaluate one of the above integrals. In order to do so, let us take the derivative with respect to θ of the TBA equation (3.17):

$$\varepsilon'(\theta) = 2e^{-y}\sinh\theta - \frac{1}{2\pi}\left[(\psi' * L)\,(\theta-\theta_0) + (\psi' * L)\,(\theta+\theta_0)\right] \tag{3.37}$$

and then integrate both sides over K_i with measure $L(\theta)\,\mathrm{d}\theta$, so that we end up with:

$$\mathcal{J}^i = \frac{\pi^2}{3}\mathcal{C}^i - \mathcal{I}^i_- - \mathcal{I}^i_+ \tag{3.38}$$

where:

$$\mathcal{J}^i \equiv \int_{K_i} \mathrm{d}\theta\, \varepsilon'(\theta) L(\theta) = \int_{\varepsilon_{i-1}}^{\varepsilon_i} d\varepsilon\, \ln\left(1+e^{-\varepsilon}\right) \tag{3.39}$$

$$\mathcal{C}^i \equiv \frac{3}{\pi^2}\int_{K_i} \mathrm{d}\theta\, 2e^{-y}\sinh(\theta) L(\theta) \tag{3.40}$$

$$\mathcal{I}^i_\pm \equiv \frac{1}{2\pi}\int_{K_i} \mathrm{d}\theta\ (\psi' * L)\,(\theta \pm \theta_0) L(\theta) \tag{3.41}$$

The right hand side of (3.40) is basically the contribution to the scaling function coming from the interval K_i when the latter is in the positive rapidity region, otherwise there is an extra minus sign. Namely:

$$2e^{-y}\sinh(\theta) \simeq \begin{cases} -e^{-y-\theta} & , \quad \theta \in K_1 \\ 0 & , \quad \theta \in K_1, K_2 \ldots, K_{2k-1} \\ e^{-y+\theta} & , \quad \theta \in K_{2k} \end{cases} \tag{3.42}$$

so that from (3.35) it follows:

$$\mathcal{C}^i = -\delta_{1,i} c_- + \delta_{2k,i} c_+\,. \tag{3.43}$$

To evaluate $\mathcal{I}_\pm$ we use the following generalized integration by parts, the proof of which can be found in [20]:

$$\int_{K_i} \mathrm{d}\theta\, (f' * A)\,(\theta) B(\theta) = -\int_{K_i} \mathrm{d}\theta\, (f' * B)\,(\theta) A(\theta) + \left(\int_{-\infty}^{+\infty} \mathrm{d}\theta f(\theta)\right) [A(\theta)B(\theta)]^{z_i}_{z_{i-1}}\,. \tag{3.44}$$

This equality is valid when f is even and exponentially decreasing outside a support centered in $\theta = 0$, while A, B are slowly varying functions on the support of f. These conditions are met if we choose $f(\theta) = \psi(\theta)$, $A(\theta) = L(\theta \pm \theta_0)$, $B(\theta) = L(\theta)$. Applying (3.44) to (3.41) we have:

$$\begin{aligned}\mathcal{I}^i_\pm &= -\frac{1}{2\pi}\int_{K_i} \mathrm{d}\theta\ (\psi' * L)(\theta) L(\theta \pm \theta_0) + \left(\frac{1}{2\pi}\int_{-\infty}^{+\infty} \mathrm{d}\theta \psi(\theta)\right) [L(\theta)L(\theta \pm \theta_0)]^{z_i}_{z_{i-1}} \\ &= -\mathcal{I}^{i\pm 2}_\mp + C^{-1}[L(\theta)L(\theta \pm \theta_0)]^{z_i}_{z_{i-1}} \end{aligned} \tag{3.45}$$

where the second line follows from a change of variable in the first integral and by noting that $z_i \pm \theta_0 = z_{i\pm 2}$. The coefficient C^{-1} has been defined in (3.15). It is convenient to define:

$$\tilde{\mathcal{I}}^i_\pm \equiv \mathcal{I}^i_\pm - \frac{1}{2} C^{-1}[L(\theta)L(\theta \pm \theta_0)]^{z_i}_{z_{i-1}}\,, \tag{3.46}$$

so that equation (3.45) simplifies to:

$$\tilde{\mathcal{I}}^i_\pm = -\tilde{\mathcal{I}}^{i\pm 2}_\mp\,. \tag{3.47}$$

Now notice that because of the double-exponential fall-off of L, $\mathcal{I}^i_\pm \simeq 0$ and $\tilde{\mathcal{I}}^i_\pm \simeq 0$ for $i < 1$ or $i > 2k$. At this point equation (3.38) can be rewritten as follows:

$$\begin{aligned}\mathcal{J}^i &= \frac{\pi^2}{3}\mathcal{C}^i - \tilde{\mathcal{I}}^i_- - \tilde{\mathcal{I}}^i_+ - \frac{1}{2}C^{-1}[L(\theta)(L(\theta+\theta_0) + L(\theta-\theta_0))]^{z_i}_{z_{i-1}} \\ &= \frac{\pi^2}{3}\mathcal{C}^i - \tilde{\mathcal{I}}^i_- - \tilde{\mathcal{I}}^i_+ + \frac{1}{2}C^{-1}[L(\theta)\varepsilon(\theta)]^{z_i}_{z_{i-1}}\,, \end{aligned} \tag{3.48}$$

where the TBA equation for the plateaux (3.30) has been used. To get rid of the surface term it is again convenient to set:

$$\tilde{\mathcal{J}}^i \equiv \mathcal{J}^i - \frac{1}{2}C^{-1}[L(\theta)\varepsilon(\theta)]^{z_i}_{z_{i-1}}\,, \tag{3.49}$$

so that (3.48) finally reads:

$$\tilde{\mathcal{J}}^i = \frac{\pi^2}{3}\mathcal{C}^i - \tilde{\mathcal{I}}^i_- - \tilde{\mathcal{I}}^i_+ = \frac{\pi^2}{3}\left[-\delta_{1,i}c_- + \delta_{2k,i}c_+\right] - \tilde{\mathcal{I}}^i_- - \tilde{\mathcal{I}}^i_+\,. \tag{3.50}$$

Equation (3.50) selects the desired integrals in (3.36) if we choose (equivalently) $i = 1$ or $i = 2k$. For $i = 1$ we have:

$$\begin{aligned} c_- &= -\frac{3}{\pi^2}\left(\tilde{\mathcal{J}}^1 + \tilde{\mathcal{I}}^1_- + \tilde{\mathcal{I}}^1_+\right) \\ &= -\frac{3}{\pi^2}\left(\tilde{\mathcal{J}}^1 - \tilde{\mathcal{I}}^3_-\right) \\ &= -\frac{3}{\pi^2}\left(\tilde{\mathcal{J}}^1 + \tilde{\mathcal{J}}^3 - \tilde{\mathcal{I}}^5_-\right) \\ &= \dots \\ &= -\frac{3}{\pi^2}\sum_{i=1}^{k}\tilde{\mathcal{J}}^{2i-1}\,, \end{aligned} \tag{3.51}$$

where the second equality follows from $\tilde{\mathcal{I}}^1_- = -\tilde{\mathcal{I}}^{-1}_+ = 0\,, \tilde{\mathcal{I}}^1_+ = -\tilde{\mathcal{I}}^3_- = 0$ and then we have repeatedly used $\tilde{\mathcal{I}}^i_- = -\tilde{\mathcal{J}}^i + \tilde{\mathcal{I}}^{i+2}_-$ for $1 < i < 2k$. The cascade stops when $\tilde{\mathcal{J}}^{2k+1} = 0$ is met. From equations (3.39) and (3.49) we get:

$$\begin{aligned} \tilde{\mathcal{J}}^{2i-1} &= \mathcal{J}^{2i-1} - \frac{1}{2}[L(\theta)\varepsilon(\theta)]^{z_{2i-1}}_{z_{2i-2}} \\ &= \int_{\varepsilon_{2i-2}}^{\varepsilon_{2i-1}} d\varepsilon\, \ln\left(1+e^{-\varepsilon}\right) - \frac{1}{2}\left[\varepsilon_{2i-1}\ln\left(1+e^{-\varepsilon_{2i-1}}\right) - \varepsilon_{2i-2}\ln\left(1+e^{-\varepsilon_{2i-2}}\right)\right]\,. \end{aligned} \tag{3.52}$$

Now if we use the representation (2.59) of the Dilogarithm function $\mathrm{Li}_2(z)$ the integral in the previous equation reads $\mathcal{J}^{2i-1} = \mathrm{Li}_2(-e^{-\varepsilon_{2i-1}}) - \mathrm{Li}_2(-e^{-\varepsilon_{2i-2}})$. Furthermore, we can combine $\mathcal{J}^{2i-1}$ and the surface term via the following relation between $\mathrm{Li}_2(z)$ and Roger's dilogarithm $\mathcal{L}(z)$, which holds for $x > -1$ and is a slight modification of (2.58):

$$\mathcal{L}\left(\frac{x}{1+x}\right) = -\mathrm{Li}_2(-x) - \ln(1+x)\ln(x) \tag{3.53}$$

so that (3.52) reads:

$$\tilde{\mathcal{J}}^{2i-1} = -\mathcal{L}\left(\frac{x_i}{1+x_i}\right) + \mathcal{L}\left(\frac{y_i}{1+y_i}\right)\,, \tag{3.54}$$

with $x_i = e^{-\varepsilon_{2i-1}}$ and $x_i = e^{-\varepsilon_{2i-2}}$ being the solutions of (3.31), $i = 1, \dots, k$. Therefore we finally obtain the UV limit of the staircase model's scaling function:

$$\lim_{y,\theta_0\to\infty} c(y,\theta) = \frac{6}{\pi^2}\sum_{i=1}^{k}\left[\mathcal{L}\left(\frac{x_i}{1+x_i}\right) - \mathcal{L}\left(\frac{y_i}{1+y_i}\right)\right] \equiv c_k \tag{3.55}$$

where the limits $y, \theta_0 \to +\infty$ are performed keeping the ratio y/θ_0 fixed as in (3.21). To evaluate the sum in the previous equation we use the fact that if the quantities x_i satisfy the chain of relations (3.31) with $C^{-1} = 1/2$ then the following sum rule for Roger's dilogarithm holds [35]:

$$\frac{6}{\pi^2} \sum_{i=1}^{k} \mathcal{L}\left(\frac{1}{1+x_i}\right) = \frac{2k}{k+3} \tag{3.56}$$

and an identical one holds substituting y_i to x_i. Using these relations and the identity:

$$\mathcal{L}\left(\frac{x}{1+x}\right) = \frac{\pi^2}{6} - \mathcal{L}\left(\frac{1}{1+x}\right) \tag{3.57}$$

the right-hand side of (3.55) yields:

$$c_k = 1 - \frac{6}{(k+2)(k+3)}\,, \quad k = 1, 2, \ldots \tag{3.58}$$

which is precisely the central charge of the unitary minimal model $\mathcal{M}_n$, with $n = k+2 \geq 3$, as expected from the numerical results in figure 3.3.

As a final remark, we mention that (3.58) can be directly obtained from the more general result proved in [20] for modified affine Toda field theories by choosing the rank of the Lie algebra (*i.e.* the number of particles) $r = 1$ and the dual Coxeter number $h = 2$, which corresponds to selecting the $\mathcal{M}_n$ series among the rational conformal field theories.

Chapter 4

Generalized hydrodynamics of the staircase model

The physics of many-body quantum systems out of thermal equilibrium has received a lot of attention in recent years, motivated by the successful experimental realization of these systems using cold atomic gases [11, 40]. It has been observed that when there are extensively many conserved charges, the time evolution of a system initially prepared in a non-thermal state does not lead to Gibbs thermalization in a traditional sense: what is instead observed is the realization of a generalized Gibbs ensemble (GGE) characterized by all the local and quasi-local charges, with non-equilibrium steady state currents due to ballistic transport [12]. These phenomena are coherently described within the theoretical framework of generalized hydrodynamics (GHD) [15, 16, 41], which is based on the assumption of local entropy maximization and provides a quasi-particle representation of GGEs by extending the TBA techniques discussed in chapter 2.

In this chapter, we present the the main principles and results of Euler-scale generalized hydrodynamics and apply them to the study of the staircase model. The peculiar features of this scattering theory, already observed when describing its TBA structure in the previous chapter, strongly affect its hydrodynamics. In particular, unlike any other massive integrable QFT studied so far within the GHD picture[1], the effective velocities of the quasi-particles are strongly non monotonic, displaying a structure which bears resemblance to the one observed in the GHD profiles of A_n massless flows [42]. In the last part of the chapter we describe how these features must be taken into account when implementing the simplest off-equilibrium setup (partitioning protocol with thermal reservoirs), leaving to the next chapter a detailed discussion of GHD steady state currents in the staircase model.

[1] To the best of the author's knowledge.

4.1 Non-equilibrium quantum systems and emergent hydrodynamics

There are different approaches which can be used to describe many-body quantum systems out of equilibrium. The one we will follow, and which is particularly suited to study the appearence of hydrodynamic features, is the Hamiltonian reservoir approach: the off-equilibrium quantum system is connected to an external thermal bath, and togheter they form a closed system with unitary time evolution. This framework finds its best practical realization in the so-called *partitioning protocol* [1, 14], which is implemented by joining together at a time $t = 0$ two quantum systems independently thermalized at temperatures T_l and T_r. In the $(1 + 1)$-dimensional case we can think of these systems as two semi-infinite halves joined at $x = 0$, with the left reservoir at $x = -\infty$ and the right reservoir at $x = +\infty$, see figure 4.1.

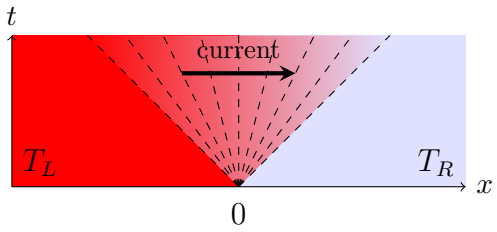

Figure 4.1: Partitioning protocol. Dashed lines represent different rays $\xi = \frac{x}{t}$. Diffusion occurs only inside the light cone defined by the particles' maximum velocity, and the reservoir are unaffected outside of it. The non equilibrium steady state lies at $\xi = 0$.

The steady state which is formed near the junction at a large time is described by a time-evolved density matrix $\rho(t) = e^{-iHt}\rho_0 e^{iHt}$, where $H = H_r + H_l + \delta H$ is the exact Hamiltonian ruling the time evolution and the initial state is:

$$\rho_0 = \rho_l \otimes \rho_r = \mathfrak{n}\left(e^{-\beta_l H_l - \beta_r H_r}\right) , \quad \mathfrak{n}(A) \equiv \frac{A}{\mathrm{Tr}[A]} \tag{4.1}$$

so that the average of any local observable O in this state is:

$$\mathcal{O}^{\mathrm{sta}} = \lim_{t\to+\infty} \mathrm{Tr}[\rho(t)O] = \lim_{t\to+\infty} \langle e^{iHt} O e^{-iHt}\rangle_0 \, . \tag{4.2}$$

If such a steady state exists, then it is a maximal entropy state involving all the conserved charges in the dynamics. Systems which possess few conserved charges usually relax towards a traditional Gibbs ensemble, where there are no steady state currents. But if there are enough charges, it is possible that the steady state admits non-equilibrium stationary currents, carried by quasi-particles at the mesoscopic level. Roughly speaking,

this means that if the system is integrable, the conserved charges are "too many" to allow for a traditional thermalization, and there is ballistic transport in the non-equilibrium steady state (NESS). Diffusion in the steady state is bound to take place inside a light cone [13] defined by the quasi-particle maximum velocity, that is $x/t = \pm 1$ in the relativistic case[2], while the asymptotic reservoirs are unaffected by the NESS currents at any finite time.

An exact result has been found [1] for the steady state energy current when the left and right subsystem are integrable QFT near a conformal critical point. In that case, there are left-movers (particles coming from the reservoir at $x = +\infty$) carrying a mean energy density $\mathrm{h}_l = \frac{\pi c}{6} T_l^2$ and right-movers (from the reservoir at $x = -\infty$) carrying a mean energy density $\mathrm{h}_r = \frac{\pi c}{6} T_r^2$. This means that if $T_l \neq T_r$ there is a non-zero energy current within the light cone, and in the UV limit $T_r\,, T_l \to +\infty$ (with T_l/T_r fixed) the NESS average energy current and density are given by:

$$\langle j \rangle^{\mathrm{sta}} = \frac{1}{2}(\mathrm{h}_l - \mathrm{h}_r) = \frac{c\pi}{12}(T_l^2 - T_r^2) \tag{4.3}$$

$$\langle h \rangle^{\mathrm{sta}} = \frac{1}{2}(\mathrm{h}_l + \mathrm{h}_r) = \frac{c\pi}{12}(T_l^2 + T_r^2) \tag{4.4}$$

with c the central charge of the CFT.

Let us now investigate how hydrodynamics emerges in a quantum many-body system out of equilibrium, starting from a homogeneous system with a finite number of local charges:

$$Q_i = \int \mathrm{d}x\, q_i(x,t)\,, \quad i = 1, 2, \ldots, N \tag{4.5}$$

which are pairwise commuting: $[Q_i, Q_j] = 0\ \forall\, i, j = 1, \ldots, N$. It is customary to identify the first two conserved charges with the Hamiltonian and the momentum, $Q_1 = H$, $Q_2 = P$, so that the conservation laws read $\dot{Q}_i = i[Q_1, Q_i] = 0$. Recall from chapter 1 that by "local" we mean that the densities $q_i(x,t)$ entering (4.5) commute with the Hamiltonian density at space-like separations. The continuity equations relating the charge densities and their currents $j_i(x,t)$ are the usual differential equations:

$$\partial_t q_i(x,t) + \partial_x j_i(x,t) = 0\,, \quad i = 1, 2, \ldots, N \tag{4.6}$$

If we believe the Boltzmann principle of entropy maximization to hold at the macroscopic scale, then after a sufficiently large time the system reaches a state ρ which maximizes $S[\rho] = -\operatorname{Tr}[\rho \ln \rho]$ under the $N + 1$ constraints coming from the separate

[2]This holds when particles can move at the speed of light $c = 1$, while in the more general case the light cone is defined by a Fermi velocity $v_F < 1$. However, equations (4.3), (4.4) for the steady state energy current and density are universal.

conservation of all the charges and the overall normalization of ρ. From the variation:

$$\delta \operatorname{Tr}\left[\rho\left(\ln\rho+\sum\beta_i Q_i+\alpha\right)\right]=0\Rightarrow \operatorname{Tr}\left[\delta\rho\left(\ln\rho+1+\sum\beta_i Q_i+\alpha\right)\right]=0\,, \tag{4.7}$$

we obtain the density matrix of the resulting Gibbs ensemble:

$$\rho=\mathfrak{n}\left(e^{-\sum_{i=1}^{N}\beta_i Q_i}\right) \tag{4.8}$$

with the normalization map defined as in (4.1). The set of generalized inverse temperatures $\boldsymbol{\beta}=(\beta_1,\beta_2,\ldots,\beta_N)$ works as a coordinate system for the manifold of maximal entropy states. The average of a local observable $O(x,t)$ in this state is given by $\langle O\rangle_{\boldsymbol{\beta}}=\operatorname{Tr}[\rho O]$ and it is independent of space-time coordinates as the system is globally homogeneous and stationary. Let us now define:

$$\mathrm{q}_i=\langle q_i(0,0)\rangle_{\boldsymbol{\beta}}\quad,\quad \mathrm{j}_i=\langle j_i(0,0)\rangle_{\boldsymbol{\beta}} \tag{4.9}$$

and notice that we can write any average of a charge density as the derivative of the model-specific free energy density:

$$f(\boldsymbol{\beta})=-\lim_{L\to+\infty}\frac{1}{L}\ln\operatorname{Tr}\left[e^{-\sum_{i=1}^{N}\beta_i Q_i}\right] \tag{4.10}$$

with respect to one of the β_i. With this sign choice in the previous equation, the Hessian matrix of $f(\boldsymbol{\beta})$ is the opposite of the static covariance matrix [43]:

$$C_{ij}=-\frac{\partial^2 f(\boldsymbol{\beta})}{\partial\beta_i\partial\beta_j}=\int \mathrm{d}x\,\langle q_j(0,0)q_i(x,0)\rangle^c_{\boldsymbol{\beta}}=C_{ji}\,, \tag{4.11}$$

and usually C is positive definite so that the map $\boldsymbol{\beta}\to\mathbf{q}\equiv(\mathrm{q}_1,\ldots,\mathrm{q}_N)$ is a bijection: the average densities of conserved charges are good coordinates to parametrize a maximal entropy state. This means that we can express also the current densities $\mathbf{j}(\boldsymbol{\beta})\equiv(\mathrm{j}_1,\ldots,\mathrm{j}_N)$ as functions of $\mathbf{q}$:

$$\mathbf{j}=\mathbf{j}(\mathbf{q})\,, \tag{4.12}$$

and once the functional dependence is made explicit, one has an equation of state for the model. Finally, it is simple to show that, because of space and time translation invariance, also the matrix:

$$B_{ij}=\frac{\partial \mathrm{j}_i(\boldsymbol{\beta})}{\partial\beta_j}=\int \mathrm{d}x\,\langle j_i(0,0)q_j(x,0)\rangle^c_{\boldsymbol{\beta}} \tag{4.13}$$

is symmetric, which means that the one-form $\sum_i \mathrm{j}_i\mathrm{d}\beta_i$ is closed. Assuming that the manifold of maximal entropy states is regular enough, this implies that it is also an

exact form, thus we can write the average current densities as derivatives of a different free energy density $g(\boldsymbol{\beta})$:

$$\mathrm{q}_i = \frac{\partial f(\boldsymbol{\beta})}{\partial \beta_i}\,, \quad \mathrm{j}_i = \frac{\partial g(\boldsymbol{\beta})}{\partial \beta_i}\,, \quad i = 1, \dots, N\,. \tag{4.14}$$

In general a system may be prepared in a state which is non-stationary and inhomogeneous, so that the observable averages $\langle O(x,t)\rangle$ explicitly depend on space-time coordinates. In this context, the emergence of hydrodynamics is based on the assumption of *local* entropy maximization: that is, the assumption that at large space and time scales the averages can be evaluated in a Gibbs ensemble with space-time dependent inverse temperatures $\beta_i(x,t)$:

$$\langle O(x,t)\rangle \approx \langle O(0,0)\rangle_{\boldsymbol{\beta}(x,t)} = \mathrm{Tr}[\rho(x,t)O]\,. \tag{4.15}$$

The validity of this assumption has to be tested model by model and it is in general very difficult to prove, but it is based on the very sensible principle of separation of scales (see figure 4.2): if we wait long enough, fluctuations in the averages are expected to take place at scales which are very large with respect to the microscopic ones, but still extremely small with respect to the macroscopic scales where the full thermalization to a global, homogeneous Gibbs ensemble takes place. Thus, the appropriate lenght scale at which hydrodynamic takes place is the *mesoscopic* one: a (locally) homogeneous Gibbs ensemble is reached at every "fluid cell"labelled by (x,t), and (4.15) is (nearly) valid after a local relaxation time τ_{rel}, with $\tau_{\mathrm{micro}} \ll \tau_{\mathrm{rel}} \ll \tau_{\mathrm{macro}}$.

Conservation laws at the mesoscopic level relate the changes of average currents and densities between neighbouring fluid cells. To see this, we can consider an integration contour $[x_1, x_2] \times [t_1, t_2]$ containing a macroscopic number of cells and integrate (4.6) along the latter:

$$\int_{x_1}^{x_2} \mathrm{d}x\, (q_i(x,t_2) - q_i(x,t_1)) + \int_{t_1}^{t_2} \mathrm{d}t\, (j_i(x_2,t) - j_i(x_1,t)) = 0\,. \tag{4.16}$$

Then, denoting space-time dependent averages by:

$$\mathrm{q}_i(x,t) = \langle q_i(0,0)\rangle_{\boldsymbol{\beta}(x,t)}\,, \quad \mathrm{j}_i(x,t) = \langle j_i(0,0)\rangle_{\boldsymbol{\beta}(x,t)} \tag{4.17}$$

and taking the expectation value of (4.16) we obtain N macroscopic conservation laws:

$$\int_{x_1}^{x_2} \mathrm{d}x\, (\mathbf{q}(x,t_2) - \mathbf{q}(x,t_1)) + \int_{t_1}^{t_2} \mathrm{d}t\, (\mathbf{j}(x_2,t) - \mathbf{j}(x_1,t)) = 0\,, \tag{4.18}$$

which can be re-written in differential form as:

$$\partial_t \mathbf{q}(x,t) + \partial_x \mathbf{j}(x,t) = 0\,. \tag{4.19}$$

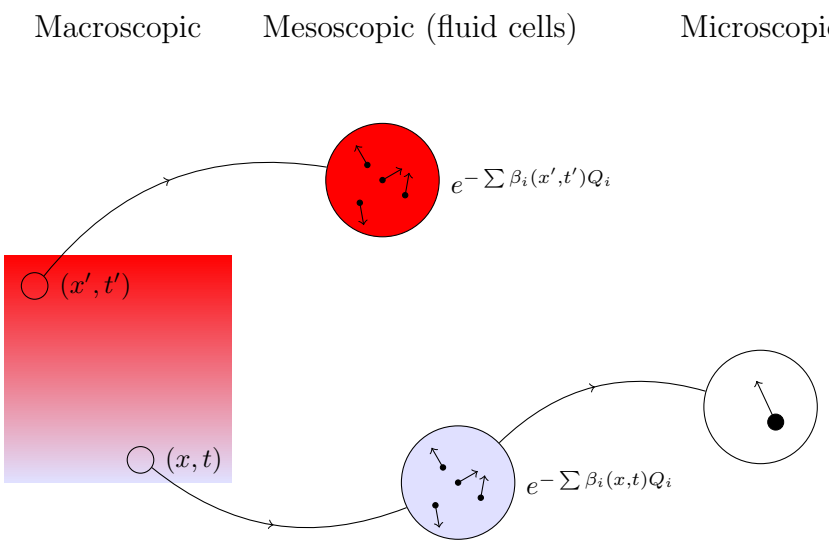

Figure 4.2: The separation of scales upon which relies the local entropy maximization hypothesis.

These are the Euler hydrodynamic equations of the model. They can be rewritten as wave equations thanks to (4.12):

$$\partial_t \mathbf{q}(x,t) + J(\mathbf{q}(x,t))\partial_x \mathbf{q}(x,t) = 0\,, \tag{4.20}$$

where $J(\mathbf{q})$ is the $N \times N$ flux Jacobian matrix of the transformation $\mathbf{q} \to \mathbf{j}(\mathbf{q})$:

$$J(\mathbf{q})_{ij} = \frac{\partial \mathrm{j}_i(\mathbf{q})}{\partial \mathrm{q}_j}\,, \quad i,j = 1,\dots,N. \tag{4.21}$$

It is possible to use a different set of coordinate to parametrize the maximal entropy state. Suppose that $\mathbf{n}(x,t) = (\mathrm{n}_1,\dots,\mathrm{n}_N)$ is such that $\mathbf{q} = \mathcal{F}^q(\mathbf{n})$ and $\mathbf{j} = \mathcal{F}^j(\mathbf{n})$, with $\mathcal{F}^q$ and $\mathcal{F}^j$ regular maps. Then $\mathbf{n}(x,t)$ are valid coordinates and (4.20) becomes:

$$\partial_t \mathbf{n}(x,t) + J(\mathbf{n}(x,t))\partial_x \mathbf{n}(x,t) = 0\,. \tag{4.22}$$

Notice that $J(\mathbf{q})$ and $J(\mathbf{n})$ are related by a similarity transformation:

$$J(\mathbf{n}) = R^{-1} J(\mathbf{q})_{\mathbf{q}=\mathcal{F}^q(\mathbf{n})} R\,, \quad R = \boldsymbol{\nabla}_{\mathbf{n}} \mathbf{j} \tag{4.23}$$

so that the spectrum of the Jacobian is independent of the coordinates. Furthermore, from the symmetry of the matrix (4.13) it is possible to show that its eigenvalues are real. It is therefore useful to choose a coordinate system in which $J(\mathbf{n})$ is diagonal, so that there are no convective derivatives and Euler equations reduce to:

$$\partial_t \mathrm{n}_i(x,t) + v_i^{\mathrm{eff}}(\mathbf{n}(x,t))\partial_x \mathrm{n}_i(x,t) = 0\,, \quad i = 1,\dots,N. \tag{4.24}$$

The quantities n_i are the normal modes of Euler hydrodynamics, and the eigenvalues $v_i^{\mathrm{eff}}(\mathbf{n}(x,t))$ are the *effective velocities* at which they propagate. In the next section we will show that it is possible to find an explicit expression for the effective velocities employing the pseudo-particle description ad the machinery of generalized TBA.

Let us now come back to the partitioning protocol introduced at the beginning of this section, using $\mathbf{q}$-coordinates for simplicity. Equations (4.20) are invariant under the scaling $(x,t) \to (ax, at)$ so that we may assume the existence of self-similar solutions (at least in the large scale limit $a \to +\infty$), which depend only on the ray $\xi = x/t$, that is $\mathbf{q}(x,t) = \mathbf{q}(\xi)$, $\boldsymbol{\beta}(x,t) = \boldsymbol{\beta}(\xi)$. Recasting the derivatives in terms of ξ, (4.20) becomes an eigenvalue equation for the ray-dependent Jacobian:

$$(J(\mathbf{q}) - \xi \mathbb{1})\partial_\xi \mathbf{q} = 0\,. \tag{4.25}$$

The initial condition $t \to 0^+$ is fixed by the state of the inhomogeneous system at the local relaxation time, which is in general unknown. However, as $|x| \to \infty$ any average is evaluated in the Gibbs state of one of the two reservoirs, which are at generalized inverse temperatures $\boldsymbol{\beta}^{r,l}$. As $|x|$ is very large, the limit $t \to 0^+$ corresponds to $\xi \to \pm\infty$, so that the initial value problem is:

$$\lim_{\xi\to\pm\infty} \mathbf{q}(\xi) = \lim_{x\to\pm\infty} \langle \underline{q}(x,0)\rangle_{\mathrm{ini}} = \mathbf{q}_{\boldsymbol{\beta}^{r,l}}\,, \tag{4.26}$$

with $\underline{q} \equiv (q_1, \dots, q_N)$. On the other hand, for every fixed x a steady state is reached in the limit $t \to +\infty$, which corresponds to $\xi \to 0$. Thus the steady state averages are:

$$\mathbf{q}^{\mathrm{sta}} = \lim_{\xi\to 0} \mathbf{q}(\xi)\,, \quad \mathbf{j}^{\mathrm{sta}} = \lim_{\xi\to 0} \mathbf{j}(\xi)\,. \tag{4.27}$$

If the two subsystems are near a conformal critical point with central charge c, then $\mathrm{j}_1^{\mathrm{sta}}$ and $\mathrm{q}_1^{\mathrm{sta}}$ are given by (4.3) and (4.4) respectively. We will present in the next chapter a generalization of these expressions for the averages of higher-spin charges.

4.2 Generalized hydrodynamics

In an integrable model there is in general an infinite number of conservation laws, and this strongly affects the thermalization properties of the systems. It is believed -and it has been successfully tested in some specific cases, both theoretically and experimentally [11, 12]- that after a long enough relaxation time the state of the system converges to a generalized Gibbs ensemble (GGE), rather than to a traditional Gibbs ensemble. The density matrix of a GGE is obtained maximizing the entropy under an infinite number of constraints, and that reduces to taking the limit $N \to +\infty$ in (4.8):

$$\rho_{\mathrm{gen}} = \mathfrak{n}\left(e^{-\sum_{i=1}^{+\infty} \beta_i Q_i}\right) \tag{4.28}$$

where again $Q_1 = H$, $Q_2 = P$ and all the charges are in involution. There are two delicate points which must be dealt with when one considers a generalized Gibbs ensemble:

- *quasi-local charges*. The sum in (4.28) is usually enlarged to include also quasi-local charges. In a continuous system a local charge is defined by the fact that it is obtained integrating a density $q(x,t)$ which is non-vanishing only in a limited spatial support. Quasi-local charges are instead characterized by densities which have an extended support but an exponentially decaying operatorial norm at large distances. Their inclusion in the GGE is necessary in order to build a complete set of conserved charges in the space of maximal entropy states, which is now infinite-dimensional [44]. Once all the charges in the model have been identified, one should define in a precise way the convergence properties of the series $\sum_{i=1}^{+\infty} \beta_i Q_i$, which is usually done by fixing the potentials β_i through successive truncations and may involve finite-volume regularization.

- *boundary conditions*. In a finite volume, the conserved quantities in the model depend on the specific boundary conditions. For instance, the presence of walls preclude any non-zero potential β_2 for the conserved momentum, as translational invariance is broken. However, given a set of allowed conserved quantities, if the volume is large enough then the boundary condition have little effects on the specific free energy and therefore on the local current and charge averages. Furthermore, it is possible to construct a GGE directly in an infinite volume, and in that case the maximal set of conserved charges is provided by periodic boundary conditions, which are precisely the ones used in the TBA approach. Therefore we will assume that the available conserved charges are those compatible with the TBA boundary conditions.

Apart from these technical problems, the physical principles underlying local entropy maximization and fluid-cell thermalization are still expected to hold: the assumption (4.15) is sufficient to evaluate all the one-point averages $\mathrm{q}_i(x,t)$ and $\mathrm{j}_i(x,t)$ in a GGE with infinite space-time dependent inverse temperatures $\beta_i(x,t)$. This is the generalized hydrodynamic (GHD) picture. Since integrability is now at play, we can extend the TBA formalism to generalized Gibbs ensembles and use the quasi-particle formulation to solve the hydrodynamic equations.

4.2.1 TBA and equations of state in a generalized Gibbs ensemble

The TBA picture is easily generalized to systems with infinitely many conserved charges. The latter are defined by their eigenvalues when acting on one-particle asymptotic states $|\theta\rangle$:

$$Q_i |\theta\rangle = h_i(\theta) |\theta\rangle , \quad i = 1, 2, \dots \tag{4.29}$$

and assuming that there is a single relativistic particle species of mass m, the first eigenvalues are parametrized in the usual way:

$$h_1(\theta) = E(\theta) = m\cosh(\theta)\,, \quad h_2(\theta) = p(\theta) = m\sinh(\theta)\,. \tag{4.30}$$

In infinite volume, a TBA state is fully described by two continuous distributions in the rapidity space: the particle density $\rho_p(\theta)$ and the hole density $\rho_h(\theta)$. In a fermionic-type system the sum $\rho_p(\theta) + \rho_h(\theta)$ is the total density of Bethe states, and the occupation function is defined by $n(\theta) = \rho_p(\theta)/(\rho_p(\theta) + \rho_h(\theta))$. In a GGE, the average charge densities $\mathrm{q}_i = \langle q_i \rangle_{\boldsymbol{\beta}}$ are given by:

$$\mathrm{q}_i = \mathrm{Tr}[\rho_{\mathrm{gen}} q_i] = \int \mathrm{d}\theta\, \rho_p(\theta) h_i(\theta)\,, \quad i = 1, 2, \dots \tag{4.31}$$

where here and below all the integrations are over $\mathbb{R}$. The previous equation generalizes (2.20) to all the conserved charges[3] and may be seen as a definition of $\rho_p(\theta)$. In the GHD setting, the TBA distributions become space-time dependent at the mesoscopic scale:

$$\rho_p(\theta) \to \rho_p(\theta; x, t)\,, \quad \rho_h(\theta) \to \rho_h(\theta; x, t)\,, \quad n(\theta) \to n(\theta; x, t) \tag{4.32}$$

and thanks to the local entropy maximization assumption (4.15) this dependence is moved to the inverse temperatures $\boldsymbol{\beta} = \boldsymbol{\beta}(x, t)$ so that $\mathrm{q}_i(x, t) = \mathrm{Tr}[\rho_{\mathrm{gen}}(x, t) q_i(0, 0)]$. The explicit dependence on (x, t) will be generally omitted from now on.

The coordinate Bethe ansatz, in the thermodynamic limit, becomes the constraint (2.24) between $\rho_p(\theta)$ and $\rho_h(\theta)$, which we rewrite as:

$$2\pi[\rho_p(\theta) + \rho_h(\theta)] = p'(\theta) + \int \mathrm{d}\alpha\, \phi(\theta - \alpha)\rho_p(\alpha)\,. \tag{4.33}$$

Now let us define the dressing of a generic function $h(\theta)$ via a linear integral operation:

$$h \mapsto h^{\mathrm{dr}}\,, \quad h^{\mathrm{dr}}(\theta) = h(\theta) + \int \frac{\mathrm{d}\alpha}{2\pi}\, \phi(\theta - \alpha) n(\alpha) h^{\mathrm{dr}}(\alpha)\,. \tag{4.34}$$

Notice that the dressing of bare observables due to a non-zero interaction kernel ϕ is not peculiar of GHD, as it can be defined already in the equilibrium TBA setting. The linearity of this operation is expressed by the relation:

$$[\alpha f(\theta) + \beta g(\theta)]^{\mathrm{dr}} = \alpha f^{\mathrm{dr}}(\theta) + \beta g^{\mathrm{dr}}(\theta)\,, \tag{4.35}$$

where α and β are constants. Moreover, the dressing equation satisfies the symmetry relation:

$$\int \mathrm{d}\theta\, f(\theta) n(\theta) g^{\mathrm{dr}}(\theta) = \int \mathrm{d}\theta\, g(\theta) n(\theta) f^{\mathrm{dr}}(\theta)\,, \tag{4.36}$$

[3] recall that q_i is a charge *density* and in a homogeneous and stationary Gibbs ensemble with finite spatial volume L it holds $Q_i = \int \mathrm{d}x\, q_i(x, t) = \int \mathrm{d}x\, q_i(0, 0) = L q_i$.

for any pair of integrable functions f and g. Both equations (4.35) and (4.36) trivially follow from (4.34) and will be extensively used in the following.

By using the definition of $n(\theta)$ and of the dressing operation, the Bethe constraint (4.33) can be rewritten as follows:

$$2\pi\rho_p(\theta) = n(\theta)[p'(\theta)]^{\mathrm{dr}} \tag{4.37}$$

or, equivalently:

$$2\pi[\rho_p(\theta) + \rho_h(\theta)] = [p'(\theta)]^{\mathrm{dr}} \,. \tag{4.38}$$

Note that the order in which the derivative with respect to θ and the dressing are performed is important, as in general[4] $[h'(\theta)]^{\mathrm{dr}} \neq [h^{\mathrm{dr}}(\theta)]'$. The right-hand side of (4.37) depends only on the occupation function, so that this relation is a map between $\rho_p(\theta)$ and $n(\theta)$ as state coordinates for the GGE in the TBA description. The map between $\rho_p(\theta)$ and the set of averages $\mathbf{q}$ is given by (4.31). The inverse temperatures $\boldsymbol{\beta} = (\beta_1, \beta_2, \dots)$ can be used as state coordinates also in a generalized Gibbs state, and they are recovered from the generalized TBA self-consistency equation satisfied by a generalized pseudoenergy ε_w, related to $n(\theta)$ as in (2.33):

$$n(\theta) = \frac{1}{1 + e^{\varepsilon_w(\theta)}} \,. \tag{4.39}$$

The derivation of the TBA equation in the GHD setting [45] follows the same lines of the procedure employed in Chapter 2, so that we will only sketch it here. The starting point is the definition of a generalized, dimensionless free energy $F(\boldsymbol{\beta}) = \lim_{L\to+\infty} Lf(\boldsymbol{\beta})$ and the corresponding GGE partition function:

$$f\left(\boldsymbol{\beta}\right) = -\lim_{L\to+\infty} \frac{1}{L} \ln \mathcal{Z}_{\mathrm{gen}} \,, \quad \mathcal{Z}_{\mathrm{gen}} = \mathrm{Tr}\left[e^{-\sum_{i=1}^{+\infty}\beta_i Q_i}\right] \,. \tag{4.40}$$

From standard thermodynamic arguments, the equilibrium densities $\rho_p(\theta)$, $\rho_h(\theta)$ are obtained by minimizing the generalized free energy functional:

$$F\left[\boldsymbol{\beta}; \rho_p, \rho_h\right] = \sum_{i=1}^{+\infty} \beta_i \langle Q_i \rangle_{\boldsymbol{\beta}} - S[\rho_p, \rho_h] \tag{4.41}$$

while enforcing the Bethe equation of state (4.33). This is of course equivalent to maximize the entropy while imposing an infinite number of constraints on the conservation

[4] It is easy to see that the two operations commute provided $(\phi * (h^{\mathrm{dr}} n'))$ is zero almost everywhere, which holds for instance if the system is prepared in a pure state, so that $n(\theta) = 0$ except at a single point.

of the charges Q_i. In the previous equation, the entropy at leading order in L is given by (2.28) and, thanks to (4.31):

$$\sum_{i=1}^{+\infty} \beta_i \langle Q_i \rangle_{\boldsymbol{\beta}} = L \sum_{i=1}^{+\infty} \beta_i \int \mathrm{d}\theta \, \rho_p(\theta) h_i(\theta) \,. \tag{4.42}$$

The functional minimization of $F\left[\boldsymbol{\beta}; \rho_p, \rho_h\right]$ with respect to ρ_p, ρ_h yields the GGE TBA equation:

$$\varepsilon_w(\theta) = w(\theta) - \int \frac{\mathrm{d}\alpha}{2\pi} \, \phi(\theta - \alpha) L_w(\alpha) \,, \quad L_w(\theta) \equiv \ln\bigl(1 + e^{-\varepsilon_w(\theta)}\bigr) \tag{4.43}$$

where now the driving term is:

$$w(\theta) \equiv \sum_{i=1}^{+\infty} \beta_i h_i(\theta) \,. \tag{4.44}$$

The free energy density $f(\boldsymbol{\beta})$ is then given by the stationary value of the functional (4.41):

$$f\left(\boldsymbol{\beta}\right) = - \int \frac{\mathrm{d}\theta}{2\pi} \, p'(\theta) L_w(\theta) \,. \tag{4.45}$$

One can use equation (4.43) in either of two ways, depending on the available data. If the set of generalized inverse temperatures is known, then the TBA equation can be solved for $\varepsilon_w(\theta)$, providing the equilibrium particle density and therefore a map $\boldsymbol{\beta} \mapsto \rho_p(\theta)$ between different GGE state coordinates. On the other hand, if somehow the equilibrium density is known from the beginning (and thus is the generalized pseudoenergy via (4.39)), then the inverse temperatures are obtained from the functional derivatives:

$$\beta_i = \frac{\delta}{\delta h_i(\theta)} \left[\varepsilon_w(\theta) + \frac{1}{2\pi} (\phi * L_w)(\theta) \right] \,, \quad i = 1, 2, \dots \tag{4.46}$$

where in the right-hand side the eigenvalues $h_j(\theta)$ are kept fixed for $j \neq i$.

The TBA machinery provides an explicit expression for the GGE average charge densities q_i. Indeed, from the definition (4.31) and equation (4.37), we have:

$$\mathbf{q}_i = \int \frac{\mathrm{d}\theta}{2\pi} \, (p')^{\mathrm{dr}}(\theta) n(\theta) h_i(\theta) = \int \frac{\mathrm{d}p(\theta)}{2\pi} \, n(\theta) h_i^{\mathrm{dr}}(\theta) \,, \tag{4.47}$$

where the second equation follows from the symmetry relation (4.36). The TBA alone is however not sufficient to derive a similar expression for the average current densities $\mathrm{j}_i = \langle j_i \rangle_{\boldsymbol{\beta}}$. For relativistic models, a way to obtain these quantities is through a *mirror*

transformation, that is, a double Wick rotation which exchanges the roles of space and time coordinates:

$$\mathcal{C} \,:\, (x,t) \,\mapsto\, (it\,,\, -ix)\,. \tag{4.48}$$

This transformation, similar to the one relating s and t-channels in the S-matrix theory, squares to the identity and is implemented on rapidities by $\theta \mapsto i\pi/2 - \theta$. Consequently, the the one-particle energy and momentum eigenvalues $E(\theta) = m\cosh(\theta)$, $p(\theta) = m\sinh(\theta)$ are exchanged as well: $(E,p) \mapsto (-ip\,,\, iE)$. Notice that the signs are consistent with the representations of the corresponding operators on (x,t)-functions, $H = i\partial_t$, $p = -i\partial_x$.

Under a relativistic mirror transformation, one expects current and charge densities to be exchanged: namely, a current density j_i is a charge density q_i in the mirror theory. If $q[h]$ and $j[h]$ are the charge and current densities associated to a one-particle eigenvalue $h(\theta)$ this means:

$$\mathcal{C}(j[h]) = iq[h^{\rm c}]\,, \quad h^{\rm c}(\theta) \equiv h(i\pi/2 - \theta)\,. \tag{4.49}$$

Let us also denote by $\langle O\rangle_w$ the average of an observable O in the GGE characterized by a driving term $w(\theta)$. When a mirror transformation is applied this expectation value transforms as $\langle \mathcal{C}(O)\rangle_w = \langle (O)\rangle_{w^{\rm c}}$, $w^{\rm c}(\theta) = w(i\pi/2-\theta)$. The average of a current density $j[h]$ follows therefore from (4.50) and $\mathcal{C}^2 = {\rm id}$:

$$\langle j[h]\rangle_w = \langle \mathcal{C}(\mathcal{C}(j[h]))\rangle_w = i\langle q[h^{\rm c}]\rangle_{w^{\rm c}} \tag{4.50}$$

thus, from equation (4.47) for $\mathrm{q}_i = \mathrm{q}[h_i]$ and the crossing exchange of E and p one obtains the expression for a current density average $\mathrm{j}_i = \mathrm{j}[h_i]$ in a GGE:

$$\mathrm{j}_i = \int \frac{{\rm d}\theta}{2\pi}\,(E')^{\rm dr}(\theta) n(\theta) h_i(\theta) = \int \frac{{\rm d}E(\theta)}{2\pi}\, n(\theta) h_i^{\rm dr}(\theta)\,. \tag{4.51}$$

We have presented an heuristic derivation of the formula above, but the latter can be rigorously proved using form factors techniques [43]. Moreover, this formula is very sensible from a physical point of view, as it can be cast in the following way:

$$\mathrm{j}_i = \int {\rm d}\theta\, \rho_c(\theta) h_i(\theta) \tag{4.52}$$

where the *spectral density* $\rho_c(\theta)$ has been introduced as the distribution which, by definition, gives a current average when integrated against its one-particle eigenvalue. From (4.37) and (4.51) one has:

$$\rho_c(\theta) = \frac{1}{2\pi} n(\theta)(E')^{\rm dr}(\theta) = v^{\rm eff}(\theta)\rho_p(\theta)\,, \tag{4.53}$$

where

$$v^{\rm eff}(\theta) \equiv \frac{(E')^{\rm dr}(\theta)}{(p')^{\rm dr}(\theta)} = \frac{p^{\rm dr}(\theta)}{E^{\rm dr}(\theta)} \tag{4.54}$$

is the effective velocity of a quasi-particle of rapidity θ. This quantity depends on the ensemble state through the occupation function entering the dressing and represents the modification of the quasi-particle's group velocity $v^{\rm gr}(\theta) = p(\theta)/E(\theta) = \tanh(\theta)$ due to the presence of interactions. A quasi-particle of rapidity θ carries conserved charge eigenvalues $h_i(\theta)$, $i = 1, 2, \ldots$, and moves with a velocity $v^{\rm eff}(\theta)$ so that the corresponding current densities are $v^{\rm eff}(\theta)h_i(\theta)$. The pair of densities (ρ_p, ρ_c) can be used as well to characterize a generalized Gibbs state, together with a self-consistent equation of state which directly follows from the definition of the effective velocity:

$$\frac{\rho_c(\theta)}{\rho_p(\theta)} = \frac{E'(\theta) + \int \mathrm{d}\alpha\, \phi(\theta-\alpha)\rho_c(\alpha)}{p'(\theta) + \int \mathrm{d}\alpha\, \phi(\theta-\alpha)\rho_p(\alpha)}\,. \tag{4.55}$$

A simple manipulation of (4.55) gives an integral equation for $v^{\rm eff}(\theta)$ which can be read as a sort of dressing equation for the group velocity:

$$v^{\rm eff}(\theta) = v^{\rm gr}(\theta) + \int \mathrm{d}\alpha\, \frac{\phi(\theta-\alpha)\rho_p(\alpha)}{p'(\theta)} \left(v^{\rm eff}(\alpha) - v^{\rm eff}(\theta)\right)\,. \tag{4.56}$$

As a concluding remark, we notice that through equations (4.47) and (4.51) the TBA formalism provides an explicit expression for the free energies which generate the expectation values $\mathbf{q}$ and $\mathbf{j}$, as in (4.14) (with $N \to +\infty$). Indeed, take $f_w(\boldsymbol{\beta}) \equiv f(\boldsymbol{\beta})$ defined by (4.45) and define likewise:

$$g_w(\boldsymbol{\beta}) = -\int \frac{\mathrm{d}E(\theta)}{2\pi}\, L_w(\theta)\,. \tag{4.57}$$

Then:

$$\mathrm{q}_i = \frac{\partial f_w}{\partial \beta_i} = \int \mathrm{d}\theta\, h_i(\theta) \frac{\delta f_w}{\delta w(\theta)}\,, \tag{4.58}$$

$$\mathrm{j}_i = \frac{\partial g_w}{\partial \beta_i} = \int \mathrm{d}\theta\, h_i(\theta) \frac{\delta g_w}{\delta w(\theta)}\,, \tag{4.59}$$

$$\tag{4.60}$$

so that a simple partial derivation of f_w and g_w with respect to the inverse temperatures β_i yields the state coordinates q_i and j_i while a functional derivation of the very same generators gives the quasi-particle coordinates $\rho_p(\theta) = \frac{\delta f_w}{\delta w(\theta)}$ and $\rho_c(\theta) = \frac{\delta g_w}{\delta w(\theta)}$

4.2.2 The partitioning protocol

The Euler equations (4.19) for the GGE averages (with again $N \to +\infty$) can be reformulated in terms of the TBA state coordinates thanks to the maps $\rho_p \mapsto \mathbf{q}$ and $\rho_c \mapsto \mathbf{j}$ explicitly provided by equations (4.31) and (4.52). At this point, the inclusion

of all the conserved charges in a generalized Gibbs ensemble (including the quasi-local ones) plays a fundamental role, as the completeness of the sets $\mathbf{q}$ and $\mathbf{j}$ suggests that the one-particle eigenvalues $h_i(\theta)$ appearing in these two equations form a complete set of functions in the rapidity space. Thus, by plugging (4.31) and (4.52) in (4.19) we get (re-introducing the explicit (x,t)-dependence):

$$\begin{aligned} 0 &= \partial_t \rho_p(\theta;x,t) + \partial_x \rho_c(\theta;x,t) \\ &= \partial_t \rho_p(\theta;x,t) + \partial_x [v^{\text{eff}}(\theta;x,t)\rho_p(\theta;x,t)] \,, \end{aligned} \tag{4.61}$$

from which we recognize the typical form of a linear hydrodynamic conservation law, with ρ_p playing the role of a fluid density. The most convenient way to parametrize the state of a GGE is by using the occupation function $n(\theta;x,t)$: indeed this is precisely the choice of coordinates which diagonalize the flux Jacobian $J(\mathbf{n})$ and allows us to rewrite the hydrodynamic equations in the form (4.24), where there are no convective derivatives. Specifically, the normal modes n_i of hydrodynamics are given by the products of one-particle eigenvalues and the TBA occupation function:

$$\mathrm{n}_i(\theta;x,t) = h_i(\theta) n(\theta;x,t) \,, \tag{4.62}$$

while the corresponding propagation velocities are nothing but the effective velocity $v^{\text{eff}}(\theta;x,t)$ defined in (4.54): indeed, at a fixed θ all the normal modes are carried by the corresponding quasi-particle and thus they form a degenerate eigenspace. In the occupation function coordinates the Euler equation (4.61) reads:

$$\partial_t n(\theta;x,t) + v^{\text{eff}}(\theta;x,t)\partial_x n(\theta;x,t) = 0 \tag{4.63}$$

The proof is as follows. First, rewrite the dressing equation (4.34) in the integral operator representation:

$$h^{\text{dr}} = (1-\varphi\mathcal{N})^{-1} h \,, \tag{4.64}$$

where for any sufficiently regular function h:

$$(\mathcal{N}h)(\theta) \equiv \int \mathrm{d}\alpha \, n(\theta)\delta(\theta-\alpha)h(\alpha) = n(\theta)h(\theta) \,, \tag{4.65}$$

$$(\varphi h)(\theta) \equiv \int \frac{\mathrm{d}\alpha}{2\pi} \, \phi(\theta-\alpha)h(\alpha) \,. \tag{4.66}$$

Then define the following symmetric[5] integral operator:

$$\mathcal{S} = \mathcal{N}(1-\varphi\mathcal{N})^{-1} \,, \tag{4.67}$$

[5]The symmetry is intended with respect to the internal product $\langle f,g\rangle \equiv \int \mathrm{d}\theta \, f(\theta)g(\theta)$, so that $\langle f,(\mathcal{S}g)\rangle = \langle g,(\mathcal{S}f)\rangle$.

so that we can rewrite (4.37) and (4.53) as:

$$(\mathcal{S}p')(\theta) = 2\pi\rho_p(\theta)\,, \quad (\mathcal{S}E')(\theta) = 2\pi\rho_c(\theta) \tag{4.68}$$

and therefore equation (4.61) becomes:

$$(\partial_t\mathcal{S})p' + (\partial_x\mathcal{S})E'\,. \tag{4.69}$$

To evaluate the derivatives of the integral operator $\mathcal{S}$ one must expand $(1-\varphi\mathcal{N})^{-1}$ in power series of $\varphi\mathcal{N}$ and then apply the Leibniz distribution rule. This yields:

$$\begin{aligned}\partial_\alpha\mathcal{S} &= \partial_\alpha[\mathcal{N}(1-\varphi\mathcal{N})^{-1}] \\ &= (1-\mathcal{N}\varphi)^{-1}(\partial_\alpha\mathcal{N})(1-\varphi\mathcal{N})^{-1}\end{aligned} \tag{4.70}$$

for $\alpha = x\,,\, t$. Therefore:

$$\begin{aligned}0 &= (1-\mathcal{N}\varphi)^{-1}\left[(\partial_t\mathcal{N})(1-\varphi\mathcal{N})^{-1}p' + (\partial_x\mathcal{N})(1-\varphi\mathcal{N})^{-1}E'\right] \\ &= (1-\mathcal{N}\varphi)^{-1}\left[(\partial_t\mathcal{N})(p')^{\mathrm{dr}} + (\partial_x\mathcal{N})(E')^{\mathrm{dr}}\right]\,,\end{aligned} \tag{4.71}$$

which clearly implies (4.63) from the definition of the effective velocity.

As a concrete application of these results, let us apply them to the solution of the partitioning protocol. Suppose that the two reservoirs are in pure Gibbs states[6] at inverse temperatures $\beta^{r,l}$. from the GHD point of view, this means that all the averages can be evaluated in these initial ensembles by using the occupation functions $n_{r,l}(\theta)$ obtained from the solution of (4.43) with $w^{r,l}(\theta) = T_{r,l}^{-1}E(\theta)$. At $t = 0$ the two systems are connected at $x = 0$ and thus the initial-value problem we have to solve is the following:

$$\begin{cases}\partial_t n(\theta;x,t) + v^{\mathrm{eff}}(\theta;x,t)\partial_x n(\theta;x,t) = 0 \\ \lim\limits_{t\to 0^+} n(\theta;x,t) = n_r\Theta_H(x) + n_l\Theta_H(-x)\end{cases} \tag{4.72}$$

where Θ_H is the Heaviside function. A first-order linear problem with this kind of initial values is called a Riemann problem. Since both the differential equation and the initial condition are invariant under a uniform rescaling of x and t we can again use a ray variable $\xi = x/t$ to rewrite the problem:

$$\begin{cases}[v^{\mathrm{eff}}(\theta;\xi) - \xi]\partial_\xi n(\theta;\xi) = 0 \\ \lim\limits_{\xi\to\pm\infty} n(\theta;\xi) = n_{r,l}(\theta)\end{cases}\,. \tag{4.73}$$

[6]This condition is not strictly necessary: one can consider the partitioning protocol in the more generic situation where the reservoirs are in GGEs with TBA driving terms $w^{r,l}(\theta) = \sum \beta_i^{r,l}h_i(\theta)$, and solve the corresponding equations (4.43) to get the asymptotic values $n_{r,l}(\theta)$. In the next chapter we will explicitly derive some GHD average in a partitioning protocol with non-thermal reservoirs.

Note that the initial-value condition has now turned into a boundary condition equivalent to (4.26), while the first equation is nothing but the eigenvalue problem (4.25) written in the normal modes coordinate system. Once a solution for $n(\theta;\xi)$ is known, one can compute the GHD averages $\mathbf{q}(\xi)$, $\mathbf{j}(\xi)$ for any value of ξ.

The solution to the previous problem is unique given these boundary conditions. Indeed, for a fixed θ, $n(\theta;\xi)$ must be a constant function of the ray ξ except possibly at the value(s) of ξ such that $v^{\rm dr}(\theta;\xi)=\xi$. But since[7] $\lim_{\xi\to\pm\infty}[v^{\rm dr}(\theta;\xi)-\xi]=\mp\infty$, the only solution compatible with the boundary conditions is the following:

$$n(\theta;\xi)=n_l(\theta)\Theta_H\left(v^{\rm eff}(\theta;\xi)-\xi\right)+n_r(\theta)\Theta_H\left(\xi-v^{\rm eff}(\theta;\xi)\right)\,. \tag{4.74}$$

For a fixed ray ξ the construction of the previous global occupation function requires to solve the transcendental equation:

$$v^{\rm eff}(\theta_*(\xi);\xi)=\xi\,, \tag{4.75}$$

and if the effective velocity is a monotonic function of the rapidity there is a unique solution $\theta_*(\xi)$ for every $\xi\in[-1,+1]$. Therefore one can recast (4.74) as:

$$n(\theta;\xi)=n_l(\theta)\Theta_H\left(\theta-\theta_*(\xi)\right)+n_r(\theta)\Theta_H\left(\theta_*(\xi)-\theta\right)\,. \tag{4.76}$$

The physical interpretation of the equation above is quite convincing: if $\theta>\theta_*(\xi)$ then $v^{\rm dr}>\xi$, so the quasi-particles which contribute at the ray ξ come from the left reservoir (that is, they are found at $x<0$ for $t\to0^+$), whereas they come from the right reservoir if $\theta<\theta_*(\xi)$, as then $v^{\rm dr}<\xi$. The solution of (4.76) is a rarefaction wave continuously interpolating between the two reservoirs: shock-like solutions are not needed as in a GGE there is a continuous distribution of normal modes which smoothly connect the asymptotic values at $\xi=\pm\infty$.

4.3 Euler-scale hydrodynamics of the staircase model: numerical results

At this point we have developed all the necessary GHD tools to study the off-equilibrium properties of the staircase model described in the previous chapter. In this section we present some of the numerical results obtained for the occupation function, effective velocity and particle density in a partitioning protocol with thermal reservoirs. The discussion of steady state currents will be carried out in the next chapter.

In order to compute any average in the partitioning protocol, one has to solve the staircase's TBA equations (3.16) for the reservoirs at inverse temperatures $\beta_{r,l}$ and plug

[7] Notice that in the relativistic case $\max_{\theta\in\mathbb{R}}\left|v^{\rm eff}(\theta;\xi)\right|=1$, while in non-relativistic systems $v^{\rm eff}(\theta;\xi)$ is in general not bounded but is finite for every finite θ.

the functions $n_r(\theta)$, $n_l(\theta)$ in equation (4.74) for the occupation function $n(\theta;\xi)$ of the joint system. In order to numerically build this quantity, the zero(s) of the effective velocities must be found in a self-consistent way by solving (4.75). $v^{\text{eff}}(\theta;\xi)$ depends on $n(\theta;\xi)$, as the global occupation function enters the dressing of $E(\theta)$ and $p(\theta)$, thus an iterative procedure must be employed to find the zero(s) of the velocity. In the simplest case where the latter is monotonic, there is only one zero $\theta_*(\xi)$ for each ξ and the iteration is rapidly convergent: one starts with an initial value, say $\theta_*^{(0)} = 0$, which is plugged in (4.76) to obtain $n^{(0)}(\theta;\xi)$. This quantity is then used to solve equation (4.75), which yields a new zero $\theta_*^{(1)}$, again to be plugged in (4.76). The iteration of this procedure thus provides a sequence $\{\theta_*^{(n)}(\xi)\}$ which converges to the true zero, $\lim_{n\to+\infty}\theta_*^{(n)}(\xi) = \theta_*(\xi)$. In practice, a few iterations are sufficient to reach $\theta_*(\xi)$ within a very small error.

Things are more complicated when the effective velocity is non monotonic. This situation is not very common, but might arise in non-diagonal models [42], where there is a multi-particle spectrum which includes magnons. However, quite surprisingly, we found that the effective velocity of the staircase model is non monotonic: to our knowledge, this is the first case to be analyzed of a diagonal, one-particle model where a non monotonic v^{eff} appears. Let us show in detail how this is indeed the case, starting from the thermal equilibrium scenario.

4.3.1 Effective velocity and quasi-particle distributions at equilibrium

To see why the staircase model's effective velocity is in general non monotonic, consider the definition (4.54): any zero of $v^{\text{eff}}(\theta)$ must be either a zero of the numerator $p^{\text{dr}}(\theta)$, or a pole of the denominator $E^{\text{dr}}(\theta)$. It is useful to notice that, by taking the derivative with respect to θ of both sides of the single-particle TBA equation (2.34) (setting $\beta = mR$) and comparing it with the definition (4.34), one has:

$$\varepsilon'(\theta) = [\beta \sinh(\theta)]^{\text{dr}} = T^{-1} p^{\text{dr}}(\theta)\,, \tag{4.77}$$

where the second equality follows from (4.35). Therefore, at any finite temperature the simple zeros of $p^{\text{dr}}(\theta)$ coincide with those of $\varepsilon'(\theta)$. Furthermore, from the definitions (2.33), (2.38) it follows:

$$L'(\theta) = -\varepsilon'(\theta) n(\theta)\,, \tag{4.78}$$

and typically $n(\theta)$ has no zeros while $L'(\theta) = 0$ only in the midpoint of the central plateau. However, as explained in the previous chapter, in the staircase model $L(\theta)$ develops an increasing number of plateaux as the ratio y/θ_0 grows, and their central points are at the positions z_i defined in (3.24), for $i = 1, \ldots, 2k-1$. Thus we expect the effective velocity to be non monotonic, with $v^{\text{eff}}(z_i) = 0$, $i = 1, \ldots, 2k-1$.

The quantity $E^{\rm dr}(\theta)$, on the other hand, does not have any simple pole. Indeed, in analogy with equation (4.77), one can write:

$$\pi'(\theta) = T^{-1} E^{\rm dr}(\theta)\,, \tag{4.79}$$

where the "pseudomomentum" $\pi(\theta)$ is the solution of (2.34) with driving term given by $\beta\sinh(\theta)$ instead of $\beta\cosh(\theta)$. The corresponding function $L_\pi(\theta) = \ln\big(1+e^{-\pi(\theta)}\big)$ displays a kinks-plateaux structure similar to that of $L(\theta)$ for positive rapidities, but quite different for negative rapidities. This is a consequence of the fact that $\pi(\theta)$ in general develops a non vanishing imaginary part for $\theta < 0$. As a result, no simple zeros are added to $v^{\rm eff}(\theta)$ from the denominator, but the global behaviour of the effective velocity, already at equilibrium, is quite involved and strongly depends on the temperature. The function $v^{\rm eff}(\theta)$ is shown in figure 4.3 together with the particle and spectral densities (4.37), (4.53) for various values of the ratio y/θ_0, $y = \ln(2/\beta)$.

Recall that when y/θ_0 is in the range (3.21) defined by the integer k, in the limit of large y and θ_0 the staircase model flows towards the minimal unitary model $\mathcal{M}_{k+2}$. Having this in mind, the global features of the equilibrium effective velocity can be summarized as follows:

- For any value of y and θ_0, $\big|v^{\rm eff}(\theta)\big| \leq 1$, and as $|\theta| \gtrsim y$, $v^{\rm eff}(\theta) \sim v^{\rm gr}(\theta) = \tanh(\theta)\,.$
- $v^{\rm eff}(\theta)$ is a monotonic function of θ only for $k = 1$, *i.e.* around the Ising critical point. For $k > 1$, the number of local extrema is $2(k-1)$, and at these points one has $\big|v^{\rm eff}\big| \to 1$ as $y, \theta_0 \to +\infty$.
- The effective velocity is not an odd function of θ. This is a general property[8] which does not depend on the temperature, but becomes evident when $k > 2$, as $v^{\rm eff}(\theta)$ starts to develop some plateaux approaching the value $v^{\rm eff} = 0$ from below at negative rapidities. Whenever k is increased by one a new plateau appears in the profile.
- For $k = 1\,,\, 2$ the zeros of $v^{\rm eff}(\theta)$ are given by $z_i = (i-k)\theta_0/2$, $k = 1, \ldots, 2k-1$. When $k \geq 3$, this is still true for the points z_i, $i = 2k-3\,,\, 2k-2\,,\, 2k-1$, while the points z_i, $i = 1, \ldots, 2k-4$ are the starting and ending points of the plateaux of $v^{\rm eff}(\theta)$. In particular this means that $v^{\rm eff}(\theta) \leq 0$ for all $\theta \leq z_{2k-3}$.

These properties of the effective velocity are quite bizarre. However, some light of them can be shred by considering in more detail the particle distribution $\rho_p(\theta)$. Looking at figure 4.3, one sees that $\rho_p(\theta)$ is even (as expected from its definition), and it has $2k$

[8] In particular, it is not a feature peculiar only to the staircase model. The reason is that in general if the kernel $\phi(\theta)$ is even, then an even function of the rapidity remains even when dressed, but an odd function of the rapidity does not remain odd: indeed, if $f(-\theta) = -f(\theta)$ the integral dressing equations for $f^{\rm dr}(-\theta)$ and $-f^{\rm dr}(\theta)$ are different.

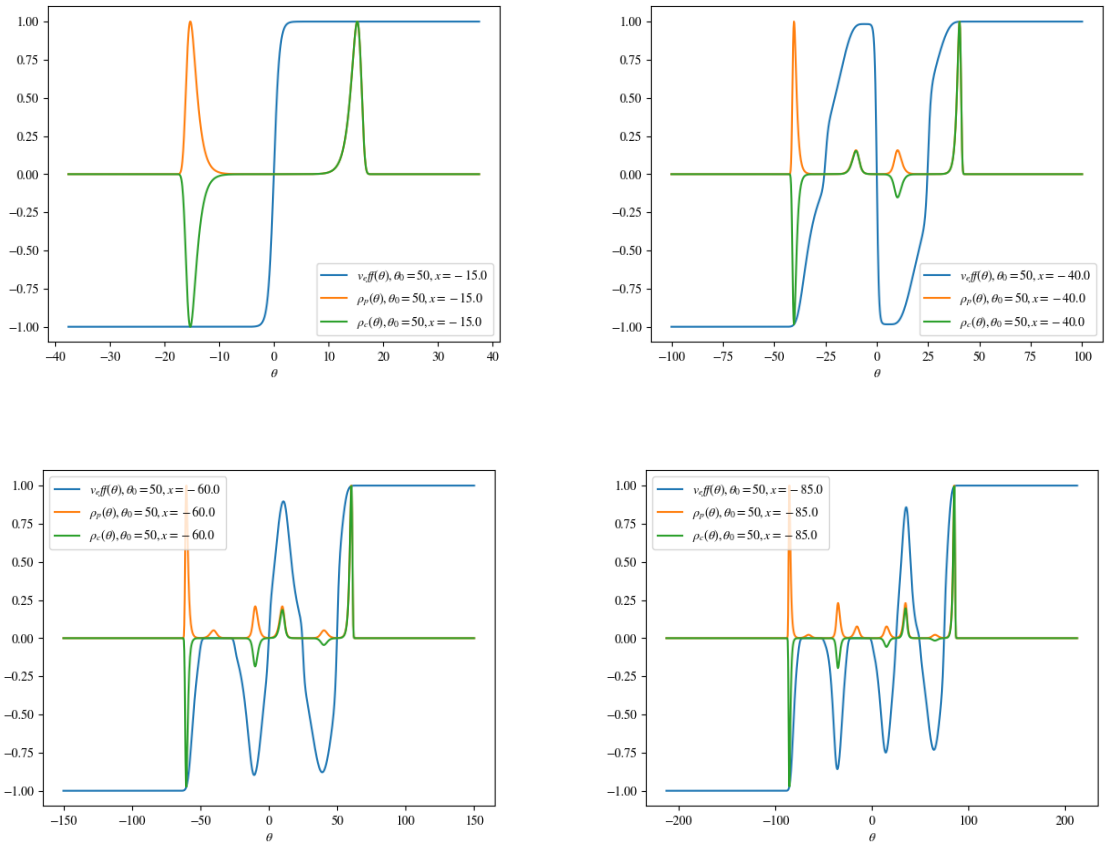

Figure 4.3: Equilibrium profiles of $v^{\text{eff}}(\theta)$, $\rho_p(\theta)$ and $\rho_c(\theta)$ for different values of $y = -x = \ln(2/\beta)$, with $\theta_0 = 50$. The particle and spectral densities are normalized to the maximum value of $\rho_p(\theta)$.

peaks when $(k-1)\theta_0/2 < y < k\theta_0/2$. For $k = 1, 2$ these peaks are at $v^{\text{eff}} = \pm 1$, and the area below the ones at $v^{\text{eff}} = +1$ and at $v^{\text{eff}} = -1$ is the same: this means that half of the particles is moving along the positive x-direction and half of them is moving the other way with the very same velocity, so that the neat current of any charge is zero, as expected at equilibrium. However, when $k \geq 3$, that is starting from the 3-state Potts model $\mathcal{M}_5$, some peaks appear in correspondence of the plateaux at $v^{\text{eff}} = 0$. Particles with a vanishing effective velocity do not carry any degree of freedom, and this is a phenomenon which happens in models with magnons in their spectrum; moreover, as we previously pointed out, the magnonic effective velocities can be non monotonic. In light of this, it is suggestive that $\mathcal{M}_5$ is the UV point of the A_3 massless flow, the first one which contains a magnon. A numerical study of the effective velocities and particle densities in

A_n massless models [18], motivated by the results above , has confirmed the surprising fact that the staircase model's effective velocity can be obtained by summing all the velocities of the particles in the A_k massless flow[9], after an appropriate translation of the latter in rapidity space. The same holds for the occupation function and the particle densities, strengthening the suggestion made at the end of the previous chapter that the staircase model can be regarded as an effective theory for non diagonal models.

4.3.2 Partitioning protocol with pure Gibbs reservoirs

In the off-equilibrium scenario the multiple solutions of equation (4.75) depend both on the ray parameter ξ and on the GGEs characterizing the states of the two reservoirs. In particular, if the latter are in pure Gibbs ensembles at temperatures $T_{r,l}$, then the zeros of (4.75) are affected by the ratio:

$$\sigma \equiv T_l/T_r \,, \tag{4.80}$$

where in the following we will always choose $\sigma \geq 1$, $\sigma = 1$ corresponding to a global homogeneous Gibbs ensemble, *i.e.* equilibrium. The iterative procedure previously described for the self-consistent determination of $\theta_*(\xi)$ with a monotonic effective velocity is straightforwardly generalized to the present case: each seed rapidity $\theta_*^{j,(0)}(\xi)$ converges after a few iteration to the actual solution $\theta_*^j(\xi)$, with j indexing the position among the multiple solutions. In particular, we have numerically observed for the staircase model that when $\xi = 0$ the zeros of (4.75) have a very weak dependence on σ. As can be seen in figure 4.4, even when $\sigma = \mathcal{O}(10^2)$, which to all practical purposes amounts to neglecting the right reservoir, there is no sensible displacement between the equilibrium zeros z_i and the actual discontinuity points of $n(\theta; \xi = 0)$.

In the next chapter we will be interested in studying current averages in the non-equilibrium steady state, that is at $\xi = 0$. On account of the previous considerations about the multiple zeros of v^{eff} at and off-equilibrium, we can rewrite the joint occupation function (4.74) as:

$$n(\theta, \xi = 0) = \chi_l(\theta) n_l(\theta) + (1 - \chi_l(\theta))\, n_r(\theta) = \begin{cases} n_l(\theta) & , \quad \theta \in L \\ n_r(\theta) & , \quad \theta \in R \end{cases} , \tag{4.81}$$

being y, θ_0 as in (3.21) and $\chi_l(\theta)$, $\chi_r(\theta) = 1 - \chi_l(\theta)$ the characteristic functions of the sets:

$$L \equiv [z_1\,,\, z_2] \,\cup\, [z_3, z_4] \,\cup\, \ldots \cup\, [z_{2k-1}\,,\, +\infty)\,, \tag{4.82}$$

$$R \equiv (-\infty\,,\, z_1] \,\cup\, [z_2, z_3] \,\cup\, \ldots \cup\, [z_{2k-2}\,,\, z_{2k-1}]\,. \tag{4.83}$$

[9] Recall that these are one right-mover, one left-mover and $k-2$ magnons.

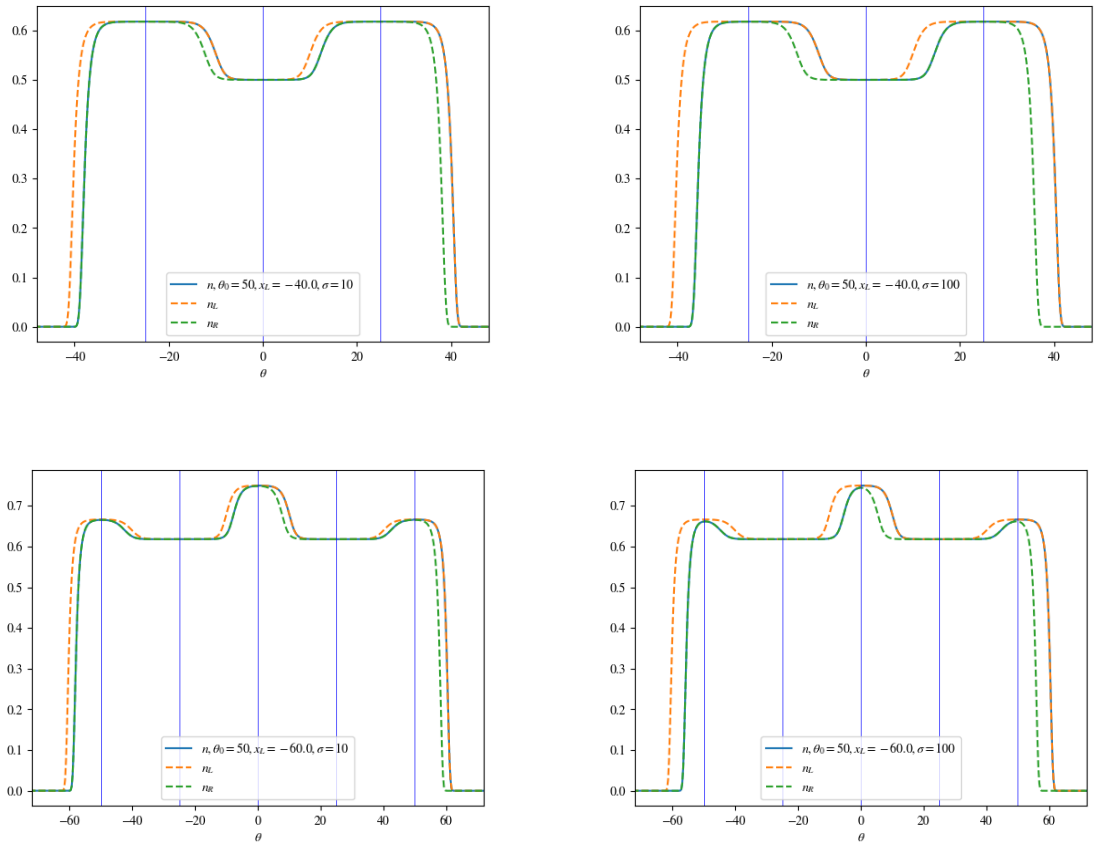

Figure 4.4: Joint occupation function $n(\theta; \xi = 0)$ for $\sigma = 10, 100$. Top (bottom) row: both the reservoirs are near the second(third) UV fixed point, respectively $k = 2$ and $k = 3$ in equation (3.21). The vertical lines are at the equilibrium zeros of $v^{\text{eff}}(\theta)$.

We remark that if z_i is the onset point of a velocity plateau rather than a simple zero, it is actually irrelevant whether $n(\theta)$ is given by $n_l(\theta)$ or $n_r(\theta)$ in $[z_i\,,\, z_{i+1}]$, as $v^{\text{eff}} \simeq 0$ everywhere in the interval. Another viable choice would be setting $n(\theta)$ equal to $n_r(\theta)$ for $\theta \leq z_{2k-3}$, without a sensible modification of the hydrodynamics. The parametrization (4.81) is just a matter of convenience.

In figure 4.5 we have plotted the off-equilibrium profiles of the effective velocity, particle and spectral densities at $\xi = 0$ for $k = 2$ and different values of $\sigma > 1$. For small values of σ, $v^{\text{eff}}(\theta; \xi = 0)$ is not sensibly different from the corresponding equilibrium function, which is coherent with the previous observation on the displacement of its zeros. On the other hand, ρ_p and ρ_c are affected by the temperature difference between the two reservoirs: the height of the peaks at $v^{\text{eff}} = -1$ is reduced, and so is the area

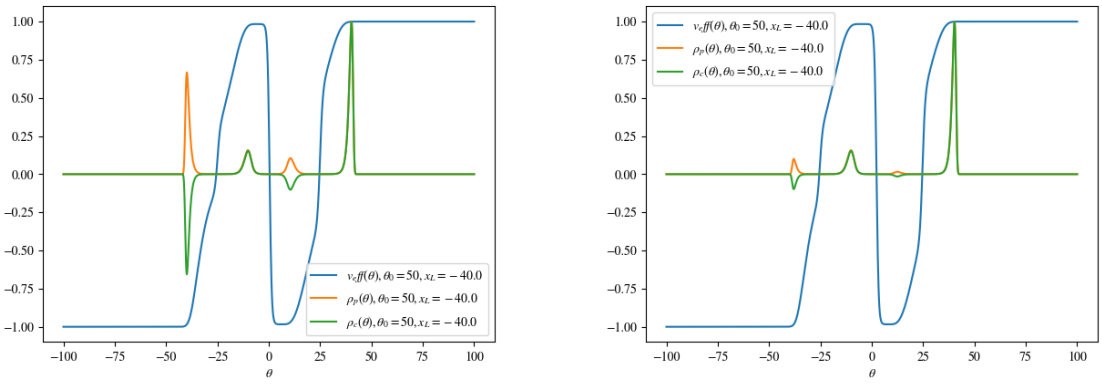

Figure 4.5: Off-equilibrium profiles of $v^{\text{eff}}(\theta)$, $\rho_p(\theta)$ and $\rho_c(\theta)$ (normalized as in figure 4.3) for $\sigma = 1.5$ (left) and $\sigma = 10$ (right). In both cases the two reservoirs are near the same critical point $k = 2$.

covered by the latter. This is an indication of the fact that as σ increases there are more charge-carriers moving from the left to the right reservoir, and the unbalance is responsible for the non-vanishing global currents (4.51).

Chapter 5

GHD currents of higher-spin charges

In this chapter we present the main theoretical achievements of this thesis. By combining TBA techniques with the generalized hydrodynamics approach, we provide an expression for the staircase model's steady state average energy current and density in an inhomogeneous setup, namely a partitioning protocol with thermal Gibbs reservoirs. By taking the UV limit of these averages we recover the exact expressions (4.3) and (4.4) for off-equilibrium CFTs. We then generalize our results to NESS averages of higher-spin currents and charge densities, obtaining a universal power-law dependence on the temperatures of the two reservoirs in the high energy limit: $\mathrm{j}_s, \mathrm{q}_s \propto T_l^{s+1} \mp T_r^{s+1}$. To a first approximation, we find that the coefficients appearing in these scaling laws are linear in the UV central charge and exponential in the spin. The expressions of these coefficient become exact when the left and right reservoirs are in generalized Gibbs ensemble and the time-evolution of the system is governed by an higher-spin conserved charge rather than a spin-1 Hamiltonian. We provide numerical results which confirm our predictions.

The arguments we present in this chapter are shaped in order to account for the very peculiar features of Zamolodchikov's staircase model, and can be extended to other models with similar properties, *i.e.* a logarithmic derivative of the S-matrix with displaced peaks [19, 20, 46]. Our results are in agreement with the ones obtained for simpler model with no staircase-like behaviour [47].

5.1 Energy current

Let us consider a partitioning protocol with two staircase scattering theories independently thermalized at temperatures T_l, T_r and joined at $x = 0$. For reasons which will become apparent later, we are interested in the situation in which the left and right subsystems tend in the UV limit to the same minimal model $\mathcal{M}_{k+2}$. According to (3.21),

this amounts to choose:

$$\frac{(k-1)\theta_0}{2} < y_r < y_l < \frac{k\theta_0}{2}\,, \quad k \in \mathbb{N}\,, \tag{5.1}$$

where we have defined:

$$y_r \equiv \ln(2/\beta_r)\,, \quad y_l \equiv \ln(2/\beta_l) = y_r + \ln(\sigma)\,, \tag{5.2}$$

with $\sigma = T_l/T_r > 1$ and as usual $\beta_{l,r} = mT_{l,r}^{-1}$ are the dimensionless inverse temperatures. If (5.1) holds and σ is not too large, then from the considerations made in the previous chapter it follows that the occupation functions $n_r(\theta)$, $n_l(\theta)$ are very similar and the zeros of the steady state effective velocity are not sensibly displaced from the equilibrium ones (see figure 4.4). Therefore the steady state occupation function $n(\theta) \equiv n(\theta;\xi=0)$ is given by (4.81), with the domains L and R defined in (4.82), (4.83).

The average energy current j_1 at $\xi = 0$ is the sum of the contributions from the right and left reservoirs, that is:

$$\mathrm{j}_1 = \mathrm{j}_1^r + \mathrm{j}_1^l \tag{5.3}$$

with:

$$\mathrm{j}_1^r = \int_R \frac{\mathrm{d}\theta}{2\pi}\, p(\theta) n(\theta) h_1^{\mathrm{dr}}(\theta) = \int_R \frac{\mathrm{d}\theta}{2\pi}\, p(\theta) n_r(\theta) h_1^{\mathrm{dr}}(\theta)\,, \tag{5.4}$$

$$\mathrm{j}_1^l = \int_L \frac{\mathrm{d}\theta}{2\pi}\, p(\theta) n(\theta) h_1^{\mathrm{dr}}(\theta) = \int_L \frac{\mathrm{d}\theta}{2\pi}\, p(\theta) n_l(\theta) h_1^{\mathrm{dr}}(\theta)\,, \tag{5.5}$$

and $h_1(\theta)$ is defined as in (4.30). Now we can take advantage of relation (4.77) between the dressed momentum and the derivative of the pseudoenergy to write:

$$\varepsilon'_{r,l}(\theta) = [\beta_{r,l}\sinh(\theta)]^{\mathrm{dr}} = T_{r,l}^{-1} p^{\mathrm{dr}}(\theta)\,, \tag{5.6}$$

where $\varepsilon'_{r,l}(\theta)$ are the solutions of the standard TBA equations for the two Gibbs reservoirs. Notice that in the equation above the dressing of $p(\theta)$ is performed with $n_r(\theta)$ in the right reservoir and with $n_l(\theta)$ in the left one, while in both (5.4) and (5.5) it is the the joint occupation function $n(\theta)$ which enters the definition of h_1^{dr}. But again, as long as (5.1) holds and σ is small we can assume that the dressing of $h_1(\theta)$ is made with $n_r(\theta)$ in (5.4) and with $n_l(\theta)$ in (5.5): this is the main assumption of our proof, and we will present a numerical check of its validity in the next section.

Using the symmetry relation (4.36) to move the dressing from $h_1(\theta)$ to $p(\theta)$ in (5.4), (5.5) and then applying (5.6), we can write:

$$\begin{aligned}\mathrm{j}_1^r = \frac{T_r}{2\pi}\int_R \mathrm{d}\theta\, \varepsilon'_r(\theta) n_r(\theta) h_1(\theta) &= -\frac{mT_r}{2\pi}\int_R \mathrm{d}\theta\, L'_r(\theta)\cosh(\theta) \\ &= -\frac{T_r^2}{2\pi}\int_R \mathrm{d}\theta\, 2e^{-y_r}\cosh(\theta) L'_r(\theta)\,,\end{aligned} \tag{5.7}$$

where the second equality is obtained from:

$$n_{r,l}(\theta)\varepsilon'_{r,l}(\theta) = -L'_{r,l}(\theta)\,, \tag{5.8}$$

and the third one from the definitions of $\beta_{r,l}$ and $y_{r,l}$. Exactly in the same way:

$$\mathrm{j}_1^l = -\frac{T_l^2}{2\pi}\int_L \mathrm{d}\theta\, 2e^{-y_l}\cosh(\theta)L'_l(\theta)\,. \tag{5.9}$$

Let us now consider in more detail the integration domains R and L. The functions $L_{r,l}(\theta)$ undergo a double exponential decay when $|\theta| \gg y_{r,l}$, and we can effectively set $L_{r,l}(z_0) = L_{r,l}(z_{2k}) = 0$ even when these quantities are multiplied by an exponentially increasing function. Of course this property is not spoiled when we derive $L_{r,l}(\theta)$ with respect to[1] θ so again we can set $L'_{r,l}(z_0) = L'_{r,l}(z_{2k}) = 0$ and R, L reduce to the compact domains $K_1 \cup K_3 \cdots \cup K_{2k-1}$ and $K_2 \cup K_4 \cdots \cup K_{2k}$ respectively, with K_i defined as in (3.25). Inside each K_i the functions $L'_{r,l}(\theta)$ are bounded for every finite y, as the width of each kink is small but independent on the temperature. Furthermore, the quantities $2e^{-y_{r,l}}\cosh(\theta)$ are effectively different from zero (in the high temperature limit) only in K_1 and K_{2k}, and we can use the approximation (3.34) for both the left and right subsystem. In light of this, equations (5.7) and (5.9) can be rewritten as:

$$\mathrm{j}_1^r = -\frac{T_r^2}{2\pi}\int_{K_1} \mathrm{d}\theta\, e^{-y_r-\theta}L'_r(\theta)\,, \tag{5.10}$$

$$\mathrm{j}_1^l = -\frac{T_l^2}{2\pi}\int_{K_{2k}} \mathrm{d}\theta\, e^{-y_l+\theta}L'_l(\theta)\,. \tag{5.11}$$

After an integration by parts, and setting $L_{r,l}(z_0) = L_{r,l}(z_{2k}) = 0$, the previous equations reduce to:

$$\mathrm{j}_1^r = -\frac{T_r^2}{2\pi}\left\{\int_{K_1} \mathrm{d}\theta\, e^{-y_r-\theta}L_r(\theta) + e^{-[y_r-(k-1)\theta_0/2]}L_r(z_1)\right\}\,, \tag{5.12}$$

$$\mathrm{j}_1^l = +\frac{T_l^2}{2\pi}\left\{\int_{K_{2k}} \mathrm{d}\theta\, e^{-y_l+\theta}L_l(\theta) + e^{-[y_l-(k-1)\theta_0/2]}L_l(z_{2k-1})\right\}\,. \tag{5.13}$$

Since $y_{r,l} > (k-1)\theta_0/2$ and $L_r(z_1) \simeq L_l(z_{2k-1})$ are bounded, the finite terms both vanish in the limit $y_{l,r} \to \infty$ with y_l/θ_0 and y_r/θ_0 fixed; thus in this limit:

$$\mathrm{j}_1^r \to -\frac{\pi T_r^2}{6}c_{-,r}\,, \quad c_{-,r} \equiv \frac{3}{\pi^2}\int_{K_1} \mathrm{d}\theta e^{-y_r-\theta}L_r(\theta)\,, \tag{5.14}$$

[1] Explicitly, one has $L(\theta) \simeq \ln\left(1+e^{-\beta\cosh(\theta)}\right) \simeq e^{-e^{\pm\theta-y}}$ as $\theta \gg y$ (+) or $\theta \ll -y$ (-). Therefore $L'(\theta) \simeq \mp\exp\left(\pm\theta - y - e^{\pm\theta-y}\right) \simeq \mp e^{-e^{\pm\theta-y}}$.

$$\mathrm{j}_1^l \to +\frac{\pi T_l^2}{6} c_{+,l}\,, \quad c_{+,l} \equiv \frac{3}{\pi^2}\int_{K_{2k}} \mathrm{d}\theta e^{-y_l+\theta} L_l(\theta)\,. \tag{5.15}$$

We recognise from (3.36) that in the high-temperature limit $c_{-,r} = c_{+,l} = c_k/2$, being c_k the central charge (3.58) of the unitary minimal model $\mathcal{M}_{k+2}$. The NESS average energy current in the UV limit $\theta_0, y_{l,r} \to +\infty$, $(k-1)\theta_0/2 < y_r < y_l < k\theta_0/2$ is therefore:

$$\mathrm{j}_1 = \mathrm{j}_1^l + \mathrm{j}_1^r \to \frac{c_k \pi}{12}\left(T_l^2 - T_r^2\right) = \frac{c_k \pi}{12} T_l^2 \left(1 - \frac{1}{\sigma^2}\right)\,, \tag{5.16}$$

which is the expected result (4.3).

To obtain the average energy density $\mathrm{q}_1 = \mathrm{q}_1^r + \mathrm{q}_1^l$ one proceeds with minimum adaptations. Up to exponentially vanishing corrections in the limit $y_{r,l} \to +\infty$, in this case one has:

$$\mathrm{q}_1^r = \int_R \frac{\mathrm{d}\theta}{2\pi} E(\theta) n_r(\theta) h_1^{\mathrm{dr}}(\theta) = +\frac{T_r^2}{2\pi}\int_{K_1} \mathrm{d}\theta\, e^{-y_r-\theta} L_r'(\theta)\,, \tag{5.17}$$

$$\mathrm{q}_1^l = \int_L \frac{\mathrm{d}\theta}{2\pi} E(\theta) n_l(\theta) h_1^{\mathrm{dr}}(\theta) = -\frac{T_l^2}{2\pi}\int_{K_{2k}} \mathrm{d}\theta\, e^{-y_l+\theta} L_l'(\theta)\,, \tag{5.18}$$

where clearly the only difference with respect to expressions (5.7), (5.9) is the overall sign in front of q_1^r due to the fact that $\sinh(\theta) \simeq -\cosh(\theta)$ when $\theta \in K_1$. Therefore in the UV limit also (4.4) is recovered:

$$\mathrm{q}_1 = \mathrm{q}_1^l + \mathrm{q}_1^r \to \frac{c_k \pi}{12}\left(T_l^2 + T_r^2\right) = \frac{c_k \pi}{12} T_l^2 \left(1 + \frac{1}{\sigma^2}\right)\,. \tag{5.19}$$

The scaled averages $12\beta_l^2 \mathrm{q}_1/\pi$ and $12\beta_l^2 \mathrm{j}_1/\pi$ are plotted in figure 5.1 as functions of y_l up to the $k = 3$ critical point, with $\sigma = 1.5$. The plateaux of these quantities are at $c_k(1 \pm \sigma^{-2})$, which precisely matches the predictions (5.16), (5.19). At this point it is clear why the choice to take y_r, y_l as in (5.1) is sensible: at large values of θ_0 (say *e.g.* $\theta_0 = 50$, the value we actually used most of the time for the numerical computations) it would take at least $\ln(\sigma) \simeq \mathcal{O}(10)$ in order to have different UV regimes in the two subsystems. But if $\sigma \simeq \mathcal{O}(e^{10})$ we see from the equations above that the contribution of the left movers (from the right reservoir) to the NESS averages j_1 and q_1 is practically zero. As we will see in the next section, this is true to an even larger extent in the case of higher-spin currents, where we have higher powers of $1/\sigma$ in the NESS averages.

5.2 Higher-spin currents from TBA: Gibbs reservoirs

The argument presented above can be easily extended to the computation of NESS higher-spin average currents in the UV limit. Namely, given any conserved charge with

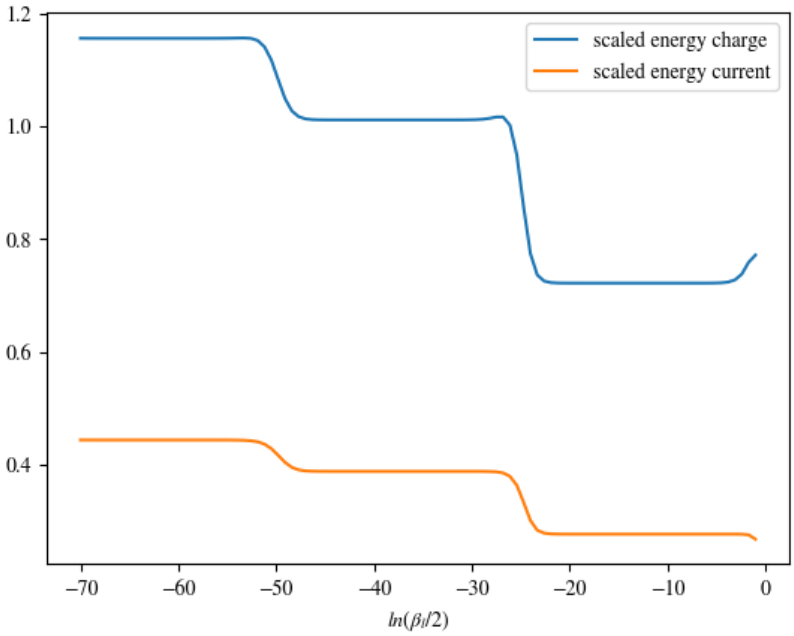

Figure 5.1: Scaled energy charge $12\beta_l^2 \mathrm{q}_1/\pi$ and current $12\beta_l^2 \mathrm{j}_1/\pi$. The plateaux start to form at the points $k\theta_0/2$, $\theta_0 = 50$.

one-particle eigenvalue $h_i(\theta)$ one obtains the steady state average of its current in an off-equilibrium massive integrable QFT through (4.51), and then take the high-temperature limit of the resulting expression to obtain the value of the latter in an off-equilibrium CFT setting. Let us apply this method to the staircase model, starting from a partitioning protocol with Gibbs reservoirs.

5.2.1 Average current densities in the UV limit

Consider the one-particle eigenvalues:

$$h_{2s-1}(\theta) \equiv \cosh(s\theta)\,, \quad h_{2s}(\theta) \equiv \sinh(s\theta)\,, \tag{5.20}$$

which correspond to the even and odd components of a spin-s conserved charge[2] (1.31). Without losing generality, we have set $m = 1$, so that $\beta_{r,l} = T_{r,l}^{-1}$. With the same definitions of the previous section, let again y_r, y_l be as in (5.1). The $\xi = 0$ average

[2]Of course in the staircase model there is only one particle type, so we can set all the quantities $\chi^{(s)}$ equal to 1. If there are more particle species, these numbers are usually obtained via bootstrap methods.

current density corresponding to the eigenvalue $h_{2s-1}(\theta)$ is:

$$\mathrm{j}_{2s-1} = \mathrm{j}^r_{2s-1} + \mathrm{j}^l_{2s-1}\,, \tag{5.21}$$

where:

$$\begin{aligned}\mathrm{j}^r_{2s-1} &= \int_R \frac{\mathrm{d}\theta}{2\pi}\,\sinh(\theta) n_r(\theta) h^{\mathrm{dr}}_{2s-1}(\theta) \\ &= \frac{T_r}{2\pi}\int_R \mathrm{d}\theta\,\varepsilon'_r(\theta) n_r(\theta)\cosh(s\theta) = -\frac{T_r^{s+1}}{2\pi}\int_R \mathrm{d}\theta L'_r(\theta)\beta_r^s\cosh(s\theta)\,,\end{aligned} \tag{5.22}$$

and:

$$\begin{aligned}\mathrm{j}^l_{2s-1} &= \int_L \frac{\mathrm{d}\theta}{2\pi}\,\sinh(\theta) n_l(\theta) h^{\mathrm{dr}}_{2s-1}(\theta) \\ &= \frac{T_l}{2\pi}\int_L \mathrm{d}\theta\,\varepsilon'_l(\theta) n_l(\theta)\cosh(s\theta) = -\frac{T_l^{s+1}}{2\pi}\int_L \mathrm{d}\theta L'_l(\theta)\beta_l^s\cosh(s\theta)\,.\end{aligned} \tag{5.23}$$

In both (5.22) and (5.23), the second equality is obtained moving the dressing operator to $p(\theta) = \sinh(\theta)$ and making use of equation (5.6) and of the considerations thereafter, while in the third equality we have factored out $T^s_{r,l}$ and used equation (5.8). Since:

$$\beta^s_{r,l} = 2^s e^{-s\,y_{r,l}}\,, \tag{5.24}$$

we can now employ the approximation:

$$2e^{-s\,y}\cosh(s\theta) \simeq \begin{cases} e^{-s(y+\theta)} & , \quad \theta \in K_1 \\ 0 & , \quad \theta \in K_2 \ldots, K_{2k-1} \\ e^{-s(y-\theta)} & , \quad \theta \in K_{2k} \end{cases}, \tag{5.25}$$

so that equations (5.22) and (5.23) read:

$$\mathrm{j}^r_{2s-1} = -\frac{2^s T_r^{s+1}}{4\pi}\int_{K_1} \mathrm{d}\theta\, e^{-s(y_r+\theta)} L'_r(\theta)\,, \tag{5.26}$$

$$\mathrm{j}^l_{2s-1} = -\frac{2^s T_l^{s+1}}{4\pi}\int_{K_{2k}} \mathrm{d}\theta\, e^{-s(y_l-\theta)} L'_l(\theta)\,. \tag{5.27}$$

Again we can integrate by parts and use the fact that for $y_{r,l}$ sufficiently large:

$$\exp\left[-s\,y_r + \frac{s(k-1)\theta_0}{2}\right] L_r(z_0) \simeq \exp\left[-s\,y_l + \frac{s(k-1)\theta_0}{2}\right] L_l(z_{2k}) \simeq 0 \tag{5.28}$$

to write:

$$\mathrm{j}^r_{2s-1} = -\frac{s\,2^s}{4\pi} T_r^{s+1}\left\{\int_{K_1} \mathrm{d}\theta\, e^{-s(y_r+\theta)} L_r(\theta) + \frac{1}{s} e^{-s[y_r-(k-1)\theta_0/2]} L_r(z_1)\right\}\,, \tag{5.29}$$

$$\mathrm{j}^l_{2s-1} = +\frac{s\,2^s}{4\pi} T_l^{s+1} \left\{ \int_{K_{2k}} \mathrm{d}\theta\, e^{-s(y_l-\theta)} L_l(\theta) + \frac{1}{s} e^{-s[y_l-(k-1)\theta_0/2]} L_l(z_{2k-1}) \right\} . \tag{5.30}$$

The surface terms exponentially vanish in the UV limit (faster with respect to the case of $s = 1$ charges). Therefore we end up with the result:

$$\mathrm{j}_{2s-1} = \mathrm{j}^l_{2s-1} + \mathrm{j}^r_{2s-1} \to \frac{s\,2^s}{4\pi} \left(\mathcal{C}_l^s T_l^{s+1} - \mathcal{C}_r^s T_r^{s+1} \right) = \frac{s\,2^s}{4\pi} \mathcal{C}_l^s T_l^{s+1} \left(1 - \frac{\mathcal{C}_r^s}{\mathcal{C}_l^s} \frac{1}{\sigma^{s+1}} \right) , \tag{5.31}$$

where the limit is specified as in (5.16) and:

$$\mathcal{C}_l^s \equiv \int_{K_{2k}} \mathrm{d}\theta\, e^{-s(y_l-\theta)} L_l(\theta) , \quad \mathcal{C}_r^s \equiv \int_{K_1} \mathrm{d}\theta\, e^{-s(y_r+\theta)} L_r(\theta) . \tag{5.32}$$

Since $L_{r,l}(\theta) = L_{r,l}(-\theta)$ and the intervals K_1, K_{2k} are symmetric with respect to the origin, we can write:

$$\mathcal{C}_l^s = \mathcal{C}^s(y = y_l) , \quad \mathcal{C}_r^s = \mathcal{C}^s(y = y_r) , \quad \mathcal{C}^s(y) \equiv \int_{K_{2k}} \mathrm{d}\theta\, e^{-s(y-\theta)} L(\theta) , \tag{5.33}$$

and we note that, for $s = 1$ and $(k-1)\theta_0/2 < y < k\theta_0/2$ it holds:

$$\lim_{y,\theta_0 \to +\infty} \mathcal{C}^1(y) = \frac{\pi^2}{6} c_k , \tag{5.34}$$

so that the energy current result (5.16) is recovered.

When we consider the one-particle eigenvalue $h_{2s}(\theta)$ the computation of the UV limit proceeds exactly in the same way as for $h_{2s-1}(\theta)$, except that now instead of (5.25) we have to use the approximation:

$$2e^{-s\,y} \sinh(s\theta) \simeq \begin{cases} -e^{-s(y+\theta)} & , \quad \theta \in K_1 \\ 0 & , \quad \theta \in K_2 \ldots, K_{2k-1} \\ e^{-s(y-\theta)} & , \quad \theta \in K_{2k} \end{cases} . \tag{5.35}$$

It follows that in the high temperature limit j^l_{2s} is given by (5.27) while j^r_{2s} differs from expression (5.26) for the overall sign. Therefore:

$$\mathrm{j}_{2s} = \mathrm{j}^l_{2s} + \mathrm{j}^r_{2s} \to \frac{s\,2^s}{4\pi} \mathcal{C}_l^s T_l^{s+1} \left(1 + \frac{\mathcal{C}_r^s}{\mathcal{C}_l^s} \frac{1}{\sigma^{s+1}} \right) . \tag{5.36}$$

The same considerations can be applied to the charge densities q_{2s-1} and q_{2s} associated to the eigenvalues (5.20), which are defined through the integration measure $\mathrm{d}p(\theta)/2\pi$ instead of $\mathrm{d}E(\theta)/2\pi$. Again, the only contributions to the integrals come from K_1 and K_{2k} and at a finite but large temperature one obtains:

$$\mathrm{q}_{2s-1} \approx \mathrm{j}_{2s} , , \quad \mathrm{q}_{2s} \approx \mathrm{j}_{2s-1} , \tag{5.37}$$

where the symbol $\approx$ stands for an equality up to terms of order $\mathcal{O}(e^{-y})$, which becomes exact in the UV limit. Notice however that because of relativistic invariance $\mathrm{q}_2 = \mathrm{j}_1$ at any finite temperature.

Let us briefly comment one delicate point in our derivation of (5.31). Even if not appreciably displaced from the equilibrium positions, the zeros of $v^{\mathrm{eff}}(\theta; \xi = 0)$ change when $T_l \neq T_r$. Moreover, as we noticed in the previous chapter, when the $k = 3$ critical point is reached, the effective velocity starts to develop plateaux exponentially approaching the value $v^{\mathrm{eff}} = 0$ from below, but without actually reaching it at any finite temperature. This is the reason why, according to the remark following (4.83), one could set $n(\theta) = n_r(\theta)$ for all the values of θ smaller than the "displaced"simple zero z_{2k-3}, $k \geq 3$. The most generic scenario is that in which the discontinuity points of $n(\theta)$ are at the positions $-y_r < \theta_*^{(1)} < \theta_*^{(2)} \cdots < \theta_*^{(n)} < y_l$, $1 \leq n \leq 2k-1$, and the definitions of the domains R and L are modified accordingly. However, because of the behaviour of $2e^{-y}\cosh(s\theta)$ and of the rapid fall-off of $L(\theta)$ for $|\theta| > y$, also in this case the contributions from the central, finite intervals vanish in the UV limit, so that (5.31) still holds, but with the intervals $\tilde{K}_1 \equiv [-k\theta_0/2, \theta_*^{(1)}]$ and $\tilde{K}_{2k} = [\theta_*^{(n)}, k\theta_0/2]$ now being the integration domains in $\mathcal{C}_r^s$, $\mathcal{C}_l^s$. In other words, as every contribution coming from the region $-y_r < \theta < y_l$ is exponentially suppressed, the only requirement for our proof is that $n = n_r$ for $\theta < z_1$ and $n = n_l$ for $\theta > z_{2k-1}$. This condition is always met.

The result we have obtained is that in the UV limit the GHD averages of spin-s charge and current densities scale proportionally to $T_l^{s+1} \pm T_r^{s+1}$, being T_l and T_r the temperatures of the asymptotic Gibbs reservoirs. This power law seems quite universal, and indeed it can be inferred from CFT first principles when the left and right subsystems are at a critical point [18]. Moreover, our derivation is based on assumptions which are peculiar to diagonal massive QFTs with non monotonic effective velocities, but the resulting formula (5.31) coincides with the one obtained in [47] for models with a kernel $\phi(\theta)$ peaked at $\theta = 0$. The specific features of the staircase model, however, are computationally advantageous for at least two reasons: first, unlike models with a monotonic v^{eff}, the coefficients (5.32) are defined by an integral over a compact interval; second, the presence of infinitely many UV fixed points in the staircase's roaming trajectory allows for a more precise numerical test of the currents' scaling behaviour. In the next subsection, we present our numerical results and study how $\mathcal{C}^s(y)$ depend on the spin and on the central charge c_k.

5.2.2 Numerical results

Let us analyze the coefficients $\mathcal{C}_l^s$ and $\mathcal{C}_r^s$ in (5.32). In both the integrals, the dominant contribution comes from the region where $|\theta| > y$, that is from $[-k\theta_0/2\,,\, -y_r]$ in $\mathcal{C}_r^s$ and from $[y_l\,,\, k\theta_0/2]$ in $\mathcal{C}_l^s$. This is so because of the finite extension of the kinks: there is an

interval of order $\mathcal{O}(1)$ where $L(\theta)$ is not yet zero and the arguments of the exponentials become positive. Furthermore, since it is only the value of the ratio y/θ_0 which fixes the UV limit of the theory, we expect that $\mathcal{C}_l^s = \mathcal{C}_r^s$ as long as the condition (5.1) is satisfied. This is indeed verified by the numerical evaluation of the function $\mathcal{C}^s(y)$ (see figure 5.2), which shows that the latter is translationally invariant in the central regions $(k-1)\theta_0/2 < y < k\theta_0/2$, and therefore by (5.33) one has $\mathcal{C}_l^s = \mathcal{C}_r^s$ when (5.1) holds.

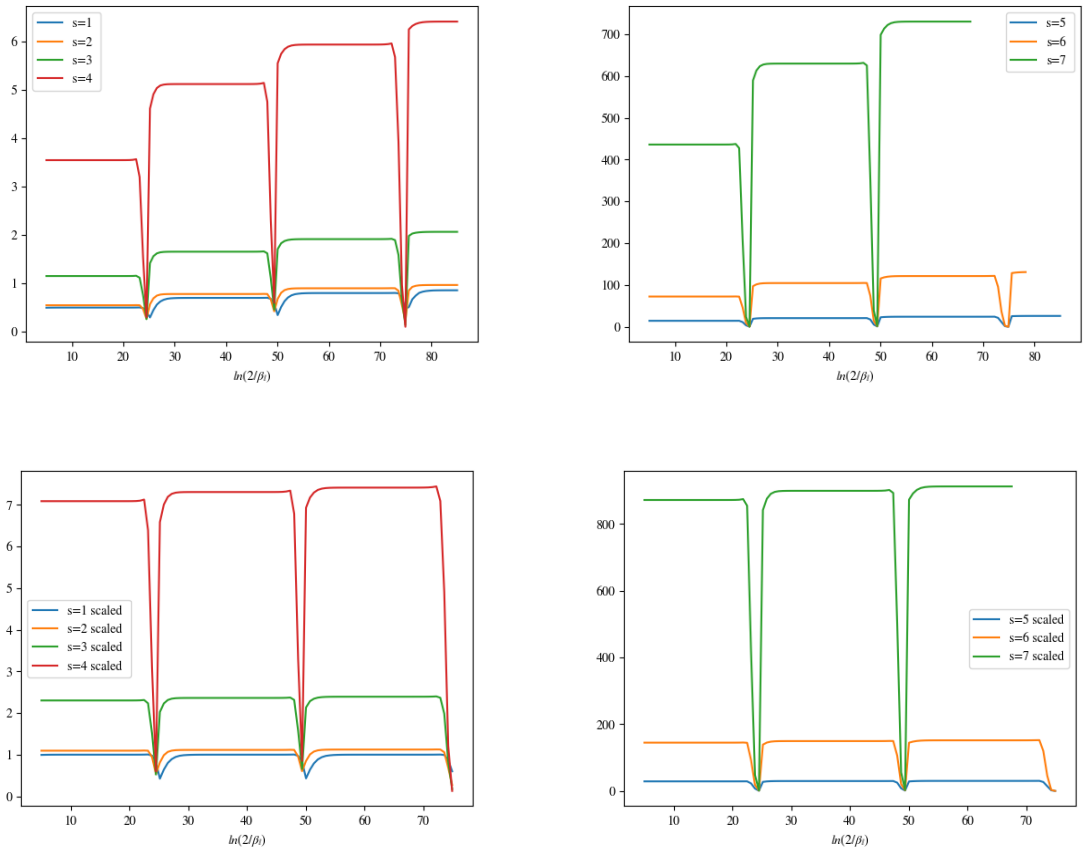

Figure 5.2: Top row: $\mathcal{C}^s(y)$ for $s = 1$ to 7 in the first four UV plateaux. Bottom row: the same coefficients scaled as specified in the main text.

Looking at the first and second plot in figure 5.2, one observes that when y/θ_0 approaches an half-integer value, the function $\mathcal{C}^s(y)$ has a sudden fall. This is consistent with (5.33), as it is easy to show that $L(z_{2k})/s \leq \lim_{y/\theta_0 \to k/2} \mathcal{C}^s(y) \leq L(z_{2k-1})/s$, where $L(z_{2k}) \simeq 0$ and $L(z_{2k-1}) \simeq 1$. In the central plateaux regions, on the other hand, to a first approximation $\mathcal{C}^s(y)$ depends linearly on the central charge and exponentially on the spin. To see this, one can treat s as a continuous variable and derive $\mathcal{C}^s(y)$ with

respect to s, so to obtain a differential equation for $\mathcal{C}^s(y)$ which is solved with the initial condition (5.34) at $s = 1$:

$$\mathcal{C}^s(y) = \frac{\pi^2}{6} c_k \exp\left\{ \left[\int_1^s \mathrm{d}s' \, \langle\theta\rangle_{s'} - (s-1)y \right] \right\}, \tag{5.38}$$

where:

$$\frac{(k-1)\theta_0}{2} \leq \langle\theta\rangle_s \equiv \frac{\int_{K_{2k}} \mathrm{d}\theta \, \theta e^{s\theta} L(\theta)}{\int_{K_{2k}} \mathrm{d}\theta \, e^{s\theta} L(\theta)} \leq \frac{k\theta_0}{2}, \quad \forall s \in \mathbb{R}, \tag{5.39}$$

so that the exponent in the right-hand side of (5.38) has an upper bound given by $(s-1)(k\theta_0/2 - y)$. When $\mathcal{C}^s(y)$ is written in this form the dependence on the spin is rather involved, but the advantage with respect to the expression given in (5.33) is that now the central charge is factored out and deviations from linearity can in principle be extracted from the exponent.

The scaled coefficients $6\mathcal{C}^s(y)/\pi^2 c_k$ are shown in the third and fourth plot of figure 5.2 for the first integer values of s, where $c_k = c_1 = 1/2$ for $y < \theta_0/2$, $c_k = c_2 = 7/10$ for $\theta_0/2 < y < \theta_0$ and so on up to the $k = 4$ plateau. As it is clear from the figure, these functions have almost the same value at every plateau: deviations from linearity in c_k are very small, even though non zero when $s > 1$.

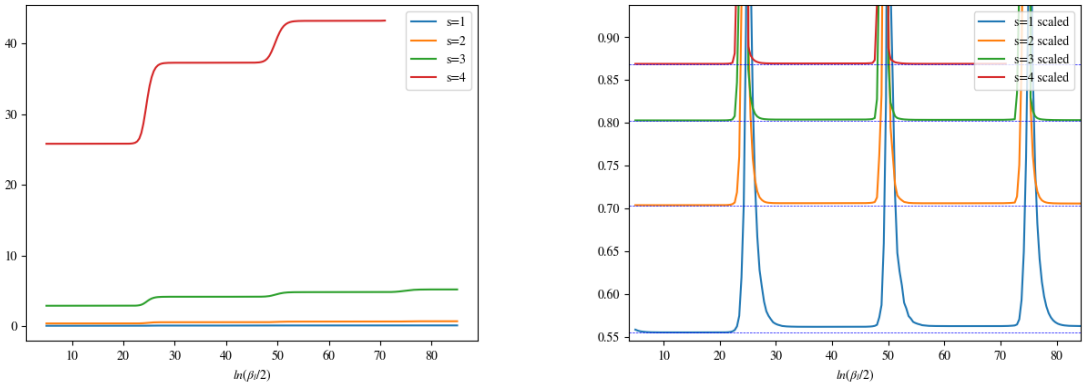

Figure 5.3: Left: currents $\beta_l^{s+1} \mathrm{j}_{2s-1}$ for $s = 1$ to 4 in the first four UV plateaux. Right: the same quantities scaled as specified in equation (5.40). Here $\theta_0 = 50$ and $\sigma = 1.5$.

Once obtained the coefficients $\mathcal{C}^s(y)$ for various values of the spin, we could proceed and numerically check the validity of our result for the average current densities. The quantities $\beta_l^{s+1} \mathrm{j}_{2s-1}$ are shown in the first plot of figure 5.3 for $s = 1, 2, 3, 4$ and y_l ranging over the first 4 plateaux, and they display the expected scaling behaviour. The

quantities shown in the second plot are instead the same currents scaled in such a way to completely eliminate the dependence on the temperature, that is:

$$\tilde{\mathrm{j}}_{2s-1} \equiv \frac{4\pi\beta_l^{s+1}\mathrm{j}_{2s-1}}{s2^s\mathcal{C}_l^s} = \left(1 - \frac{\mathcal{C}_r^s}{\mathcal{C}_l^s}\frac{1}{\sigma^{s+1}}\right) \simeq \left(1 - \frac{1}{\sigma^{s+1}}\right) , \tag{5.40}$$

where the approximate equality holds as long as y_l/θ_0 is not an integer or an half-integer. Notice the presence of peaks in $\tilde{\mathrm{j}}_{2s-1}$ when $y_l/\theta_0 = k/2$, corresponding to the drops in $\mathcal{C}_l^s$ at the same values[3].

The horizontal dashed lines in the second plot of figure 5.3 are at $y = 1-\sigma^{-(s+1)}$, and the deviations of the scaled currents from these values in the plateaux are an estimation of the global error made when deriving equation (5.31). Recall that our main assumption was that it is possible to use $n(\theta) = n_r(\theta)$ in the definition of the dressed eigenvalues $h_i^{\mathrm{dr}}(\theta)$ when $\theta \in R$ (respectively $n(\theta) = n_l(\theta)$ when $\theta \in L$). This seems reasonable when we look at the numerics, as when σ is of order $\mathcal{O}(1 \div 10)$ the functions $n_l(\theta)$ and $n_r(\theta)$ are almost indistinguishable; however, this is the only approximation not justified by some exponentially-decreasing bound, thus we believe it to be the main source of error. By looking at the deviations from the constant values in the regions where $y_l/\theta_0 \neq k/2$ we see that the error is very small: the deviations slightly increase with y_l and at a fixed temperature they seem to decrease exponentially with the spin (the absolute error is of order $\mathcal{O}(10^{-2})$ for $s = 1, 2$ and $\mathcal{O}(10^{-4})$ for $s = 4$).

There is a comment to make regarding the values of s. Figure 5.3 shows that when we join two systems prepared in thermal states, the average current densities have a staircase behaviour regardless of whether the spin is even or odd. Moreover, the same result holds for any real and positive value of s, as our derivation of (5.31) and (5.36) proceeds without having to make any assumption on s as long as $s > 0$. Of course this does not imply that the staircase model admits conserved charges for every positive value of the spin: in order for s to be the actual spin of a conserved charge in the staircase model, there must exist an operator Q_s such that its eigenvalue on a one-particle state $|\theta\rangle$ is a linear combination of $h_{2s-1}(\theta)$ and $h_{2s}(\theta)$. If Q_s is a local conserved quantum charge then $s \in \mathbb{N}$ and the charge transforms according to an integer spin representation of the Lorentz group. The local charges in the staircase model are obtained via an analytic continuation (3.10) of the corresponding ones in the sinh-Gordon model, which exist for odd values of s [2, 29]. Nonetheless, it is still meaningful to consider even or non-integer values of s in the one-particle eigenvalues, as in the most generic GGE setup one has to include also non local charges, and the latter have in general fractional and

[3]One should keep in mind that these peaks do not reflect the physical behaviour of the current averages at the points $y_l/\theta_0 = k/2$. Indeed, not only the functions $\mathcal{C}^s(y)$ lose their translational invariance therein, but the approximations used in the derivation of (5.31) are no more valid. In particular, when $y_l/\theta_0 = k/2$ the coefficients (5.32) are defined by integrals over the whole non-compact domains R, L.

coupling-dependent spin. For instance, in [48] it has been shown that the sine-Gordon model in the repulsive regime admits a set of charges with spins $s = 2\pi k/p$, being $p > 1$ a parameter dependent on the coupling β. Since sine-Gordon is analytically continued to sinh-Gordon, and the latter to the staircase model, we expect local charges with similar fractional spins to appear also in the GGE description of the staircase model.

5.3 Higher-spin currents in non-thermal steady states

In the previous sections we derived and discussed the expressions of higher-spin current averages in the staircase model when the the asymptotic reservoirs are in Gibbs states. In this scenario we have a universal dependence on the temperatures T_l, T_r in the UV limit, but unless $s = 1$ the exact dependence of the coefficients $\mathcal{C}_l^s$, $\mathcal{C}_r^s$ on the central charge is not available. There is, however, a situation in which these coefficients are exactly linear in the central charge: namely, this is the case when the reservoirs are in non-thermal states, described by generalized TBA equations of the form (4.43). The derivation of this result proceeds in two steps.

First, consider the following generalized TBA equation for the staircase model:

$$\begin{aligned}\varepsilon_s(\theta) &= \beta^s \cosh(s\theta) - \frac{1}{2\pi}\left[(\psi * L_s)(\theta-\theta_0) + (\psi * L_s)(\theta+\theta_0)\right] \\ &= 2^s e^{-sy}\cosh(s\theta) - \frac{1}{2\pi}\left[(\psi * L_s)(\theta-\theta_0) + (\psi * L_s)(\theta+\theta_0)\right], \end{aligned} \tag{5.41}$$

where again $m = 1$ and $(k-1)\theta_0/2 < y = \ln(2/\beta) < k\theta_0/2$ for some positive integer k. This equation corresponds to a GGE where the only non vanishing β_i is coupled to a spin-s charge eigenvalue[4] $h_s(\theta) = \cosh(s\theta)$. We have numerically solved (5.41) and obtained the plots of the functions $L_s(\theta) \equiv \ln\left(1 + e^{-\varepsilon_s(\theta)}\right)$ at different temperatures and for the first integer values of s. These functions display a kinks-plateaux structure which is extremely similar to that of $L_1(\theta) \equiv L(\theta)$, described in section 3.2.1: in fact, the only difference with respect to the latter is that the first and last kinks of L_s (at $\mp y$ respectively) are steeper than the ones of L. This is a consequence of the fact that $\varepsilon_s(\theta)$ grows with a larger exponent when $|\theta| > y$. The positions of kinks and plateaux are untouched and at the midpoints $L_s(z_i) = L(z_i)$, as the driving term can still be neglected when we derive the coupled transcendental equations for $\varepsilon_s(z_i)$, which are thus given by (3.30). We remark that only the first and last kinks of $L_s(\theta)$ are affected by the driving term: the central kinks of L_s are not steeper then the ones of L (they are in fact practically indistinguishable when the functions are superimposed), because their width depends only on the support of the kernel.

[4] We are using a lighter notation with respect to the one in (5.20) since we focus here on even eigenvalues. The case $h_s(\theta) = \sinh(s\theta)$ is a straightforward generalization.

The fact that $L_s(\theta)$ and $L(\theta)$ have the same properties allows us to obtain an explicit relation between the coefficients $\mathcal{C}^s(y)$ and the central charges c_k starting from the generalized TBA equation (5.41), namely:

$$\mathcal{C}^s(y) \equiv \int_{K_{2k}} \mathrm{d}\theta\, e^{-s(y-\theta)} L_s(\theta) \to \frac{\pi^2}{3}\frac{c_k}{s2^s}\,, \tag{5.42}$$

in the usual limit y, $\theta_0 \to \infty$ and y/θ_0 fixed. To obtain the expression above one has to proceed along the lines of what we did in section 3.3 for the standard TBA scaling function, the only difference being that in this case one has to derive both members of equation (5.41) with respect to θ and integrate them over K_i with measure $L_s(\theta)\,\mathrm{d}\theta$. Notice that $L_s(z_i) = L(z_i)$ is a crucial property, as it is the specific form of the coupled equations (3.30) which ensure the validity of the dilogarithm sum rule.

With relation (5.42) at hand we can proceed to the evaluation of higher-spin current averages in a GGE. Before turning to the partitioning protocol, however, we have to generalize the TBA-derived formulas (4.47) and (4.51) for the average charge and current densities. Recall that in the quasi-particle description the GHD average q_i is defined by (4.31), which is equivalent to equation (4.47) thanks to the Bethe constitutive relation (4.33). Equation (4.51) for the current average is then obtained by means of a crossing symmetry argument. Suppose that we now modify equation (4.33) in the following way:

$$\rho_p(\theta) + \rho_h(\theta) = \frac{1}{2\pi} h(\theta) + (\phi * \rho_p)(\theta)\,, \tag{5.43}$$

that is, a generic regular function $h(\theta)$ replaces $p'(\theta)$ in the right hand side. An explicit calculation shows that the minimization of the GGE free energy functional (4.41) with respect to ρ_p and ρ_h is not affected by this replacement in the constraint, so that the resulting generalized TBA equation is still (4.43). On the other hand, the equilibrium free energy density $f(\boldsymbol{\beta})$ is now given by:

$$f(\boldsymbol{\beta}) = -\int \frac{\mathrm{d}\theta}{2\pi}\, h(\theta) \ln\bigl(1 + e^{-\epsilon_w(\theta)}\bigr) \tag{5.44}$$

instead of (4.45). This means that there is a large freedom in the choice of $f(\boldsymbol{\beta})$ keeping fixed the TBA equation, *i.e.* the generalized Gibbs ensemble. At first sight, equation (5.43) might seem physically meaningless when $h(\theta) \neq p'(\theta)$, because on a more fundamental level the constitutive relation (4.33) directly follows from the Bethe quantization condition (2.15) in the thermodynamic limit. However, there is a precise meaning underlying the choice of a generalized free energy density of the form (5.44). We will spend a few words on this at the end of the section.

Let us take $h(\theta) = h_s(\theta) = \cosh(\theta)$, *i.e.* precisely the driving term of the GGE TBA equation. Then from (5.43) we now have:

$$\rho_p(\theta) + \rho_h(\theta) = \frac{[h_s(\theta)]^{\mathrm{dr}}}{2\pi}\,, \quad \rho_p(\theta) = n_s(\theta)\frac{[h_s(\theta)]^{\mathrm{dr}}}{2\pi}\,, \tag{5.45}$$

so that the average density of a charge with eigenvalue $h_k(\theta)$ becomes:

$$\mathrm{q}_k^{(s)} \equiv \int_{-\infty}^{+\infty} \mathrm{d}\theta \rho_p(\theta) h_k(\theta) = \int_{-\infty}^{+\infty} \frac{\mathrm{d}\theta}{2\pi} \left[h_s(\theta)\right]^{\mathrm{dr}} n_s(\theta) h_k(\theta)\,, \tag{5.46}$$

where the superscript denotes the spin of the GGE charge and the subscript the spin of the charge we are averaging. We are interested in the case $k = s$ so we can stick to the usual notation q_s with no risk of ambiguity. The corresponding current density average j_s is now obtained by implementing the crossing transformation $\theta \to i\pi/2 - \theta$, which acts on higher-spin eigenvalues as:

$$\cosh\left(s\theta\right) \mapsto \begin{cases} (-1)^k \cosh\left(s\theta\right) & , \quad s = 2k \\ -i(-1)^k \sinh\left(s\theta\right) & , \quad s = 2k+1 \end{cases} . \tag{5.47}$$

Selecting the odd values of s, up to an irrelevant minus sign[5]:

$$\mathrm{j}_s = \int_{-\infty}^{+\infty} \frac{\mathrm{d}\theta}{2\pi} \left[\sinh\left(s\theta\right)\right]^{\mathrm{dr}} n_s(\theta) h_s(\theta) \tag{5.48}$$

for a system in the specified GGE. Using the fact that:

$$\varepsilon_s'(\theta) = s\beta^s [\sinh\left(\theta\right)]^{\mathrm{dr}}\,, \tag{5.49}$$

together with $\varepsilon_s'(\theta) n_s(\theta) = -L_s'(\theta)$ and $\beta = 2e^{-y}$, (5.48) reduces to:

$$\mathrm{j}_s = -\frac{2^{s-1}}{2\pi s \beta^{2s}} \int_{-\infty}^{+\infty} \mathrm{d}\theta 2e^{-sy} \cosh\left(s\theta\right) L_s'(\theta)\,. \tag{5.50}$$

Notice that now we have an overall factor of β^{-2s} instead of the characteristic $\beta^{-(s+1)}$ of a pure thermal state: the dependence of current averages on the (generalized) inverse temperatures is peculiar to a given GGE. If we join two subsystems prepared in states described by (5.41) (with $\beta = \beta_{r,l}$) at generalized temperatures $T_{r,l} = \beta_{r,l}^{-1}$ such that (5.1) holds, the integration interval in (5.50) reduces to K_{2k} for j_s^l and to K_1 for j_s^r. Proceeding exactly as in the standard TBA case but using the fact that now the scaling function is (5.42), we end up with the expression for the UV limit of $\mathrm{j}_s = \mathrm{j}_s^l + \mathrm{j}_s^r$ in a partitioning protocol with non-thermal asymptotic reservoirs:

$$\mathrm{j}_s^{l,r} = \pm \frac{2^{s-1}}{2\pi\beta^{2s}} \mathcal{C}_{L,R}^s \Rightarrow \mathrm{j}_s = \mathrm{j}_s^l + \mathrm{j}_s^r \to \frac{\pi c_k}{12 s} \left(T_l^{2s} - T_r^{2s}\right)\,. \tag{5.51}$$

As announced, an exact linear dependence on the UV central charge is obtained. This is in spite of a different power law in $T_{l,r}$ with respect to the one in (5.31), which is a

[5] This can be always re-absorbed by including a factor of $(-1)^k$ in $h_s(\theta)$.

direct consequence of the modified current equation (5.48). We remark that the latter is consistent with the result (D13) derived in [15] by means of form factors. In particular, the form factor approach shows that a charge density $q_k^{(s)}$ with GGE average (5.46) and the corresponding current density $j_k^{(s)}$ are related by a continuity equation of the form:

$$i[Q_s, q_k^{(s)}] + \partial_x j_k^{(s)} = 0\,, \tag{5.52}$$

which clarifies the role of $h(\theta) = h_s(\theta)$ in (5.44) as the eigenvalue of the higher-spin charge Q_s now ruling the time evolution. Therefore we conclude that GGE averages of higher-spin current (and charge) densities depend linearly on the central charge whenever the only non-vanishing conserved charge in the ensemble coincides with the generator of time evolution, be it the Hamiltonian or an higher-spin charge.

Conclusions and outlooks

The purpose of this work was to perform a detailed study of Zamolodchikov's staircase model within the recently developed framework of generalized hydrodynamics. In order to do so, we needed to present a vast set of theoretical tools. The first part of this thesis was therefore entirely devoted to the discussion of integrability techniques, from the analytic S-matrix theory to the thermodynamic Bethe ansatz for diagonal integrable QFTs in one spatial dimension.

Within this context, we introduced the staircase model and outlined its TBA structure. Despite the simplicity of its mass spectrum and S-matrix, the peculiar features displayed by this model make it worth a thorough investigation. In particular, the roaming behaviour of the staircase model's scaling function, which approaches all the minimal unitary models as the temperature varies, suggested a connection with the A_n series of massless, non-diagonal models flowing between the very same critical theories. This suggestion was found to be true at the TBA level, and motivated a further study of the staircase model in the context of generalized hydrodynamics, to which a large part of this thesis was dedicated. The hydrodynamic features of Zamolodchikov's staircase model are quite peculiar, as non-monotonic effective velocities were never observed in any other diagonal theory with a single-particle spectrum. Again, we found similarities with the off-equilibrium behaviour of A_n massless flows. A comprehensive review of this connection will be the object of a future publication.

The last chapter of this thesis was entirely devoted to the investigation of non equilibrium steady-state currents arising after the implementation of a partitioning protocol. Because of its infinitely many UV fixed points, the staircase model revealed to be extremely suited for this study, as we could numerically check our results in more than one critical regime. Even though the computations we performed were based on specific features of staircase-like models, the resulting expressions are universal, as the very same scaling laws are found in diagonal models having a monotonic effective velocity [47].

There are several directions in which further research can (and hopefully will) be pursued:

- At the pure S-matrix level, it is still unclear whether the scattering amplitude of the staircase model can be derived from a QFT with a consistent lagrangian formulation. A candidate action is given in (3.13), and even if apparently physically

ill-defined, it gives rises to a consistent perturbative expansion [17].

- Generalized staircase-like theories can be obtained from affine Toda field theories through a suitable analytic continuation of the coupling constant [19, 20], and the resulting scaling functions roam between coset conformal models. Since affine Toda field theories are diagonal models, their TBA equations are derived with little effort. Thus it would be interesting to investigate whether it is possible to relate also these models to some non-diagonal theories.

- Finally, the results we obtained for the UV limits of higher-spin currents could in principle be obtained from CFT first principles, by making use of Zamolodchikov's mirror argument to study the finite-size scaling of higher-spin conformal fields in a cylindrical geometry.

Bibliography

[1] Denis Bernard and Benjamin Doyon. Energy flow in non-equilibrium conformal field theory. *Journal of Physics A: Mathematical and Theoretical*, 45(36):362001, 2012.

[2] Alexander B Zamolodchikov and Alexey B Zamolodchikov. Factorized S-matrices in two dimensions as the exact solutions of certain relativistic quantum field theory models. In *Yang-Baxter Equation In Integrable Systems*, pages 82–120. World Scientific, 1990.

[3] Patrick Dorey. Exact S-matrices. In *Conformal field theories and integrable models*, pages 85–125. Springer, 1997.

[4] Sidney Coleman and Jeffrey Mandula. All possible symmetries of the S-matrix. *Physical Review*, 159(5):1251, 1967.

[5] Al B Zamolodchikov. Thermodynamic Bethe ansatz in relativistic models: Scaling 3-state Potts and Lee-Yang models. *Nuclear Physics B*, 342(3):695–720, 1990.

[6] Al B Zamolodchikov. From tricritical Ising to critical Ising by thermodynamic Bethe ansatz. *Nuclear Physics B*, 358(3):524–546, 1991.

[7] Al B Zamolodchikov. Thermodynamic Bethe ansatz for RSOS scattering theories. *Nuclear Physics B*, 358(3):497–523, 1991.

[8] Chen-Ning Yang and Cheng P Yang. Thermodynamics of a one-dimensional system of bosons with repulsive delta-function interaction. *Journal of Mathematical Physics*, 10(7):1115–1122, 1969.

[9] M Steiner, J Villain, and CG Windsor. Theoretical and experimental studies on one-dimensional magnetic systems. *Advances in Physics*, 25(2):87–209, 1976.

[10] Toshiya Kinoshita, Trevor Wenger, and David S Weiss. Local pair correlations in one-dimensional Bose gases. *Physical review letters*, 95(19):190406, 2005.

[11] Toshiya Kinoshita, Trevor Wenger, and David S Weiss. A quantum Newton's cradle. *Nature*, 440(7086):900–903, 2006.

[12] Tim Langen, Sebastian Erne, Remi Geiger, Bernhard Rauer, Thomas Schweigler, Maximilian Kuhnert, Wolfgang Rohringer, Igor E Mazets, Thomas Gasenzer, and Jörg Schmiedmayer. Experimental observation of a generalized Gibbs ensemble. *Science*, 348(6231):207–211, 2015.

[13] Marc Cheneau, Peter Barmettler, Dario Poletti, Manuel Endres, Peter Schauß, Takeshi Fukuhara, Christian Gross, Immanuel Bloch, Corinna Kollath, and Stefan Kuhr. Light-cone-like spreading of correlations in a quantum many-body system. *Nature*, 481(7382):484–487, 2012.

[14] Denis Bernard and Benjamin Doyon. Non-equilibrium steady states in conformal field theory. In *Annales Henri Poincaré*, volume 16, pages 113–161. Springer, 2015.

[15] Olalla A Castro-Alvaredo, Benjamin Doyon, and Takato Yoshimura. Emergent hydrodynamics in integrable quantum systems out of equilibrium. *Physical Review X*, 6(4):041065, 2016.

[16] Bruno Bertini, Mario Collura, Jacopo De Nardis, and Maurizio Fagotti. Transport in out-of-equilibrium XXZ chains: Exact profiles of charges and currents. *Physical review letters*, 117(20):207201, 2016.

[17] Al B Zamolodchikov. Resonance factorized scattering and roaming trajectories. Technical report, 1991.

[18] Francesco Ravanini, Olalla A. Castro-Alvaredo, Octavio Pomponio, and Michele Mazzoni. In preparation, 2021.

[19] Patrick Dorey and Francesco Ravanini. Generalising the staircase models. *Nuclear Physics B*, 406(3):708–726, 1993.

[20] Patrick Dorey and Francesco Ravanini. Staircase models from affine Toda field theory. *International Journal of Modern Physics A*, 8(05):873–893, 1993.

[21] Olivier Babelon, Denis Bernard, and Michel Talon. *Introduction to classical integrable systems*. Cambridge University Press, 2003.

[22] Benjamin Doyon. Lecture Notes on integrability, King's College London taught course, 2012.

[23] Fabio Franchini. Notes on Bethe ansatz techniques. *International School for Advanced Studies-Trieste, Lecture Notes*, 2011.

[24] Paul Ginsparg. Applied conformal field theory. *arXiv preprint hep-th/9108028*, 1988.

[25] Philippe Di Francesco, Pierre Mathieu, and David Sénéchal. *Conformal field theory*. Springer Science & Business Media, 2012.

[26] Giuseppe Mussardo. *Statistical field theory: an introduction to exactly solved models in statistical physics*. Oxford University Press, 2010.

[27] Alexander B Zamolodchikov. Integrable field theory from conformal field theory. In *Integrable Systems in Quantum Field Theory and Statistical Mechanics*, pages 641–674. Elsevier, 1989.

[28] Stephen Parke. Absence of particle production and factorization of the S-matrix in (1+1)-dimensional models. *Nuclear Physics B*, 174(1):166–182, 1980.

[29] Timothy R Klassen and Ezer Melzer. Purely elastic scattering theories and their ultraviolet limits. *Nuclear Physics B*, 338(3):485–528, 1990.

[30] AE Arinshtein, VA Fateyev, and Al B Zamolodchikov. Quantum S-matrix of the (1+ 1)-dimensional Todd chain. *Physics Letters B*, 87(4):389–392, 1979.

[31] Timothy R Klassen and Ezer Melzer. The thermodynamics of purely elastic scattering theories and conformal perturbation theory. *Nuclear Physics B*, 350(3):635–689, 1991.

[32] Al B Zamolodchikov. On the thermodynamic Bethe ansatz equations for reflectionless ADE scattering theories. *Physics Letters B*, 253(3-4):391–394, 1991.

[33] Francesco Ravanini, Angelo Valleriani, and Roberto Tateo. Dynkin TBA's. *International Journal of Modern Physics A*, 8(10):1707–1727, 1993.

[34] Patrick Dorey and Roberto Tateo. Excited states by analytic continuation of TBA equations. *Nuclear Physics B*, 482(3):639–659, 1996.

[35] Anatol N Kirillov. Dilogarithm identities. *Progress of theoretical physics supplement*, 118:61–142, 1995.

[36] AB Zamolodchikov. Integrals of motion in scaling 3-state Potts model field theory. *International Journal of Modern Physics A*, 3(03):743–750, 1988.

[37] Andrea Cappelli and Jean-Bernard Zuber. ADE classification of conformal field theories.

[38] Al B Zamolodchikov. TBA equations for integrable perturbed $SU(2)_k \times SU(2)_l/SU(2)_{k+l}$ coset models. *Nuclear Physics B*, 366(1):122–132, 1991.

[39] F Ravanini. Thermodynamic Bethe ansatz for $\mathcal{G}_k \otimes \mathcal{G}_l/\mathcal{G}_{k+l}$ coset models perturbed by their $\phi_{1,1,\mathrm{Adj}}$ operator. *Physics Letters B*, 282(1-2):73–79, 1992.

[40] Jean-Sébastien Caux, Benjamin Doyon, Jerome Dubail, Robert Konik, and Takato Yoshimura. Hydrodynamics of the interacting Bose gas in the Quantum Newton Cradle setup. *SciPost Phys*, 6:070, 2019.

[41] Maximilian Schemmer, Isabelle Bouchoule, Benjamin Doyon, and J'erome Dubail. Generalized hydrodynamics on an atom chip. *Physical review letters*, 122(9):090601, 2019.

[42] David X Horvath. Hydrodynamics of massless integrable RG flows and a non-equilibrium c-theorem. *Journal of High Energy Physics*, 2019(10):1–40, 2019.

[43] Jacopo De Nardis, Denis Bernard, and Benjamin Doyon. Diffusion in generalized hydrodynamics and quasiparticle scattering. *SciPost Phys.*, 6(4):049, 2019.

[44] Benjamin Doyon. Thermalization and pseudolocality in extended quantum systems. *Communications in Mathematical Physics*, 351(1):155–200, 2017.

[45] Jorn Mossel and Jean-Sébastien Caux. Generalized TBA and generalized Gibbs. *Journal of Physics A: Mathematical and Theoretical*, 45(25):255001, 2012.

[46] Olalla A Castro-Alvaredo, Cecilia De Fazio, Benjamin Doyon, and Francesco Ravanini. On the hydrodynamics of unstable excitations. *Journal of High Energy Physics*, 2020(9):1–37, 2020.

[47] Tim Thomas, Olalla A. Castro-Alvaredo, and Benjamin Doyon. Non-Equilibrium Steady State Currents in Critical Systems from Generalized Hydrodynamics . unpublished, 2018.

[48] Eric Vernier and Axel Cortés Cubero. Quasilocal charges and progress towards the complete GGE for field theories with nondiagonal scattering. *Journal of Statistical Mechanics: Theory and Experiment*, 2017(2):023101, 2017.